VAN DYK, ANTONIE CHRISTOFFEL

SURFACE TREATMENT OF TIO2 POWDERS

PhD UP 1997

Surface Treatment of TiO_2 Powders

by

Antonie Christoffel van Dyk

Presented in partial fulfilment of the requirements for the degree

Philosophiae Doctor

Chemistry

in the Faculty of Science

University of Pretoria

Pretoria

April 1997

ACKNOWLEDGEMENTS

I would like to express my sincere gratitude to the following people and institutions for their support throughout my studies:

- My promoter, Professor Anton M. Heyns for his guidance, inspirational vision and financial support.
- My wife and family for their support
- The rest of the research group for their advice
- MINTEK for the use of their facilities and financial support
- Dr de Villiers and Dr Giesekke for arrangements at MINTEK to complete this study and technical advice

SUMMARY

Surface Treatment of TiO_2 Powders

by

Antonie Christoffel van Dyk
Presented for the degree Ph.D (Chemistry)

Supervisor
Professor A.M. Heyns
Department of Chemistry
University of Pretoria

TiO_2 was treated with inorganic and organic surface agents under different conditions and the aim was to improve the qualities of the pigment and to determine the role of the adsorbed hydroxyl ions in these qualities. Good dispersion and durability are two important qualities in the TiO_2 pigment industry that are investigated in this study.

It is a difficult matter to quantify the effectiveness of the coating, but in this study the surface treatment of TiO_2 was evaluated by using sedimentation and the degradation of methylene blue.

Surface area measurements, zeta potential measurements and infrared spectroscopy were used to characterize the TiO_2 surface. The surface area of treated TiO_2 powders showed that the alumina-bearing chemical and the precipitation procedure have a tremendous effect on the morphology of the coating and therefore also on the qualities of the final pigment. The large negative zeta potential values reported for silica treated samples, are responsible for the good dispersion stability while structural viscosity, created by hydrogen bonding, is responsible for the stability in organic treated samples.

This study proved that hydroxyl and water molecules, adsorbed on the surface, play a very important role in the dispersion stability and photo-activity of the TiO_2 pigment. For optimum pigment qualities it is therefore important to control the terminal hydroxyl groups on the rutile surface by surface treatment.

OPSOMMING

Surface Treatment of TiO_2 Powders

deur

Antonie Christoffel van Dyk

Voorgelê vir die graad Ph.D (Chemie)

Promotor

Professor A.M. Heyns

Departement Chemie

Universiteit van Pretoria

TiO_2 was behandel met anorganiese en organiese oppervlak agente onder verskillende kondisies en die doel was om die eienskappe van die pigment te verbeter en om vas te stel watter rol speel die hidroksiel ione in hierdie eienskappe. Goeie dispersie en duursaamheid is twee belangrike eienskappe in die TiO_2 pigment industrie en hulle word in hierdie studie ondersoek.

Kwantifisering van die effektiwiteit van die bedekking is 'n moeilike kwessie maar in hierdie studie is die oppervlak behandeling van TiO_2 geëvalueer deur die gebruik van sedimentasie en die degradasie van metileen blou.

Oppervlak area metings, zeta potensiaal metings en infrarooi spektroskopie was gebruik om die TiO_2 oppervlak te karakteriseer. Die oppervlak area van die behandelde TiO_2 poeier het aangetoon dat die aluminium-draende chemikalieë en die presipitasie prosedure, 'n yslike effek op die morfologie van die bedekking het en daarom ook op die eienskappe van die finale pigment. Die groot negatiewe zeta potensiaal waardes, wat vir silika behandelde monsters geraporteer is, is verantwoordelik vir die goeie dispersie stabiliteit terwyl

struktuele viskositeit, geskep deur waterstof binding, is verantwoordelik vir die stabiliteit in organies behandelde monsters.

Hierdie studie het getoon dat die hidroksiel en water molekules, wat op die oppervlak geadsorbeer is, 'n baie belangrike rol speel in die dispersie stabiliteit en foto-aktiwiteit van TiO_2 pigmente. Vir optimum pigment eienskappe is dit dus belangrik om die terminale hidroksiel groepe, op die rutiel oppervlak, te beheer deur oppervlakbehandeling.

CONTENTS

To my wife, Elna

CHAPTER 1

Introduction

CHAPTER 1

INTRODUCTION

1.1. THE IMPORTANCE OF TITANIUM DIOXIDE POWDERS

Titanium is a natural mineral and found in beach sands around the coasts of South Africa, Canada, Australia and the U.S.A. According to The Economics of Titanium [1] over 90% of the world supply of titanium feedstock is used in the production of titanium dioxide pigment. Titanium dioxide (TiO_2) occurs naturally in ilmenite, leucoxine and rutile, but must be further processed to produce a bright white pigment. The purity and particle size of the product are important in determining the brightness and whiteness of the pigment. Pure TiO_2 is a white crystalline solid and like the other d-block elements, in its group of the Periodic Table, the TiO_2 is stable, nonvolatile, largely insoluble and rendered refractory by strong ignition. The TiO_2 exist in three fundamental crystal forms namely: tetragonal rutile, tetragonal prisms of anatase and orthorhombic brookite.

Only anatase and rutile are produced commercially with rutile the more important in volume terms. The rutile crystal has a more compact structure than anatase and this accounts for important differences between the two crystal forms. The higher refractive index of rutile (2.71), which leads to greater opacifying power, and superior exterior durability are the major reasons for its preferred use relative to anatase (2.55) and other white pigments like antimony oxide (2.20), Zinc oxide (2.01) and basic lead carbonate (2.00).

TiO_2 pigments are the most widely used of all white pigments and produced via the sulphate and chloride process. The widespread use of TiO_2 is attributable to its physical characteristics, the most important of which is a high refractive index, good brilliance, chemical inertness and non-absorption of visible light.

Paints, varnishes and other coatings are the principle end-usage of TiO_2 pigments with other applications being in paper, plastics, rubber, inks, fibres and cosmetics. Figure 1.1 shows the world demand for TiO_2 pigments in the major end-uses.

Figure 1.1: World demand for TiO_2 in 1991.

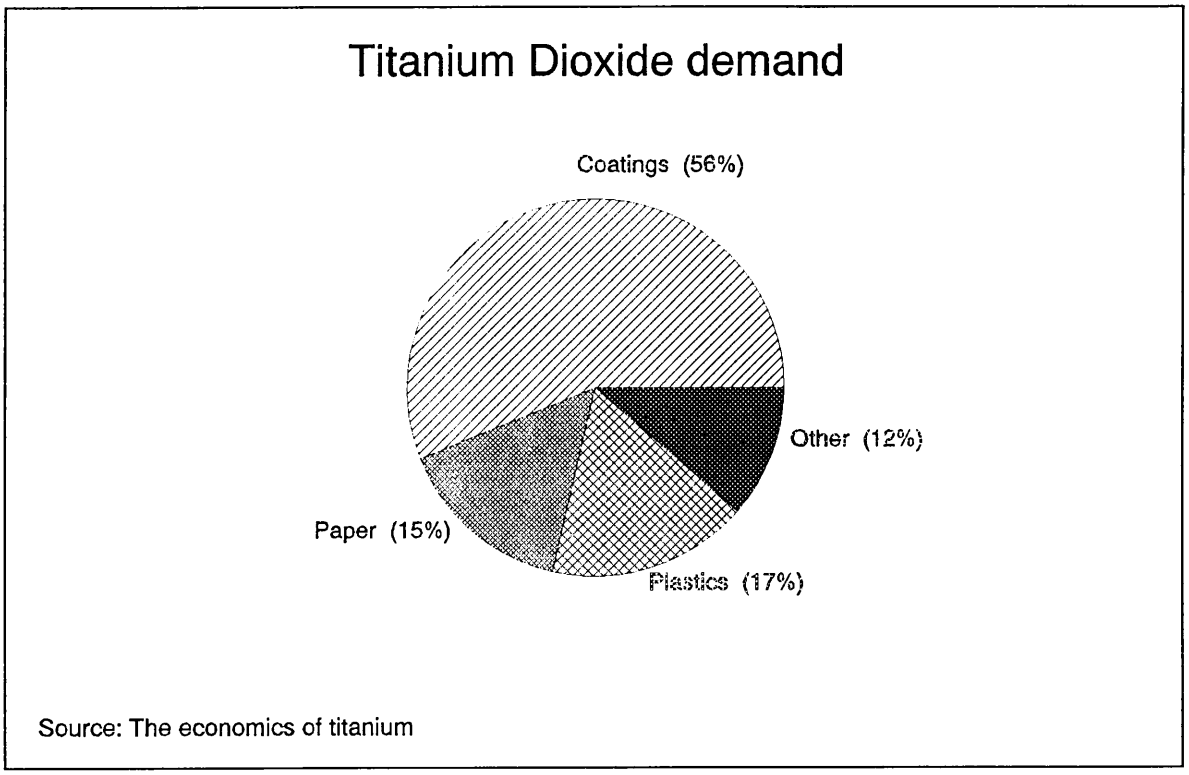

In 1994 the world supply of TiO_2 was approximately 3.5m tonnes and at a average price of US$2000/ton this is a big industry [2]. The paints manufacturing industry is a major consumer of TiO_2 pigments and use it for white and light coloured paints and coatings. TiO_2 pigments are used in three different media:

i) Systems where there is appreciable pigment-medium interaction for example most paints;
ii) Systems in which there is little pigment-medium interaction for example plastics;
iii) Systems in which there is a phase change involving the pigment for example emulsion paints.

The paper industry accounts for 15% of the TiO_2 consumption. TiO_2 is used in papermaking mainly as a filler and opacity, brightness, particle size and hardness are some of the properties needed. Anatase grade (3.85g/cm^3) is preferred over rutile grade (4.15g/cm^3) for paper filling because it has a lower specific gravity, which avoids retention at the wet-end of the paper machine and imparts a bluish whiteness, which is considered more acceptable than the yellow tinge sometimes found with rutile.

The chemical inertness and high refractive index of TiO_2 has made it an ideal opacifier for most plastics. South Africa's main paint producer AECI also consumes substantial quantities of TiO_2 in plastics processing. TiO_2 is also used in polyolefins to provide opacity because it is suitable for prevention of light damage. TiO_2 is used in inks for colour, controlling bulk, opacity, specific gravity, viscosity and printing quality and is available with coatings of zinc, aluminium and silicon oxides.

The TiO_2 content of world reserves of ilmenite and rutile is given in Table 1. The main economic reserves of ilmenite are as follows: South Africa 18%, Norway 16%, India and China 15% each, Canada 13% and Australia 12%.

Table 1: World titanium reserves in 1991 (mill.t TiO_2)

Country	Ilmenite	Rutile & Anatase	Total
Canada	27.0	-	27.0
USA	7.8	0.3	8.1
Brazil	1.6	66.0	67.6
Norway	32.0	-	32.0
South Africa	**36.0**	**3.6**	**39.6**
China	30.0	-	30.0
India	31.0	4.4	35.4
Australia	24.0	5.3	29.3
Other	14.2	5.4	19.6
Total	203.6	85.0	288.6

Source: The economics of Titanium [1]

In South Africa there is only one company, S.A. Tioxide, that produces TiO_2 pigment mainly in the rutile form for the paint industry with a capacity of approximately 40kt per annum. Considering the big amount of money involved in the industry and the fact that South Africa has the largest economic reserve base of titanium minerals, it is important for South Africa to build a basic knowledge of the chemistry and processes involved in the production of TiO_2.

1.2. SURFACE TREATMENT OF TITANIUM DIOXIDE

Most TiO_2 pigments undergo surface treatment to improve the quality of the pigment. This is done by precipitation or adsorption of organic and inorganic materials on the surface of the particles. The surface treatment gives certain qualities to the pigment depending on the surface agent used. The most important qualities are good dispersion in binders and a decrease in photo-activity. The material on the surface isolates the TiO_2 particle from the binder to reduce photo-activity and interacts with the binder to give a good dispersion. The surface treatment can also play a role in the optical qualities of the pigment although to a lesser extend.

In the 1940's coatings were applied to TiO_2 pigments, principally to improve their dispersibility and durability [1]. Inorganic oxides of Al, Si, P, Zn, Zr, etc. are mainly used as surface agents for the treatment of TiO_2 powders. This is followed by organic treatment which is usually a polyol, amine or silicone-based material.

Silica-alumina treatments is mainly used. The coating of TiO_2 powders takes place by adding aluminium sulphate to a dispersion of TiO_2 and a alkaline silica at a temperature of 318K. The final pH of the dispersion is adjusted between 5 en 7. A silica solution can also be added to a concentrate of the pigment and an aluminium salt. The first method is preferred because the alkaline silica acts as a dispersion agent for the TiO_2 and the final product is of a better quality.

Zirconium sulphate is also used as a surface agent to precipitate zirconium oxide on the TiO_2 surface and because of ZrO_2's low reactivity Solomon en Hawthorne [3] stated that this lessens the photo-reactivity of TiO_2.

The treatment of TiO_2, with different concentrations of alumina, silica and organic reagents, was investigated in this study. This treatment was done, as discussed above, to improve the dispersion stability and the photo-activity of the pigment. The aim of this study is to investigate why the surface treatment improved certain qualities and to what extend.

Because of the difficulty, and lack of instrumentation in measuring the degradation and dispersion of pigments in a medium, different methods needed to be found. The photo-activity of TiO_2 powders were evaluated by using the degradation of methylene blue which can be measured with a spectrophotometer. Dispersion stability was evaluated by sedimentation under gravity.

The characterization of the TiO_2 surface was done by surface area measurements, zeta potential and infrared spectroscopy. These measurements were used to explain the observations in the dispersion stability and photo-activity experiments and will give a better knowledge about the surface and the influencing factors.

1.3. REFERENCES

1. Roskill Information Services Ltd. 1993. The Economics of Titanium. 8th Edition. November.

2. Adams, R. 1995. TiO_2 in the Decade Ahead. TiO_2 95 Conference. Munich, Germany, 8-10 May.

3. Solomon, D.H. Hawthorne, D.G. 1983. *Chemistry of Pigments and Fillers.* New York and Brisbane: John Wiley & Sons.

CHAPTER 2

Surface Treatment of TiO_2 Powders

CHAPTER 2

SURFACE TREATMENT OF TiO_2

2.1. INTRODUCTION

Most TiO_2 pigments undergo surface treatment to improve the quality of the pigment. This is done by precipitation or adsorption of organic and inorganic materials on the surface of the particles. The surface treatment gives certain qualities to the pigment depending on the surface agent used. The most important qualities are good dispersion in binders and a decrease in photo-activity. As coatings are applied to TiO_2 in aqueous suspension, the pigment surface is hydrated and therefore a technique like, for example, infrared reflectance is able to give useful information about the surface. This will be discussed in chapter 6.

The mechanism of the inorganic surface modification of TiO_2 may be classified as co-precipitation onto a substrate. If the rate of addition and hydrolysis is too high the surface compounds might precipitate in solution and not on TiO_2. The two components may form a molecular mixture in the precipitate or alternatively one component may precipitate first and form nuclei onto which the other component then precipitates. The most common additives are silica and alumina which will be investigated in this study but other hydrous inorganic oxides like zirconium, tin, zinc etc. were also reported in the literature [1].

Hughes [2] suggested that the role of coating alumina is that of a strong electron acceptor attached to the surface Ti-OH groups of the titania crystal, preventing the formation of hydroxyl or peroxy free radicals. Wiseman [3] argued that the pseudo-boehmite structure of alumina resulted in higher surface hydroxyl coverage.

Wiseman [3] claimed low surface area and porosity to be indicative of greater physical coherence of the surface layer and concluded that compact, coherent coatings of alumina and silica reduce the photo-activity of the pigment and improve the weathering resistance of the pigmented film.

Wiseman also claimed that the proportions of alumina and silica added are usually such that a large excess of alumina is present which precipitates as interstitial alumina. The hydroxylated aluminium species adsorbed on the silica gel particles will inhibit polymerization of the silica gel. Silica-aluminas can exist in compositions ranging from the true alumino-silica, with aluminium ion tetrahedrally bound in a silicon-oxygen network, to inter-mixtures of silica and alumina in separate domains.

After the inorganic coating is applied, additional organic treatments may be added. Organic treatment can play a role in the dispersion stability and the dry flow of pigments but often organics are added as a milling aid.

In this chapter the experimental procedure, to add a surface coating onto the TiO_2, will be discussed. Factors like pH, temperature and rate of precipitation that can influence the precipitation will be investigated.

2.2. EXPERIMENTAL

2.2.1. INORGANIC SURFACE TREATMENT

2.2.1.1. *Alumina*

Titanium dioxide (5g), with a purity of 99% (Saarchem) and in the rutile crystal structure, was dispersed in 100ml of water by stirring it with a magnetic stirrer and placing it in an ultrasonic bath for 2 minutes. The sample was then heated to 318K and the pH was determined. This procedure was repeated every time before any addition of inorganic materials. Sodium aluminate (Glassworld CP) was added separately to these dispersions in the following volumes (100g/l): 0.5ml (A1), 1.0ml (A2), 2.0ml (A3) and 3.0ml (A4). The pH was then measured and HCl (6 mol/dm^3) was added to neutralize the pH to 6.5. The powder was then filtered, washed and dried at 383K for 3 hours. All the pH measurements were done with a Mettler Delta 340 pH meter.

The experiment was repeated with different initial temperatures at 291K (A4(291)), 303K, 318K, 323K and 353K to observe the effect of various temperatures on the coatings. Only 3.0ml $NaAlO_2$ and 3.0ml $Al_2(SO_4)_3$ (100g/l) was used in these experiments.

The same procedure as mentioned above was followed using 0.5ml(A5), 1ml(A6) and 3ml(A7) $Al_2(SO_4)_3$ (100g/l) and 0.5ml(A8), 1ml(A9) and 3ml(A10) (100g/l) $AlCl_3$ (99% Protea Chem) as reagent. In this case the pH was adjusted with NaOH (300g/l).

2.2.1.2 *Silica*

Titanium dioxide (5g), with a purity of 99% and in the rutile crystal structure, was dispersed in 100ml of water by stirring it with a magnetic stirrer and placing it in an ultrasonic bath for 2 minutes. The sample was then heated to 318K and the pH was determined. This procedure was repeated every time before any addition of inorganic materials. Sodium silicate (Glassworld CP) was added separately to these dispersions in the following volumes (100g/l): 0.5ml (S1), 1.0ml (S2), 2.0ml (S3) and 3.0ml (S4). The pH was then measured and HCl (6 mol/dm^3) was added to neutralize the pH to 6.5. The neutralization took place between 45 and 60 minutes. The powder was then filtered, washed and dried at 383K for 3 hours.

The experiment was repeated with different initial temperatures at 291K(S4(291)), 303K, 318K, 323K and 353K to observe the effect of various temperatures on the coatings. Only 3.0ml Na_2SiO_3 (100g/l) was used in these experiments.

After analysis, which will be discussed later in this chapter, the yield on the silica treated samples were poor and a reason for this might have been the neutralization time. It was therefore decided to do another two experiments with silica as surface agent. TiO_2 (10g) was dispersed in 200ml of water as discussed previously. Na_2SiO_3, (100g/l) 5ml(S5), 10ml(S6), was added continuously in 1 hour. Neutralization with hydrochloric acid was done over 3 hours and the temperature was kept at 318K for the period. The powder was filtered and washed as discussed before.

2.2.1.3. *Combination of silica and alumina*

Different combinations of the oxides were used to treat TiO_2, also with different methods of precipitation. In all the experiments the silica was added before the alumina.

Experiment AS1- AS5

Suspensions of TiO_2 (5g) in 100ml water were prepared and dispersed in a ultrasonic bath for 2 minutes. The pH of the suspensions were 7.3 and they were kept at room temperature. The suspensions were treated with different volumes of Na_2SiO_3 and $NaAlO_2$ as follows:

Exp AS1: 0.5ml Na_2SiO_3 + 1ml $NaAlO_2$

Exp AS2: 0.5ml Na_2SiO_3 + 2ml $NaAlO_2$

Exp AS3: 2ml Na_2SiO_3 + 2ml $NaAlO_2$

Exp AS4: 2ml Na_2SiO_3 + 0.5ml $NaAlO_2$

Exp AS5: 1ml Na_2SiO_3 + 0.5ml $NaAlO_2$

The pH was then measured and HCl (6 mol/dm^3) was added to neutralize the pH to 6.5. The neutralization was done in 60 minutes. The powder was then filtered, washed and dried at 383K for 3 hours.

Experiment AS6-AS9

Because of the low yield of silica precipitated on the surface in the previous experiments, the following experiments were done in order to improve the percentage of silica on the surface. Suspensions of TiO_2 (10g) dispersed in water (200ml) were prepared using a magnetic stirrer and ultrasonic bath. The suspensions were treated with different volumes of Na_2SiO_3 and $NaAlO_2$ at room temperature as follows:

Exp AS6: 4ml Na_2SiO_3 + 1ml $NaAlO_2$

Exp AS7: 2ml Na_2SiO_3 + 1ml $NaAlO_2$

Exp AS8: 6ml Na_2SiO_3 + 2ml $NaAlO_2$

Exp AS9: 4ml Na_2SiO_3 + 2ml $NaAlO_2$

The pH was then measured and HCl (6 mol/dm^3) was added to neutralize the pH to 6.5. The neutralization time was increased to 3 hours. The powder was then filtered, washed and dried at 383K for 3 hours.

Experiment AS10-AS16

Suspensions of TiO_2 (5g) in 100ml water were prepared and dispersed in a ultrasonic bath for 2 minutes. The pH of the suspensions were 7.3 and they were heated to 318K. The suspensions were treated with different volumes of Na_2SiO_3 and $Al_2(SO_4)_3$ as follows:

Exp AS10: 0.5ml Na_2SiO_3 + 2ml $Al_2(SO_4)_3$

Exp AS11: 1ml Na_2SiO_3 + 2ml $Al_2(SO_4)_3$

Exp AS12: 2ml Na_2SiO_3 + 2ml $Al_2(SO_4)_3$

Exp AS13: 3ml Na_2SiO_3 + 2ml $Al_2(SO_4)_3$

Exp AS14: 2ml Na_2SiO_3 + 0.5ml $Al_2(SO_4)_3$

The pH was adjusted afterwards with NaOH to 6.5 over a period 60 minutes. The powder was then filtered, washed and dried at 383K for 3 hours.

Two additional experiments were done to improve the yield of the silica. Suspensions of TiO_2 (10g) were dispersed in water (200ml) as discussed previously. The following additions were made at room temperature:

Exp AS15: 1.5ml Na_2SiO_3 + 4ml $Al_2(SO_4)_3$

Exp AS16: 2ml Na_2SiO_3 + 4ml $Al_2(SO_4)_3$

The pH was adjusted afterwards with NaOH to 6.5 over a period of 3 hours. The powder was then filtered, washed and dried at 383K for 3 hours.

2.1.1.4 *Summary*

A summary of the surface treatment of TiO_2 as described in the experiments above can be seen in table 2.1. Al_2O_3% and SiO_2% are expressed as the weight percentage of surface agent added over the total weight of TiO_2 (eg. Al_2O_3/TiO_2 %). Surface agent in the content of this study means the different precursor salts of Al_2O_3 and SiO_2 used in the experiments.

TABLE 2.1: Summary of the surface treatment of TiO_2

Sample	Surface agent	SiO_2%	Al_2O_3%	Sample	Surface agent	SiO_2%	Al_2O_3%
A1	$NaAlO_2$		0.62	AS1	Na_2SiO_3	0.49	1.24
A2			1.24	AS2	+	0.49	2.49
A3			2.49	AS3	$NaAlO_2$	1.97	2.49
A4			3.73	AS4		1.97	0.62
				AS5		0.98	0.62
A5	$Al_2(SO_4)_3$		0.3	AS6		1.97	0.62
A6			0.6	AS7		0.98	0.62
A7			1.79	AS8		2.95	1.24
				AS9		1.97	1.24
A8	$AlCl_3$		0.38				
A9			0.76	AS10	Na_2SiO_3	0.49	1.19
A10			2.29	AS11	+	0.98	1.19
				AS12	$Al_2(SO_4)_3$	1.97	1.19
S1	Na_2SiO_3	0.49		AS13		2.95	1.19
S2		0.98		AS14		1.97	0.3
S3		1.97		AS15		0.74	2.49
S4		2.95		AS16		0.98	2.49
S5		2.46					
S6		4.92					

2.2.2. ORGANIC SURFACE TREATMENT

A suspension of TiO_2 (5g) was dispersed in water (100 ml) using a ultrasonic bath for 2 minutes. The suspension was heated to 318K. The 0.5 ml, 1 ml and 3 ml of the organic reagent was added separately and the suspension was stirred for half an hour. The treated TiO_2 was filtered and dried. The organic reagent used can be seen in the following table.

The organic reagents are added to a water dispersion of TiO_2 to see if some of the organics will adsorb on the surface. The adsorption was investigated with infra-red spectroscopy. The dispersion stability of the samples was tested and the samples with the best results were used for further investigation. The organic treatment will be discussed in another chapter.

Table 2.2 : Organic reagents used for surface treatment

Sample	Organic agent	Volume added (ml)	Sample	Organic agent	Volume added (ml)
PEG.5	Polyethylene glycol	0.5	TEA.5	Triethanolamine	0.5
PEG1	(Merck 6000)	1	TEA1	(Palchem 85%)	1
PEG3		3	TEA3		3
ED.5	Ethanediol	0.5	PET.5	Phenylethanol	0.5
ED1	(Saarchem 99%)	1	PET1	(Merck 99%)	1
ED3		3	PET3	"	3
PD.5	Propanediol(1,2)	0.5	EDA.5	Ethylene	0.5
PD1	(Merck 99%)	1	EDA1	diamine (Merck	1
PD3		3	EDA3	99%)	3
AC.5	Acetic acid	0.5	DMA.5	Dimethylamine	0.5
AC1	(Merck 99%)	1	DMA1	(BDH Chem	1
AC3		3	DMA3	30%)	3
ET.5	Ethanol	0.5	AM.5	Ammonia	0.5
ET1	(NT 99%)	1	AM1	(Sastec 35%)	1
ET3		3	AM3		3
PR.5	2-Propanol	0.5			
PR1	(Merck 99%)	1			
PR3		3			

2.2.3. ANALYSIS

Analysis were done at Mintek to determine the percentage TiO_2, SiO_2 and Al_2O_3 on the treated TiO_2. The samples were analyzed for Al, Si and Ti using Inductive Coupled Plasma Emission Spectrometry at Mintek. Sample preparations were done by fusing samples with sodium carbonate and sodium peroxide and dissolving the sample afterwards in hydrochloric acid. The samples were diluted and measurements were taken.

2.3. RESULTS AND DISCUSSION

2.3.1. TEMPERATURE- AND pH DEPENDENCE OF SURFACE TREATMENT

The efficiency of the coating technique will be discussed in this section by comparing the percentage of coating material added with the chemical analysis of the coated powder. In the first experiment the influence of the pH on the precipitation was investigated. Experiment S4 and A4 were repeated and samples were taken at different pH values and analyzed. The results for this experiment can be seen in table 2.3.

Table 2.3 : Composition of samples at different pH values

Sample	pH	TiO_2%	SiO_2%	Al_2O_3%
S4	11.36	99.4	<0.2	<0.25
	10.15	99.1	<0.2	<0.25
2.95% SiO_2	9.04	98.1	0.97	<0.25
	8.05	99.0	0.30	<0.25
	6.82	98.8	0.39	0.39
	5.66	98.9	0.31	<0.25
A4	11.00	99.4	<0.2	0.36
	10.00	97.9	<0.2	1.23
3.73% Al_2O_3	8.98	95.3	<0.2	3.07
	7.92	94.9	<0.2	3.17
	6.87	95.2	<0.2	2.90
	4.30	96.0	<0.2	1.98

Coating TiO_2 with SiO_2 as seen in sample S4 is not very effective because a great percentage of the coating is washed away in the filtration. Although 2.95% SiO_2 was added only 1% (yield- 30%) remained on the surface at a pH of 9. Although the pH was lowered over 30 minutes a reason for the low yield might be the aging time especially at a pH of 9. The results from Howard and Parfitt [4] also showed that SiO_2 precipitated more effectively at a pH of 8-9 and at this pH the highest yield was 24%. Desorption of silica from the TiO_2 substrate as the pH was lowered, was also visible in their data.

Coating TiO_2 with Al_2O_3 was more effective as seen in the results from sample A4 with a highest yield of 85% at a pH of 7.9. Incomplete precipitation occurred before neutralization in both cases.

Another interesting result is that SiO_2 precipitates at a higher pH than Al_2O_3 and therefore the conclusion can be made that SiO_2 precipitates before Al_2O_3. In the combination reactions it can be assumed that silica first form a layer around the TiO_2 particle and then the alumina precipitates on the spaces not covered by the silica. All the silica is not precipitated at the time that the alumina starts to precipitate and therefore a aluminosilicate compound can be formed. Once the oxides start to precipitate out they are insoluble in water even if the pH increases again. This is also an indication that SiO_2 and Al_2O_3 are formed and not an intermediate compound.

The 0.39% alumina in sample S4 might be due to a detection error in the analytical measurements or due to alumina added during the manufacturing stage which is too small to detect accurate with the technique used here.

Treatment of TiO_2 with $Al_2(SO_4)_3$, Na_2SiO_3 and $NaAlO_2$ at different temperatures can be seen in table 2.4 - 2.6. The temperature does not seem to have a big influence on the precipitation of Al_2O_3 when $Al_2(SO_4)_3$ is used as starting material.

Table 2.4 : Treatment of TiO_2 with 1.79% $Al_2(SO_4)_3$ at different temperatures

Sample	Temp (K)	TiO_2%	SiO_2%	Al_2O_3%
A7(303)	303	96.4	<0.2	1.25
A7(323)	323	94.6	0.24	1.24
A7(333)	333	96.6	<0.2	1.30
A7(353)	353	96.4	0.22	1.26

With $NaAlO_2$ and Na_2SiO_3 as starting material, the temperature caused a slight difference in the yield. $NaAlO_2$ gave a yield of 90% at 291K and a lowest yield of 74% at 323K. The latest result is in good agreement with sample A4 at a pH of 6.8 in table 2.3 which was done under similar experimental conditions. No linear relationship could be found between the temperature and the yield.

Table 2.5 : Treatment of TiO_2 with 3.73% $NaAlO_2$ at different temperatures

Sample	Temp (K)	TiO_2	SiO_2	Al_2O_3
A4(291)	291	93.7	<0.2	3.36
A4(303)	303	90.6	<0.2	3.09
A4(318)	318	94.2	<0.2	3.26
A4(323)	323	94.2	<0.2	2.75
A4(353)	353	91.9	<0.2	3.11

Table 2.6 : Treatment of TiO_2 with 2.95% Na_2SiO_3 at different temperatures

Sample	Temp (K)	TiO_2	SiO_2	Al_2O_3
S4(291)	291	98.9	<0.2	0.33
S4(303)	303	97.4	0.61	0.44
S4(318)	318	98.1	0.33	0.29
S4(323)	323	97.0	0.39	0.38
S4(353)	353	96.7	0.38	0.61

Treatment using Na_2SiO_3 as starting material gave a highest yield of 21% at 303K. Again the silica yield is very poor as in the previous experiment and at this stage the only reason might be the aging time.

Bruni, Visca, Garbassi and MelloCeresa [5] reported better results for precipitating SiO_2 and said that this is due to the higher temperature used (333K). Looking at table 2.6 this conclusion does not seem to be true. Another reason might be the difference in experimental techniques.

2.3.2. CHEMICAL ANALYSIS OF TREATED POWDERS

Treatment of TiO_2 with SiO_2 was not very effective as seen in table 2.7. The yield was very low and therefore a great percentage of the coating was washed away in the filtration process. Although the pH was lowered over 30 minutes this might not be adequate time for the silica to precipitate on the surface. Further experiments were done to increase the yield by decreasing the rate of precipitation. In a previous section it was shown that silica precipitate close to a pH of 9 and therefore the sample must be kept at this pH for a longer time.

This seems to be only part of the explanation because the yield in samples S5 and S6, which were neutralised slowly, was still very low at 30%. The yield in these samples is therefore considerable higher compared to samples S1-S4 and is equal to the highest yield precipitated in the previous section at different pH values. The higher yield of these two samples can also be seen in figure 2.1. A linear relation with a small coefficient (0.111), indicating a low yield, exist between the percentage added and precipitated for samples S1-S4. The slope of this line increase (0.307) when the neutralization time is increased as seen at sample S5 and S6. These results show the benefit of slow controlled precipitation when sodium silicate is used as coating agent. The correlation coefficient for samples S1-S4 is 0.980 and for samples S5-S6 it is 0.999 indicating a good least-squares fit.

Coating TiO_2 with Al_2O_3 using sodium aluminate as reagent gave a good yield as seen from the slope (0.865) in figure 2.1. The alumina is less dependant on the rate of neutralization than silica.

Table 2.7 : Analytical results of surface treated TiO_2

Sample	Surface agent	Added (%)		Precipitated (%)	
		SiO_2	Al_2O_3	SiO_2	Al_2O_3
S1	Na_2SiO_3	0.49	0	0.10	<0.2
S2		0.98	0	0.14	<0.2
S3		1.97	0	0.28	<0.2
S4		2.95	0	0.33	0.29
S5		2.46	0	0.69	<0.2
S6		4.92	0	1.51	<0.2
A1	$NaAlO_2$	0	0.62	<0.1	0.73
A2		0	1.24	<0.1	1.25
A3		0	2.49	<0.1	2.39
A4		0	3.73	<0.2	3.25
A5	$Al_2(SO_4)_3$	0	0.3	<0.1	0.37
A6		0	0.60	<0.1	0.33
A7		0	1.79	<0.2	0.48
A8	$AlCl_3$	0	0.29	<0.1	0.29
A9		0	0.76	<0.1	0.30
A10		0	2.29	<0.1	0.31
AS1	Na_2SiO_3	0.49	1.24	0.37	1.31
AS2	+	0.49	2.49	0.39	2.37
AS3	$NaAlO_2$	1.97	2.49	1.17	2.90
AS4		1.97	0.62	0.77	0.74
AS5		0.98	0.62	0.52	0.79
AS6		1.97	0.62	0.80	0.58
AS7		0.98	0.62	0.36	0.58
AS8		2.95	1.24	1.49	1.11
AS9		1.97	1.24	1.14	1.18
AS10	Na_2SiO_3	0.49	1.19	<0.2	0.67
AS11	+	0.98	1.19	0.29	0.65
AS12	$Al_2(SO_4)_3$	1.97	1.19	0.75	0.73
AS13		2.95	1.19	0.71	0.58
AS14		1.97	0.30	0.35	0.29
AS15		0.74	2.49	0.29	0.83
AS16		0.98	2.49	0.44	0.82

Figure 2.1: Yield of silica and alumina coated on TiO_2

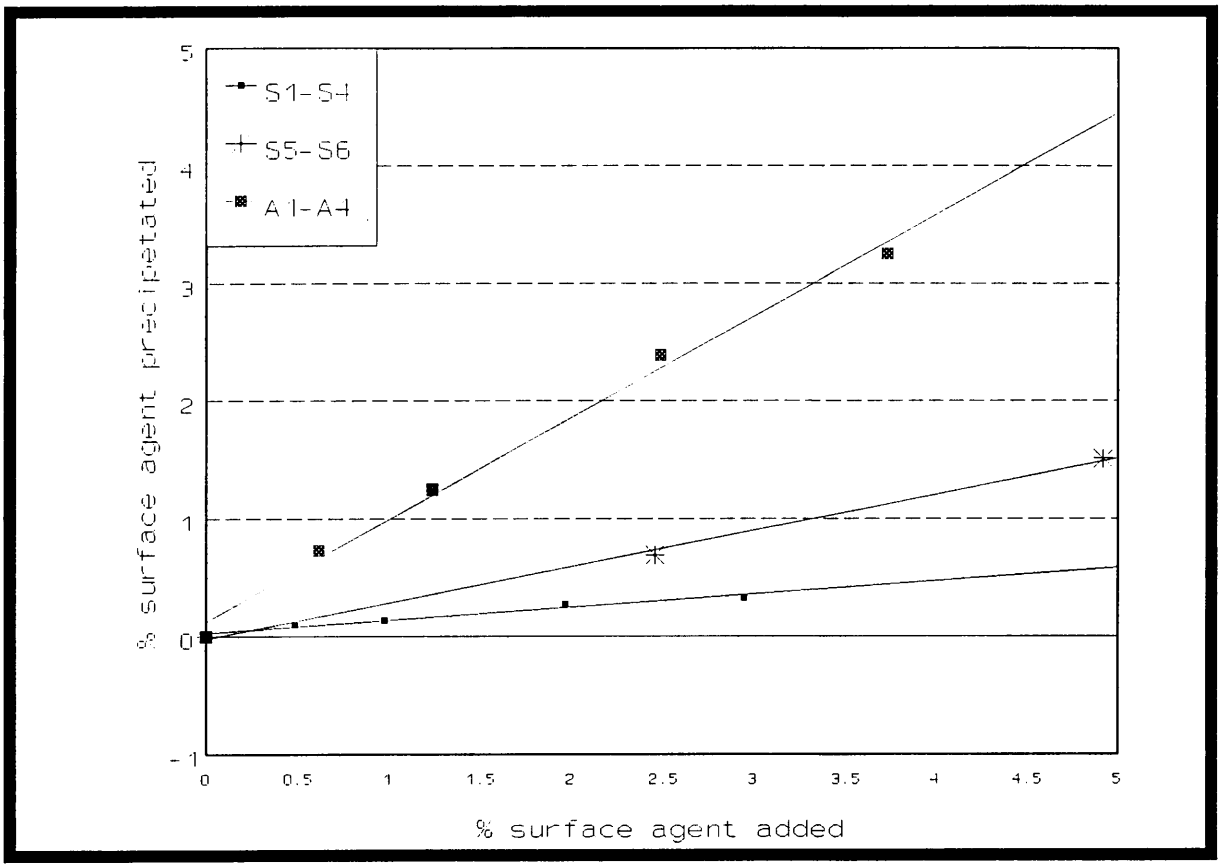

Precipitation of $Al_2(SO_4)_3$ gave a slightly lower yield than $NaAlO_2$ as seen in the analytical results from samples A5-A7. Sample A7 gave a poor yield but this could be due to an experimental problem because the samples in table 2.4 indicated a higher yield. $AlCl_3$, on the other hand gave a very poor yield as seen in sample A9 and A10.

Although rather incomplete Baroucci and Tarlaschi [6] showed the benefit of slow controlled precipitation of coating agents, in that coatings precipitated from aluminium sulphate and sodium silicate reagents by neutralization with alkali were less protective than the same quantities of coating oxides precipitated slowly from sodium aluminate and sodium silicate solutions.

The chemical analysis of the TiO_2 treated with different ratios of alumina and silica can be seen in samples AS1-AS16 in table 2.7. Samples AS6-AS9 were neutralised over a longer period than samples AS1-AS5 but the difference in the yield for silica is not as visible as when silica was precipitated alone. In the presence of alumina the silica is therefore less dependant on the rate of precipitation. The yield for alumina in these samples were again very good and the higher percentage precipitated on some of the samples might be due to a detection error.

Another interesting result from these samples is that the silica yield is higher when more alumina is used. This can be seen by comparing the percentage of silica precipitated on the surface with the percentage of alumina added in samples AS1 and AS2, AS3 and AS4, AS6 and AS9. This and the fact that the silica is less dependant on the rate of precipitation in the presence of alumina give enough reason to believe that the two components form a molecular mixture rather than precipitating in separate domains.

The higher yield of both the silica and alumina can be seen in figure 2.2. The AS1-AS9(A) line represent the precipitation of alumina in sample AS1-AS9 and the AS1-AS9(S) line represent the precipitation of silica. The silica gave a yield of 45% and correlation coefficient of 0.956 and the yield for alumina was 103% with a correlation coefficient of 0.979. The decrease in the correlation coefficient, especially for silica, is due to the dependence on the percentage of alumina added as discussed in the previous paragraph.

Surface treatment using aluminium sulphate and sodium silicate as starting reagents resulted in low surface coverage because of the low yield. The trend that the silica yield increases and is less dependant on the rate of precipitation in the presence of alumina, is still applicable.

Figure 2.2: Yield of the combination of surface agents

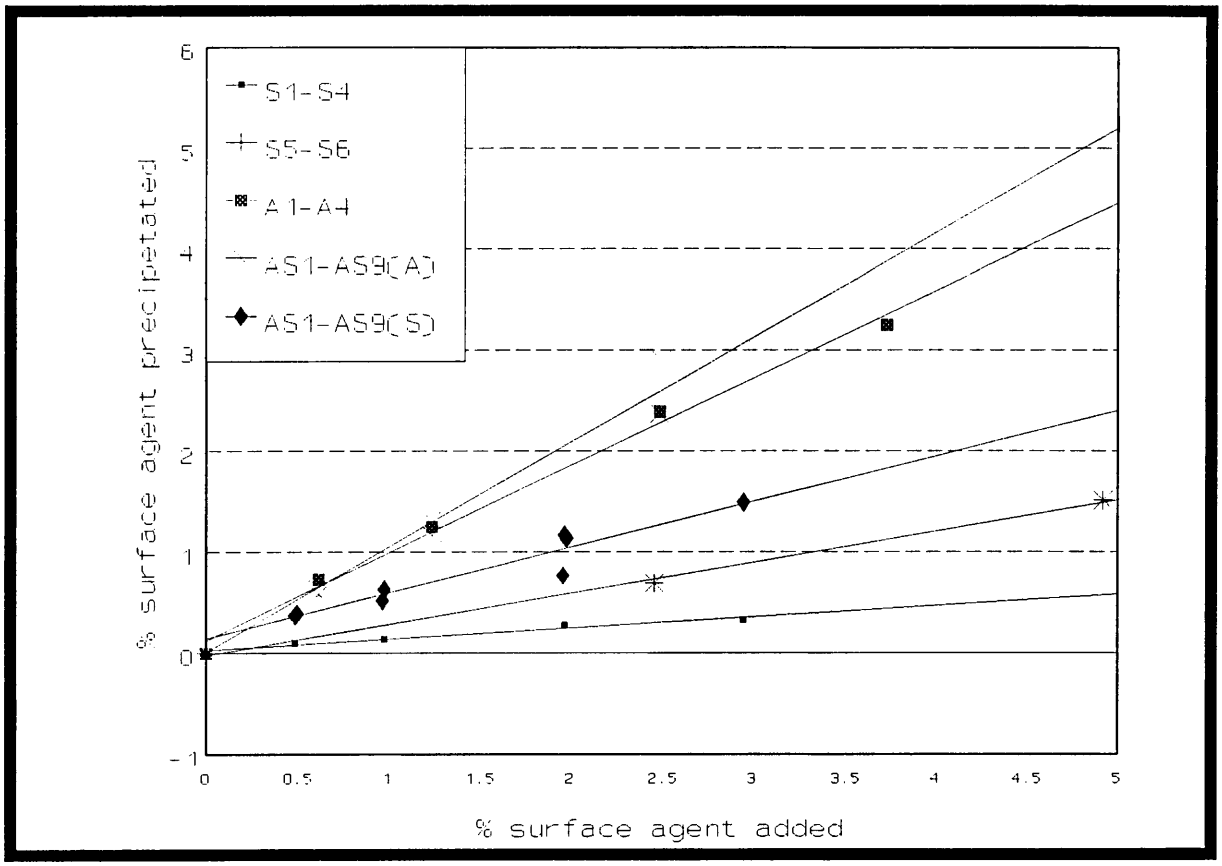

2.4. CONCLUSION

The precipitation behaviour of silica and alumina is strongly dependant upon the experimental conditions. Silica precipitated with a highest yield of 24% at a pH of 9 and alumina precipitated with a 85% yield at a pH of 8 when sodium silicate and sodium aluminate were used as starting materials. No precipitation took place at higher pH values while the yield was considerable lower at lower pH values.

Temperature did not have a significant influence on the coating of TiO_2, independent of what surface agent was used.

The rate of precipitation is one of the conditions that can influence the precipitation of silica. It was proofed that, when sodium silicate is used, the yield of silica precipitated on the surface can be increased by increasing the neutralization time, especially in the region of pH 9. This seems to be only one of the reasons for the low yield of silica because increasing the neutralization time gave a yield of 30% which is still small.

Sodium aluminate gave the best yield (87%) for the surface treatment and is less dependant on the rate of precipitation. Aluminium sulphate and aluminium chloride gave poor yields.

When TiO_2 is treated with silica and alumina simultaneously, the yield of the silica precipitated on the surface increases and the silica is also less dependant on the rate of precipitation.

It can therefore be concluded that the coating of TiO_2 with alumina and silica is a complex co-precipitation process where the silica is believed to precipitate first, followed by the formation of an alumino-silica intermolecular mixture.

The amphoteric dissociation of hydroxyl groups on the TiO_2 particle plays an important roll in the surface charge and therefore the precipitation of other particles on the surface. It is therefore expected that the low yield of the silica can be explained by investigating the charge on the surface. This will be discussed comprehensively in chapter 6.

2.5. REFERENCES

1. Howard P.B. 1977. Treatment of Pigment. *U.S. Patent 4052223.*

2. Hughes, W. 1970. In Parfitt, G.D. Sing, K.S.W. 1976. *Characterization of Powder Surfaces.* Academic Press: London. p 177.

3. Wiseman, T.J. 1976. In Parfitt, G.D. Sing, K.S.W. 1976. *Characterization of Powder Surfaces.* Academic Press: London. p 178.

4. Howard, P.B, Parfitt, G.D. 1977. The Precipitation of Silica/Alumina on Titanium Dioxide Surfaces. *Croatica Chemica Acta.* 50(1-4): p 15.

5. Bruni, M. Visca, M. Garbassi, F. MelloCeresa, E. 1985. Precipitation of Aluminosilicates on the Surface of Titanium Dioxide. *Industrial and Engineering Chemistry Product Research and Development.* 24(4):p 579.

6. Baroucci, V. Tarlaschi, S. 1968. 9th FATIPEC Congress Book, Section 1. In Parfitt, G.D. Sing, K.S.W. 1976. *Characterization of Powder Surfaces.* Academic Press: London. p 178.

CHAPTER 3

Surface Area of TiO_2 Powders

CHAPTER 3

SURFACE AREA OF TiO_2 POWDERS

3.1. INTRODUCTION

The specific surface area is the surface area of the particles per unit mass or volume of material. For a porous material, the surface area determined experimentally depends on the size of the adsorbed molecule relative to the size of the pores. Gas is often used to adsorb on the surface because of its ability to penetrate small pores.

The most popular experimental method of measuring specific surface area is that of gas adsorption. In essence, if the amount of gas required to cover the surface with a complete monolayer can be evaluated, the specific surface area can be calculated, if the area occupied by a single molecule is known. The best known technique to determine the surface area of a solid surface is the Brunauer, Emmett and Teller (BET) method [1].

The importance of surface coatings on TiO_2 was already mentioned but the nature of the coating is just as important. A series of patents [1] claimed low surface area and porosity to be indicative of greater physical coherence of the surface layer and therefore the coating is more effective. Studies by Rechmann [2] concluded that the BET surface area was related to the type of neutralization agent and to the alumina content. Ermolaeva et al. [4] came to similar conclusions about a linear relation between the specific surface area and the amount of coating contained by the pigment. No explanation was offered for the increase in area on coating apart from the comment that the surface roughness increased.

In this chapter attention will be given to the surface area of the coated TiO_2 powders, prepared in the previous chapter. The results obtained here will give information about the nature of the coatings.

3.2. EXPERIMENTAL

The surface area of the powders was determined by low-temperature N_2 adsorption using the Brunauer-Emmett-Teller (BET) method. Measurements were done on a Micromeritics Flowsorb ii 2300 apparatus. The theoretical aspects of this method will be discussed in appendix 1.

3.3. RESULTS AND DISCUSSION

The surface area of the samples as measured by BET method can be seen in table 3.1. The surface area of most of the coated TiO_2 differ from the untreated rutile which is used as starting material. A surface area of 7.36 m^2/g is reported for the rutile and also reported in table 3.1 is the surface areas of the coatings, precipitated in the absence of a substrate. It can be concluded from these measurements that $AlCl_3$ formed a very dense coating because of the low surface area reported. Sodium aluminate also formed a dense coating relative to aluminium sulphate, but when silica and alumina precipitated simultaneously, a porous mixture of the coating materials formed.

The influence of different alumina concentrations on the surface area can be seen in figure 3.1. Higher concentrations of alumina on the surface is responsible for a increase in surface area but the same correlation could not found between the percentage SiO_2 on the surface and the surface area. In the presence of silica the alumina seems to have a bigger influence on the surface area as observed from the bigger slope for samples AS1-AS16 compared to samples A1-A7. The correlation coefficient for the AS-samples is 0.968 with coefficients a = 6.441 and b = 2.293. This indicates an increase of 2.293 m^2/g per percentage alumina on the surface. Rechmann [2] reported an increase of 2.6-3 m^2/g per Al_2O_3% added. The correlation coefficient for the A samples is 0.686 which indicates a poor fit and coefficient a = 6.993 and b = 0.410.

The increase in surface area with increasing alumina concentrations might be due to interstitial material or due to a porous alumina layer on the surface. At low concentrations

TiO_2 treated with sodium aluminate gives a lower surface area than samples treated with aluminium chloride and aluminium sulphate which indicates a more dense coating. Higher alumina concentrations resulted in more interstitial material, therefore a increase in surface area.

Table 3.1 : Surface area of treated TiO_2 powders

Sample	Area (m^2/g)	Sample	Area (m^2/g)
Rutile	7.36	AS1	9.14
		AS2	11.25
$AlCl_3$	3.82	pH 4	7.11
$Al_2(SO_4)_3$	69.20	pH 8	11.75
$NaAlO_2$	22.82	AS3	13.93
Na_2SiO_3	16.18	AS4	8.29
Na_2SiO_3 + $NaAlO_2$ (1:1)	46.82	AS5	8.43
		AS6	7.77
S1	7.39	AS7	7.79
S2	6.20	AS8	8.99
S3	7.04	AS9	9.03
S4	8.00	AS10	7.53
S5	8.12	AS11	7.42
S6	7.56	AS12	7.78
		AS13	7.91
A1	6.82	AS14	7.11
A2	6.70	AS15	7.55
A3	8.77	AS16	7.48
A4	8.12		
A5	7.30		
A6	7.28		
A7	7.20		
A8	7.21		
A9	7.24		
A10	7.10		

These results are similar to those of Cornell, Posner and Quirk [3] who also found a linear relation between the Al_2O_3% and the surface area. Because of the low yield for aluminium chloride and aluminium sulphate most of the alumina precipitated on the surface, but it is assumed that at higher concentrations more interstitial material will precipitate. Other factors such as the rate of precipitation have a influence on the porosity and hence the area of the coating. This can explain the lower surface area for samples S2, A1 and A2. Sample S5 and S6 give an indication that slow controlled precipitation of silica results in a dense coating.

Figure 3.1: Surface area as a function of Al_2O_3%

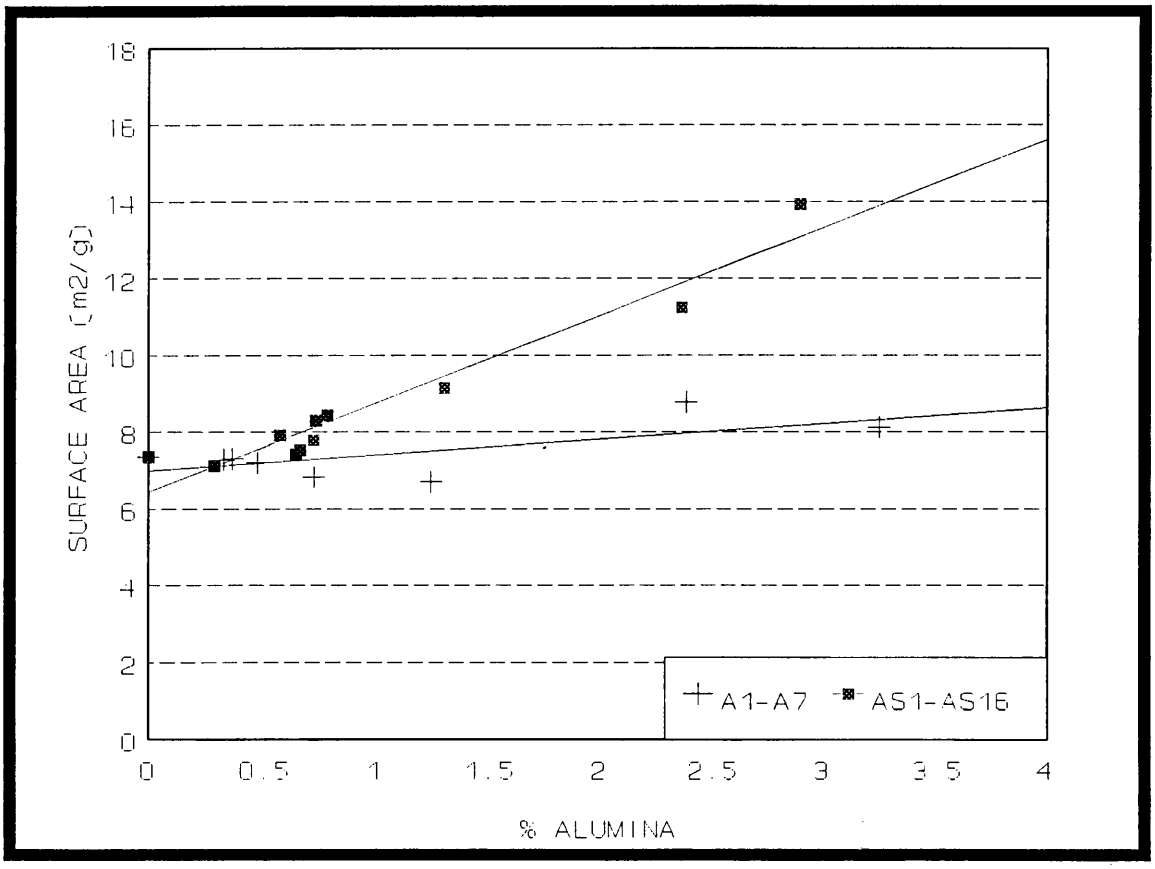

The importance of the experimental conditions were also proved by varying the end pH of sample AS2. The samples were prepared in the same way as sample AS2 after which the pH was adjusted to 4 and 8. Measurements show that the coated TiO_2 with a end pH value of 8 has a higher surface area than TiO_2 with a end pH value of 4. This can be explained using

Wiseman's [4] assumption that a low surface area is indicative of greater physical coherence. At a pH of 4 the precipitation is more complete and therefore the coating will be more dense at this pH value. The TiO_2 also seems to agglomerate more at pH values under 6, judging by the ease of filtration of the sample at a pH value of 4. This causes aggregation in the drying stage which can influence the surface area. The agglomeration is due to electrostatic forces which will be investigated in chapter 5.

3.4. CONCLUSION

The specific surface area of TiO_2 is measured by the Brunauer, Emmett and Teller method. A surface area of 7.36 m^2/g was reported for rutile and this value changed when TiO_2 is treated with inorganic oxides.

The precipitation of Al_2O_3 causes the surface area of the TiO_2 samples to sharply increase and this effect is more evident when silica is also present in the coating. An increase of 2.293 m^2/g is observed for each Al_2O_3 % coated on the surface. This increase might be due to interstitial material not bounded to the surface and a porous alumina layer. A more dense coating of alumina is formed at lower alumina concentrations and when the rate of precipitation is controlled.

The surface area of treated TiO_2 powders showed that the alumina-bearing chemical and the precipitation procedure have a tremendous effect on the morphology of the coating and therefore also on the qualities of the final pigment.

3.5. REFERENCES

1. Parfitt, G.D. 1974. Dispersion of Powders in Liquids. Second Edition. Applied Science Publishers. London.

2. Rechmann, H. 1969. *Farbe und Lack*. 75, p51

3. Cornell, R.M. Posner, A.M. Quirk, J.P. 1980. The precipitation and some properties of Alumina coatings on rutile. *J. Chem. Tech. Biotechnol.* 30: 187-199.

4. Wiseman, T.J. 1976. In Parfitt, G.D. Sing, K.S.W. 1976. *Characterization of Powder Surfaces*. Academic Press: London. p 178.

5. Ermolaeva, T.A. Potapova, M.P. Abramson, D.L. 1972. In Parfitt, G.D. Sing, K.S.W. 1976. *Characterization of Powder Surfaces*. Academic Press: London. p 178.

CHAPTER 4

Dispersion Stability and Photo-activity of TiO_2 Powders

CHAPTER 4

DISPERSION STABILITY AND PHOTO-ACTIVITY OF TiO_2 POWDERS

4.1. INTRODUCTION

4.1.1. DISPERSION OF TiO_2 POWDERS

The formation of a dispersion of pigment in a liquid is the basic step in the manufacturing of ink and paint. Only in exceptional cases for instance in cosmetics, pigments are used in a dry medium and it is therefore important to investigate the dispersion of pigments in a liquid, since dispersion is one of the more important factors determining the performance of a coating. An important aspect of pigment surface chemistry is the dependence of adsorption of simple ions, surfactants and paint polymers on pigment acid/base character. Because of the increasing importance of water base formulations, the dispersion of TiO_2 in water will be investigated in this study.

The term dispersion is used here to refer to the complete process of incorporating a powder into a liquid medium such that the final product consists of fine particles distributed throughout the medium. The dispersion process consists of three stages according Parfitt [1], which are quite distinct in their nature, but in practise they overlap. The three stages are:

1) wetting of the powder,
2) breaking up of clusters or disintegration and
3) dispersion stability.

The first two steps can be controlled mechanically by dispersion equipment and is also influenced by the particle size distribution, while stabilization can be controlled by surface chemistry.

Sedimentation behaviour is of considerable practical importance in dispersions because it gives a good indication of the state of dispersion. The sedimentation behaviour of a dispersion is dependant upon a number of factors, including the degree of dispersion and dispersion stability or in other words the prevention of flocculation during storage. Because of practical and instrumental reasons sedimentation will be used as a measurement for dispersion stability in this study.

For dispersions of solid particles in liquid media the primary cause of instability is flocculation in which particles under the influence of random motion come into close contact and form clusters. The function of the pigment coating is to assist in preventing this flocculation in addition to reduce the degree of cohesion.

At least three major types of interaction are involved in the approach of colloidal particles, namely;

1) the London-van der Waals force of attraction,
2) the Coulombic force associated with charged particles, and
3) the repulsive force arising from solvation, adsorbed layers etc.

A colloidal dispersion will in general be stable for a reasonable period, if interaction 2 and 3 exceeds 1 by such a factor that an energy barrier exists which is of magnitude, several orders higher than the thermal energy of the particles.

According to Entwistle [2] the dispersed particles will tend to flocculate under the action of London-van der Waals forces of attraction in the absence of repulsive forces. Dispersion stability can only be maintained if the pigment particles are separated sufficiently for the repulsive forces to exceed those of attraction. The same author proposed two mechanisms for stabilising dispersions:

1) Electrostatic repulsion due to the presence of charges on the particle surface,
2) Steric repulsion resulting from the adsorption of polymer chains on to the particle surface.

Electrostatic repulsion is mainly responsible for the stability of TiO_2 pigments which are

coated with inorganic oxides while steric repulsion creates stability when organics adsorb on the surface.

It has long been recognized that the zeta potential is a very good index of the magnitude of the repulsive interaction between colloidal particles [3] and measurements of zeta potential are commonly used to assess the stability of a colloidal sol. This will be discussed comprehensively in the next chapter.

4.1.2. PHOTO-ACTIVITY OF TiO_2 POWDERS

The surface of titania is capable of oxidizing or reducing a wide variety of adsorbed or contacted organic compounds when exposed to light having wavelengths of 300 to 400nm. This is particularly true for oxygen-containing organic molecules which commonly undergo dehydration, dehydrogenation, deoxygenation and self-disproportionation reactions. This result in a progressive loss of gloss and chalking, which is the destructive effect of TiO_2 on the binder in a paint medium. The photo-activity of TiO_2 is responsible for the breakdown of the polymer in a coating system and therefore the durability of the paint decreases.

When TiO_2 is irradiated, electrons are excited from the valence band to the conduction band, generating positive holes and free electrons. This is done by the conversion of light quanta into excited species. According Solomon [4] the energy gap between these bands in the rutile lattice is approximately 3.05eV, and 3.2eV in the anatase lattice. These energy levels correspond to light quanta having the respective wavelengths of 420 and 390nm. Light having wavelengths shorter than these critical values is absorbed with the formation of electron-hole pairs. These can dissociate into free, mobile holes and electrons. If the electrons and holes, which is free to move, reach the surface of the particle they are capable of forming hydroxy and perhydroxy radicals. These radicals are capable of breaking down organic binders. The reaction can be summarized as follow:

$$TiO_2 + hv \dashrightarrow e^- + [hole]^+$$

$$[hole]^+ + OH^- \dashrightarrow OH\cdot$$

$$e^- + O_2 \dashrightarrow O_2^-$$

$$O_2^- + H_2O \dashrightarrow OH^- + HO_2\cdot$$

$$3HO\cdot + 3HO_2\cdot + 2(-CH_2-) \dashrightarrow 2CO_2 + 5H_2O$$

According to Lewis [5] the rate of photochemical degradation is dependent on the following:

1. The wavelength of the incident radiation.
2. The intensity of the radiation.
3. The absorption characteristics of the binder.

To reduce the surface photo-activity the TiO_2 are treated with inorganic oxides. The durability of a paint is therefore related to the photo-activity of the pigment.

Durability is usually measured by the quality of loose pigment particles and according to Buxbaum [6] it may be determined by the Kempf, Adhesive Tape and Photographic methods. These methods use special equipment to simulate open-air weathering after the pigment is applied to a coating and judgement are often done visually. Because of the difficulties in these methods a new method had to be found to determine the photo-activity of TiO_2.

Nogueira and Jardim [7] investigated the photodegradation of methylene blue using solar light and TiO_2. Methylene blue can be mineralized according to the equation:

$$C_{16}H_{18}N_3SCl + 5.5O_2 \dashrightarrow HCL + H_2SO_4 + 3HNO_3 + 16CO_2 + 6H_2O$$

The extend of degradation can be monitored at 660nm with a spectrophotometer which gives a easier way to determine the photo-activity of TiO_2. Other organic materials like phenol, atrazine and propan-2-ol were also reported to act as indicator for the photo-activity of TiO_2 [8,9].

4.2. EXPERIMENTAL

4.2.1. MEASUREMENT OF DISPERSION STABILITY

Dispersion is a difficult property to be measured because of all the influencing factors. Sedimentation is one of the methods known to test the degree of dispersion and especially the stability of the pigment in binders and therefore the stability of treated TiO_2 is investigated in this study by sedimentation under gravity.

The samples (0.050g) were dispersed in 100 ml measuring cylinders filled to the 100ml mark with distilled water using a ultrasonic bath for 5 minutes. The dispersion was left on the shelf for 48 hours to settle. After two days a pipette was used to take off the uppermost 10ml of the dispersion. The absorption of the uppermost 10ml of the dispersions were measured on a Genesis spectrophotometer at 604nm.

4.2.2. MEASUREMENT OF PHOTO-ACTIVITY

Many pigments show typical colour or structural changes when subjected to intense radiation or weathering. The photo-activity or chalking resistance of TiO_2 is measured by using methylene blue. Treated TiO_2 samples (0.050g) were added to 25ml methylene blue (2×10^{-5}M) in a Petri dish and stirred with a glass tube to improve the dispersion. The samples were exposed to sunlight for 35 minutes at noon during the summer. The samples were centrifuged to separate the TiO_2 from solution and the adsorption at 660nm of the clear solutions were done on a Genesis spectrophotometer. Because the intensity of the sunlight is not always the same, all the samples were treated at the same time. All treated TiO_2 was in the rutile structure.

4.3. RESULTS AND DISCUSSION

4.3.1. DISPERSION STABILITY

4.3.1.1 *TiO_2 treated with inorganic oxides*

The influence of pH on the stability of TiO_2 can be seen in figure 4.1. The stability increased with the pH to a value of ± 9 from where the stability decreased. The stability at different pH values is a direct consequence of surface charge and will be discussed further in the next chapter.

Figure 4.1: The influence of pH on dispersion stability

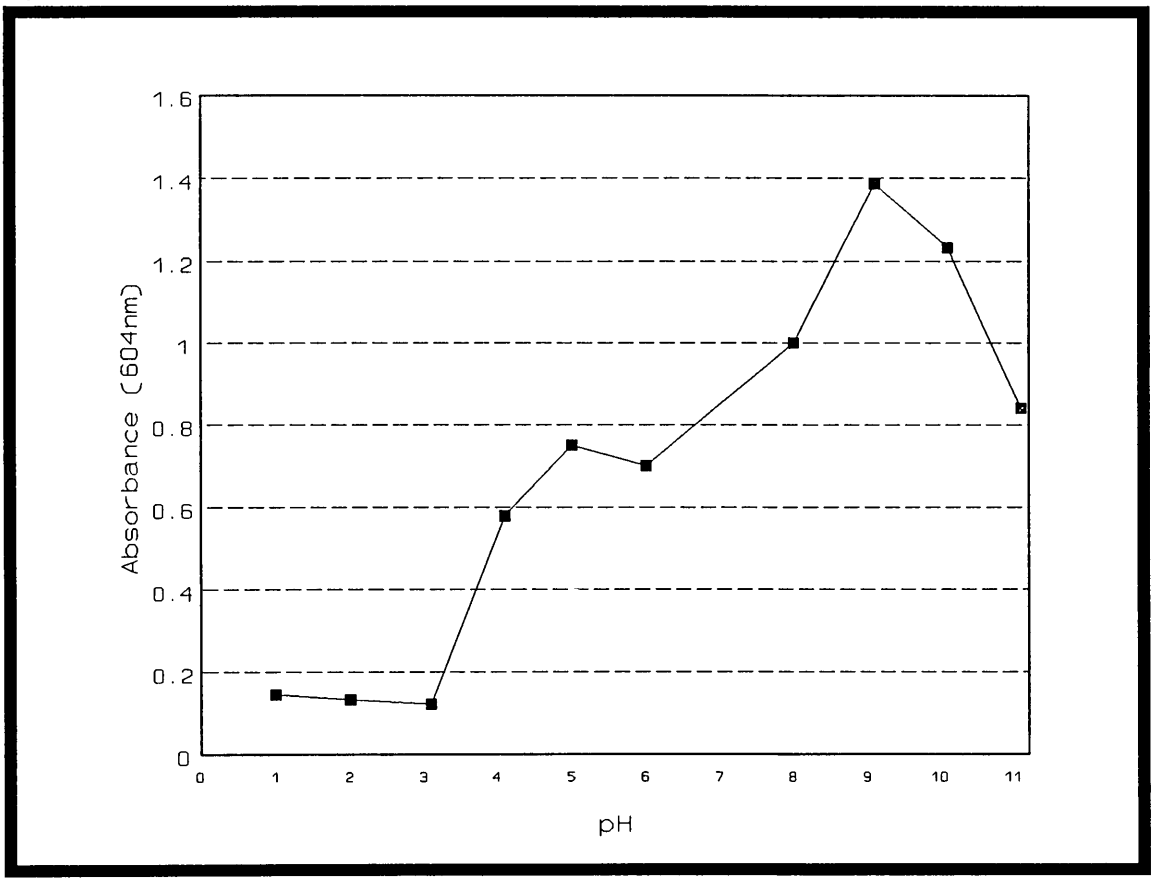

The absorbance, at 604nm, of the uppermost 10 ml for the TiO_2 samples can be seen in table 4.1. Different reagent concentrations do not seem to influence the stability of the treated TiO_2 dispersions, however the samples treated with SiO_2 were significant more stable than the samples treated with Al_2O_3 as seen in figure 4.2. This result agrees with those of Rechmann [10] who showed that the high silica pigments had good stability whilst the high alumina pigments all had equal instability in aqueous solutions. A reason might be the higher molecular mass of Al_2O_3 and more likely electrostatic forces which will be explained in the next chapter using zeta potential measurements.

Table 4.1 : Absorbance values for the sedimentation of inorganic treated TiO_2

Sample	SiO_2%	Al_2O_3%	Absor-bance	Sample	SiO_2%	Al_2O_3%	Absor-bance
Rutile	<0.2	<0.2	0.416	AS1	0.37	1.31	0.064
				AS2	0.39	2.37	0.233
S1	0.10	<0.2	0.595	AS3	1.17	2.90	0.087
S2	0.14	<0.2	0.462	AS4	0.77	0.74	0.459
S3	0.28	<0.2	0.630	AS5	0.52	0.79	0.421
S4	0.33	<0.2	0.789	AS6	0.80	0.58	0.819
S5	0.69	<0.2	0.657	AS7	0.36	0.58	0.770
S6	1.51	<0.2	0.813	AS8	1.49	1.11	0.581
				AS9	1.14	1.18	0.547
A1	<0.1	0.73	0.265	AS10	<0.2	0.67	0.112
A2	<0.1	1.25	0.057	AS11	0.29	0.65	0.114
A3	<0.1	2.39	0.311	AS12	0.75	0.73	0.569
A4	<0.2	3.25	0.353	AS13	0.71	0.58	0.545
A5	<0.1	0.37	0.263	AS14	0.35	0.29	0.868
A6	<0.1	0.33	0.287	AS15	0.29	0.83	0.070
A7	<0.2	0.48	0.206	AS16	0.44	0.82	0.247
A8	<0.1	0.29	0.138				
A9	<0.1	0.30	0.338				
A10	<0.1	0.31	0.292				

The influence of the SiO_2/Al_2O_3 weight ratio on the stability of the dispersions can be seen in figure 4.3. Again no linear relation can be found between the stability and the weight

ratio, but a significant increase in stability was observed when the weight ratio increased higher than 0.6.

Another interesting observation in figure 4.3 is the difference in stability for samples with more or less the same coating ratio especially when the following samples are compared: AS5 and AS7, AS13 and AS14, AS6 and AS8. The difference in stability might be due to the molecular mass of the alumina as stated previously because all the samples with lower stability have a higher percentage and therefore molecular mass of alumina on the surface.

Because electrostatic repulsion are responsible for the dispersion stability of inorganic treated TiO_2, the sedimentation behaviour will be explained in a later report using zeta potential measurements.

Figure 4.2: The influence of Si and Al on the dispersion stability

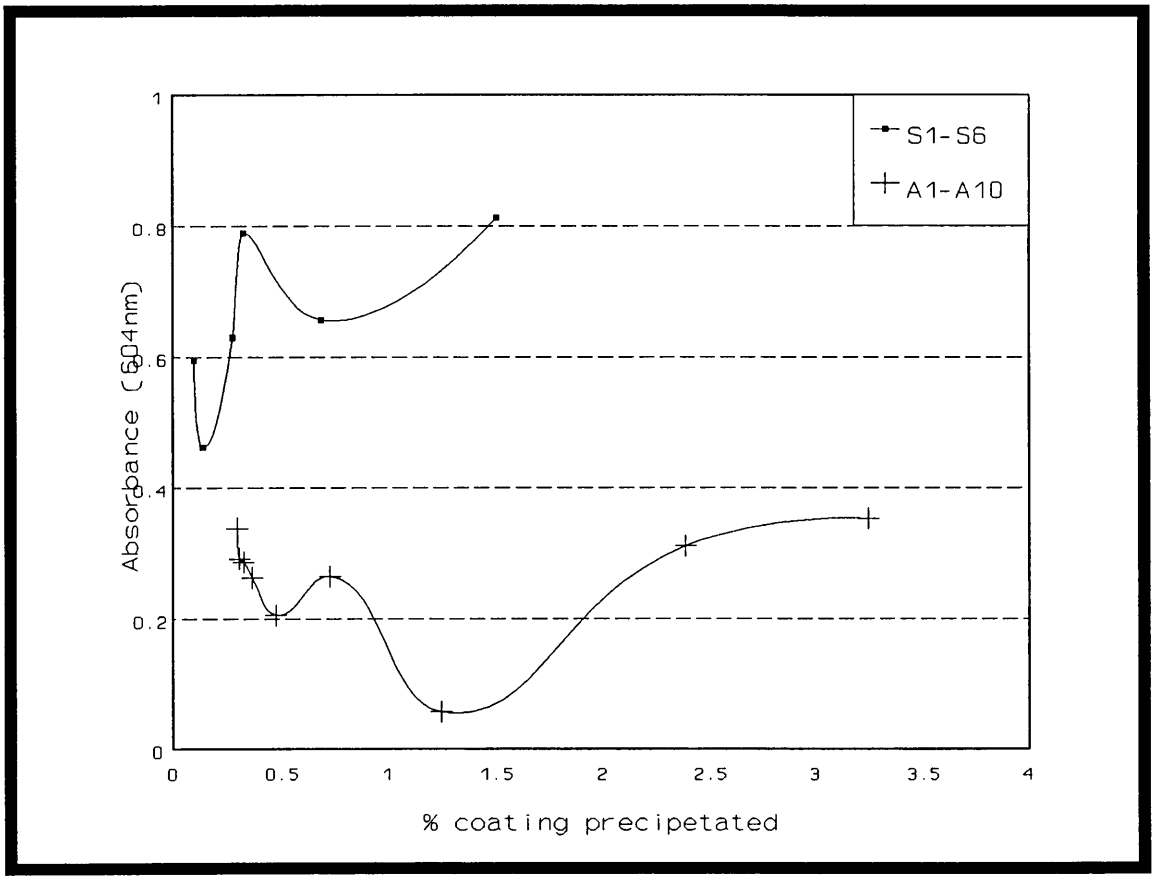

Figure 4.3: The influence of the Si/Al ratio on the dispersion stability

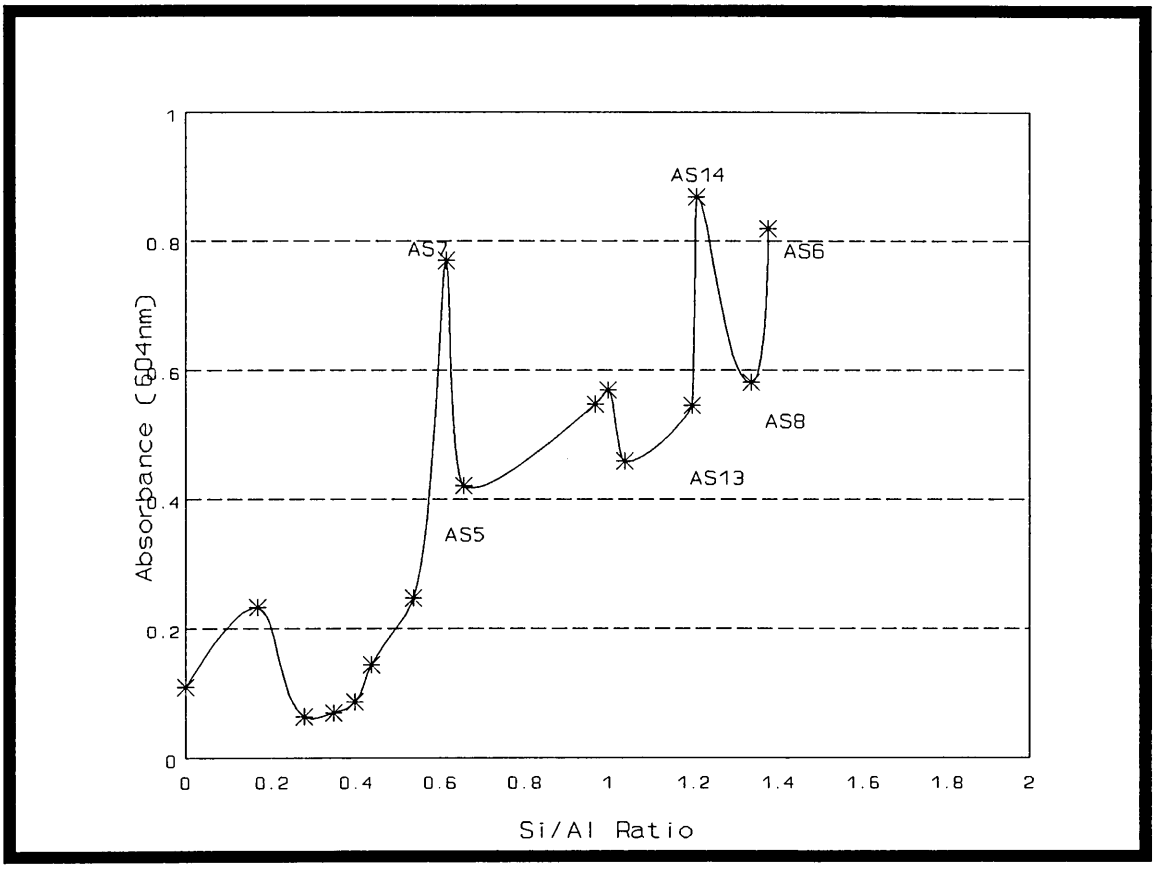

4.3.1.2 *TiO_2 treated with organic reagents*

The sedimentation values of the TiO_2 treated with organic reagents can be seen in table 4.2. The importance of steric stabilization can be seen in the high absorbance values for most of the organic treated samples compared with the inorganic treated samples in the previous section. As mentioned in section 4.1.1 the repulsive forces should exceed the attractive forces to provide a stable suspension and attractive forces only become active at small distances. When the particles collide, large organic molecules on the surface cause an increase in distance of approximately twice the thickness of the adsorbed layer. The attractive forces are therefore weakened and this is the reason why organic treated TiO_2 is more stable in a suspension compared to inorganic treated TiO_2. For some additives there is a significant difference in stability between the concentrations of the coating. This is because the colloidal

particles and the TiO_2 surface can be oppositely charged in certain cases, resulting in charge neutralisation associated with the adsorption of the additives, whereas at higher concentrations protection can result.

Table 4.2 : Absorbance values for the sedimentation of organic treated TiO_2

Sample	Organic agent	Absor-bance	Sample	Organic agent	Absor-bance
PEG.5	Polyethylene glycol	0.106	TEA.5	Triethanolamine	0.660
PEG1	"	0.522	TEA1	"	0.968
PEG3	"	0.438	TEA3	"	0.597
ED.5	Ethanediol	0.118	PET.5	Phenylethanol	0.663
ED1	"	0.319	PET1	"	0.692
ED3	"	0.434	PET3	"	0.904
PD.5	Propanediol(1,2)	0.540	EDA.5	Ethylene	0.762
PD1	"	0.318	EDA1	diamine	1.005
PD3	"	0.145	EDA3		0.445
AC.5	Acetic acid	0.093	DMA.5	Dimethylamine	0.485
AC1	"	0.397	DMA1	"	0.637
AC3	"	0.217	DMA3	"	0.624
ET.5	Ethanol	0.690	AM.5	Ammonia	0.661
ET1	"	0.302	AM1	"	0.405
ET3	"	0.735	AM3	"	0.771
PR.5	2-Propanol	0.378			
PR1	"	0.409			
PR3	"	0.556			

From these values it is also evident that the powders treated with an amine is more stable in a water solution than samples treated with an alcohol. This might be due to ester formation with the alcohol and the OH groups on the surface but can also occur with a dehydroxylated surface as proofed by Shchekochikhin [11]. Ester formation can take place between two different TiO_2 particles. The relative instability of samples treated with ethanediol, propanediol and acetic acid might be due to bridging where part of the adsorbed molecules are attached to a TiO_2 particle and the other part to a different particle. Therefore aggregation occurs and the dispersion is less stable. Amine solutions are alkaline which also enhances stabilization.

Because of the high dipole moment and slight ionization potential of amines, polyamines can serve as excellent dispersants. The samples treated with amines might be more stable due to interaction between the water and the adsorbed layer. This interaction can take place because of hydrogen bonding between the water and the amine. The hydrogen bonding creates structural viscosity. The involvement of hydrogen bonding will be investigated in chapter 6 with infrared spectroscopy. Conley [12] also proved the importance of amines as dispersants especially ethylene diamine because of the smaller possibility of surface chelation, which can occur with longer chain amines.

4.3.2. PHOTO DEGRADATION OF METHYLENE BLUE (MB)

The photo degradation of methylene blue (MB) by sunlight irradiation using rutile and anatase as photo catalyst are shown in figure 4.4. From these results it can be seen that MB was completely degraded by the sunlight in the presence of anatase after 30 minutes. As expected the photo degradation of MB in the presence of rutile is not as completed as in the presence of anatase. An early explanation, according to Solomon [4], was based on the observation that the Ti-O-Ti interatomic distances are smaller in the rutile lattice than those in anatase and this was equated with an existence of stronger bonds in rutile. The reasons for the quantitative differences between the photochemical activities of rutile and anatase are not readily apparent, and many of the published explanations are facile or contradictory but Diebold [13] offered a more accessible explanation. An important role of TiO_2 in most paints is binder protector by absorbing UV radiation and preventing direct degradation from occurring. Since anatase absorb less UV radiation than rutile, direct degradation is greater in anatase.

The photo degradation of methylene blue (MB) by sunlight and with different samples of TiO_2 as catalysis can be seen in table 4.3. The first sample represent the rutile which was used as starting material in the coating experiments. In the following samples the rutile was also used as catalysis but the pH was adjusted with HCl and NaOH to the indicated values. The influence of the pH on the photo-activity of TiO_2 is indicated in figure 4.5. At higher

pH values more hydroxyl ions adsorb on the surface and are therefore available to form more hydroxyl radicals and accelerate the degradation of the MB.

Figure 4.4: Degradation of MB with TiO_2 as catalysis

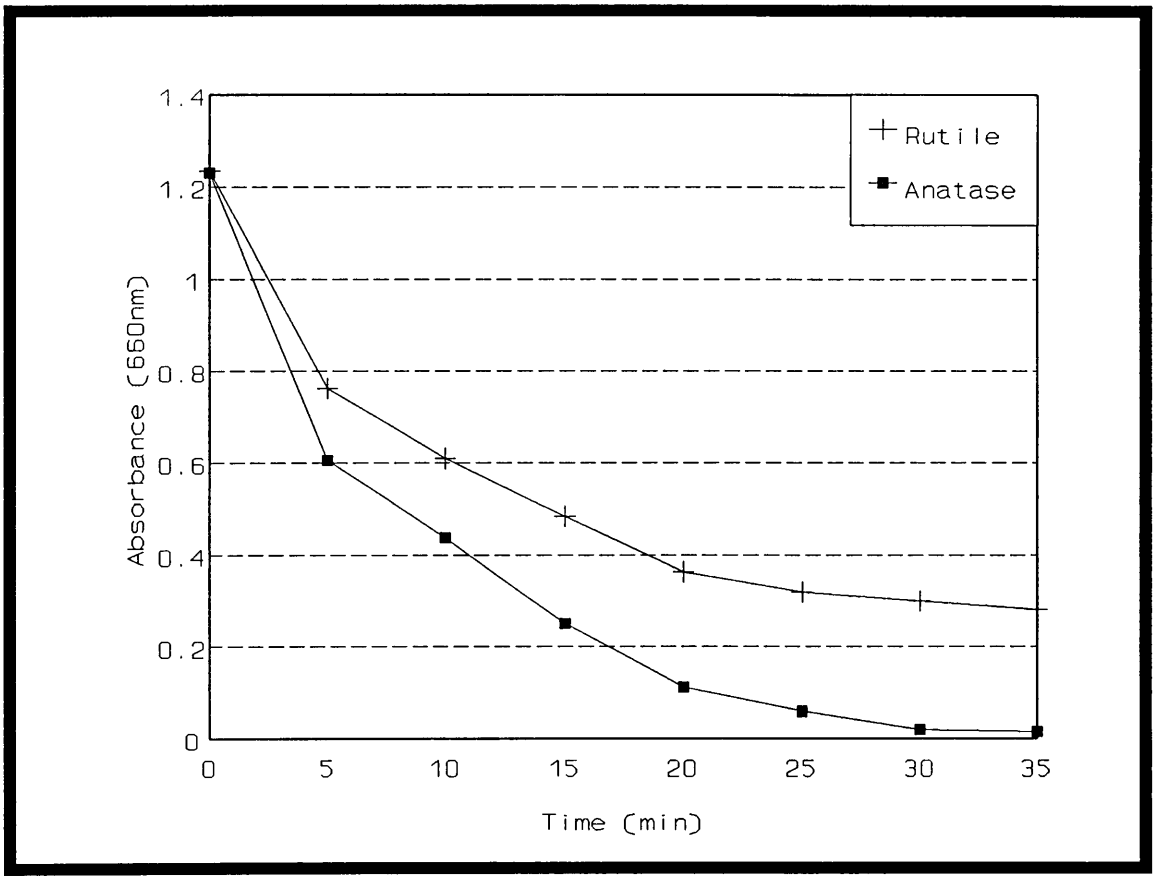

Also shown in table 4.3 is the absorbance value of the starting MB and MB exposed to sunlight for 35 minutes. Only a small deviation in colour occurred indicating the strong catalytic effect of TiO_2 on the degradation process. Although photo degradation can occur in the absence of TiO_2 it is of such small magnitude that it is beyond the scope of this study, which is intended to compare the different coated TiO_2.

TABLE 4.3 : Absorbance values for the degradation of MB

Sample	SiO_2%	Al_2O_3%	Absor-bance	Sample	SiO_2%	Al_2O_3%	Absor-bance
Rutile	<0.2	<0.2	0.282	AS1	0.37	1.31	0.974
pH 1			1.009	AS2	0.39	2.37	0.941
pH 2.6			0.836	AS3	1.17	2.90	0.977
pH 3.2			0.830	AS4	0.77	0.74	0.569
pH 8.8			0.084	AS5	0.52	0.79	0.797
pH 11			0.072	AS6	0.80	0.58	0.775
MB			1.246	AS7	0.36	0.58	1.004
MB (sun)			1.052	AS8	1.49	1.11	0.672
				AS9	1.14	1.18	0.796
S1	0.10	<0.2	0.147	AS10	<0.2	0.67	0.732
S2	0.14	<0.2	0.198	AS11	0.29	0.65	0.865
S3	0.28	<0.2	0.199	AS12	0.75	0.73	0.862
S4	0.33	<0.2	0.145	AS13	0.71	0.58	0.778
S5	0.69	<0.2	0.138	AS14	0.35	0.29	0.238
S6	1.51	<0.2	0.166	AS15	0.29	0.83	0.801
				AS16	0.44	0.82	0.427
A1	<0.1	0.73	0.511				
A2	<0.1	1.25	0.913				
A3	<0.1	2.39	1.034				
A4	<0.2	3.25	1.052				
A5	<0.1	0.37	0.629				
A6	<0.1	0.33	0.627				
A7	<0.2	0.48	0.620				
A8	<0.1	0.29	0.670				
A9	<0.1	0.30	0.637				
A10	<0.1	0.31	0.669				

The results for the A and S samples, indicating the effect of SiO_2 and Al_2O_3 treatment, can be seen in figure 4.6. It is evident that the TiO_2 treated with SiO_2 is much more photoactive than those treated with Al_2O_3 and even more reactive than untreated TiO_2. This is an interesting result because SiO_2 is expected to isolate the TiO_2 particle to some extend from the MB and prevent photo degradation. Diebold [13] stated that silica is the only barrier coating capable of the highest levels of durability. The increase in photo-activity for the

samples treated with SiO_2 compared to untreated TiO_2 might be due to the increased adsorption of MB on SiO_2 as discussed by Anderson and Bart [14].

Figure 4.5: The influence of pH on the degradation of MB

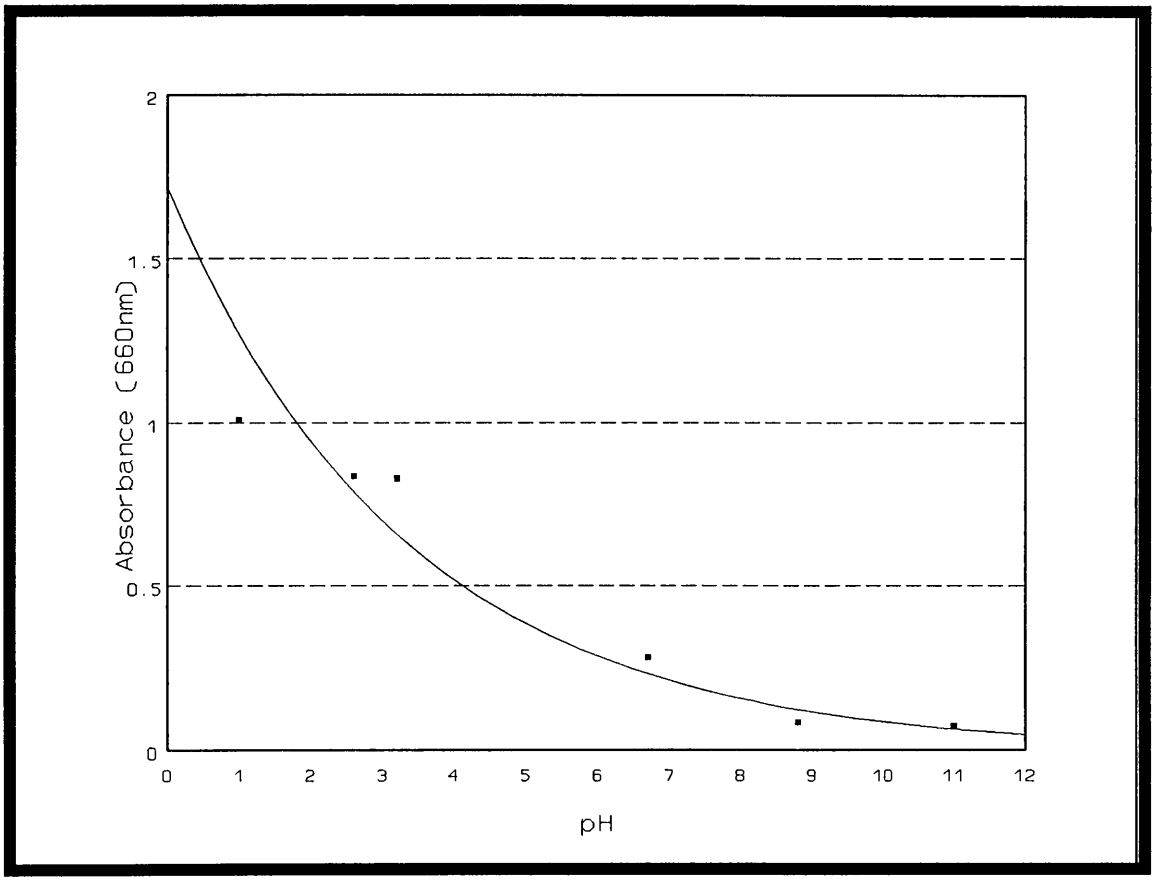

MB adsorbed on the SiO_2 surface bring the MB more in contact with the hydroxyl radicals and therefore the degradation increased. The better dispersion stability of SiO_2 treated samples might also be a reason for the increased photo-activity because a better dispersion bring the MB more in contact with the TiO_2 surface. This was proved by dispersing the rutile to different extends, first using a ultrasonic bath and secondly the rutile was added without stirring. The sample dispersed in a ultrasonic bath gave an absorbance of 0.183 and the absorbance value for the un-stirred sample was 0.297. This proofs that the state of

Figure 4.6: Influence of Si and Al on the degradation of MB

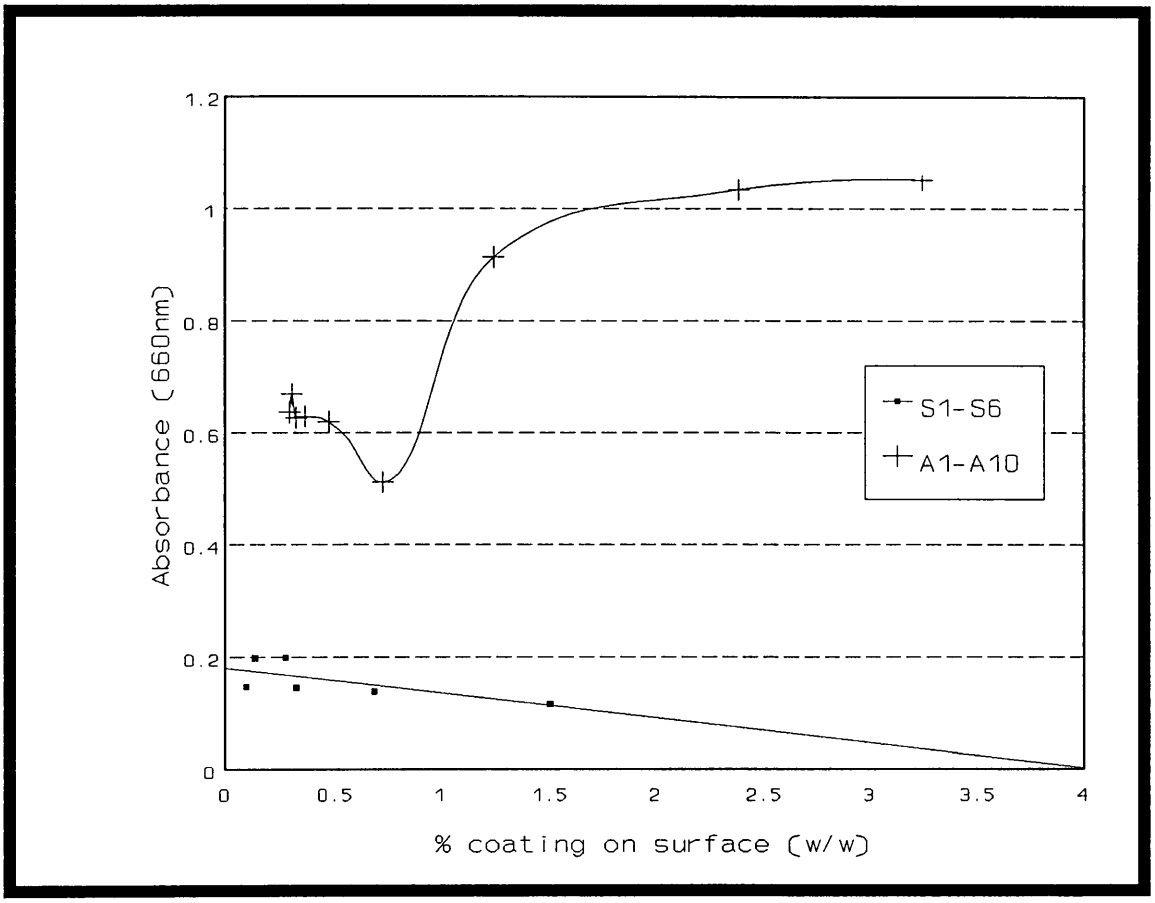

dispersion can influence the photo-activity of TiO_2 although to a lesser extend. Anderson et al [14] also showed an increased photo-activity for SiO_2 treated samples and argued that the increase can partly be attributed to an increased surface area but most probably due to the preferential adsorbance on SiO_2.

The TiO_2 treated with Al_2O_3 is less reactive than the untreated TiO_2 because the alumina acts as a strong electron acceptor on the surface and prevent the formation of hydroxyl radicals. Al_2O_3 acts as a physical barrier over the TiO_2 surface and this prevent the electron holes to move to the surface.

The samples treated with more than 1% Al_2O_3 gave the best durability and a reason for this

might be that the TiO_2 surface is not completely covered at low percentages allowing the formation of hydroxyl radicals. When the surface is covered, higher percentages of alumina does not seem to improve the durability. According Diebold [13] 0.3-0.4% coating is sufficient to make a coating layer of just one atom thick and electron holes can tunnel through thin oxide layers. This explains the sharp increase observed in figure 4.6 at surface coatings higher than 1%.

The results for the AS samples can be seen in figure 4.7 where the silica-alumina ratio is plotted against the absorbance values. Although the samples with a high Si/Al ratio gave a much better durability than the samples treated with silica only, the silica content still resulted in a decrease in durability. It can be concluded that TiO_2 coated with more than one percentage alumina will have good durability and the percentage silica in the coating will determine to which extend this durability decreases.

Figure 4.7: The influence of the Si/Al ratio on the degradation of MB

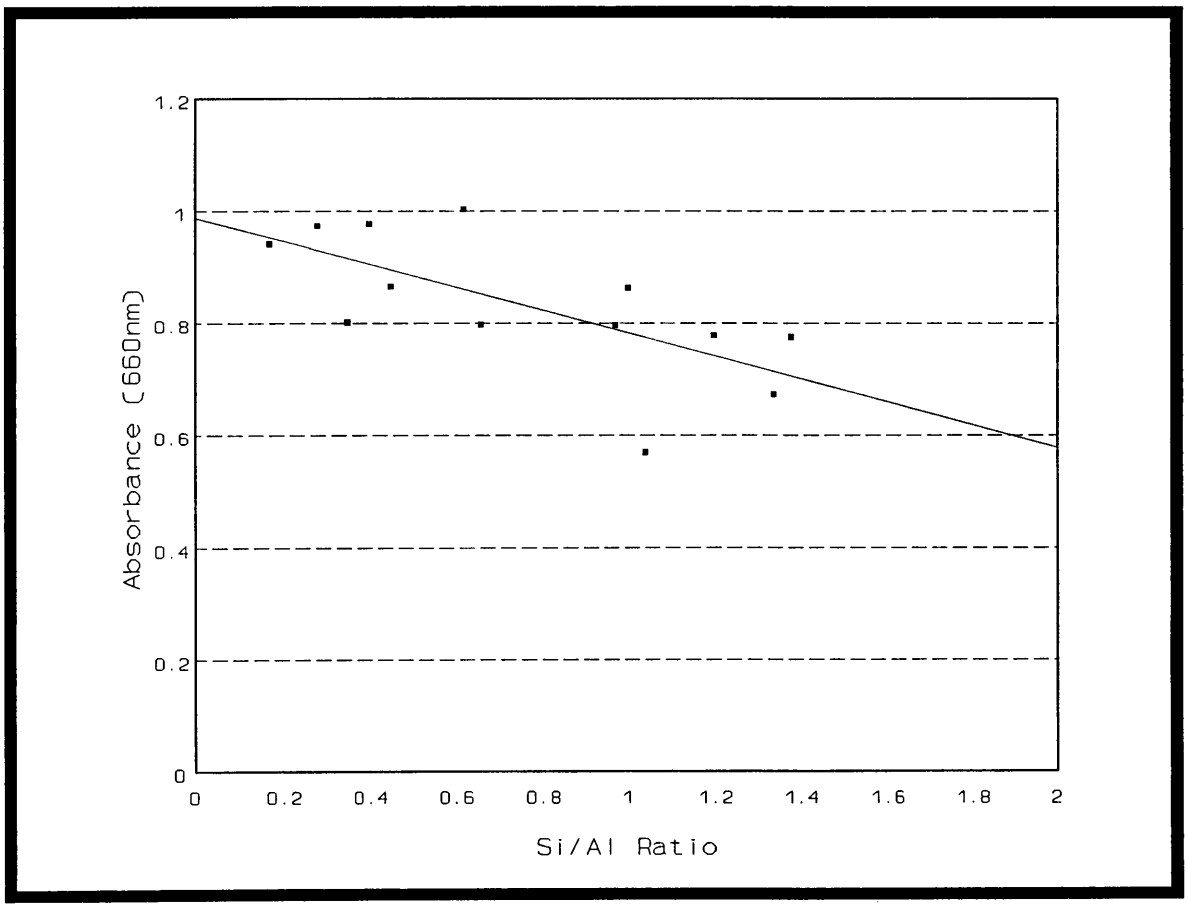

4.4. CONCLUSION

Good dispersion and durability are two important qualities in the TiO_2 pigment industry. These qualities can be controlled by coating the pigment with organic and inorganic materials. It is a difficult matter to quantify the effectiveness of the coating. In this study the surface treatment of TiO_2 was evaluated by firstly using sedimentation under gravity to give an indication of the dispersion stability and secondly the degradation of methylene blue was used to measure the photo-activity.

The pH of the solution had a big influence on both the dispersion stability and photo-activity of TiO_2. Lower pH values gave a low photo-activity and poor dispersion stability, while at pH values higher than 3 the dispersion stability improved, but pH values higher than 5 showed high photo-activity.

Silica treated samples gave a good dispersion stability and a high photo-activity and the percentage precipitated did not have a significant influence on these qualities. Alumina treated samples on the other hand gave poor stability and low photo-activity especially at coating percentages higher than one. The reason for the low photo-activity is because alumina act as a strong electron acceptor on the surface and prevent the formation of hydroxyl radicals, while it is expected that methylene blue adsorbs more on silica treated samples which bring the molecules in closer contact with the hydroxyl radicals. The better dispersion stability of silica treated samples is because of electrostatic forces and will be explained in the next chapter.

TiO_2 treated with mixtures of silica and alumina showed improved qualities. Good dispersion stability was observed with a Si/Al ratio higher than 0.6 but at this ratio the molecular mass of alumina had an effect on the stability. Higher Si/Al ratio's resulted in a slight increase in photo-activity.

The importance of steric stabilization was proved by the good dispersion stability of the samples treated an amine. It is expected that this might be due to hydrogen bonding which created structural viscosity but this will be investigated further in chapter 6.

For optimum durability and dispersion stability it is therefore suggested that TiO_2 is treated with a mixture of silica and alumina and preferably with a Si/Al ratio between 0.7 and 1. Additional treatment with an amine will increase the dispersion stability. The importance of surface treatment to improve the quality of TiO_2 pigments is clearly visible from these results.

4.5. REFERENCES

1. Parfitt, G.D. 1974. Dispersion of Powders in Liquids. Second Edition. Applied Science Publishers. London.

2. Entwistle, T. 1986. Titanium Dioxide for surface Coatings. In *Surface Coatings-2*. p183.

3. Tuorilla, P. 1928. Kolloid-Beith. **27**, 44.

4. Solomon, D.H. Hawthorne, D.G. 1983. *Chemistry of Pigments and Fillers*. New York en Brisbane: John Wiley & Sons.

5. Lewis, P.A. 1993. *Pigment Handbook*. Second Edition. Volume 1, 22.

6. Buxbaum, G. 1993. *Industrial Inorganic Pigments*. VCH Weinheim

7. Nogueira, R.F.P.Jardim, W.F. 1993. Photodegradation of Methylene Blue. *Journal of Chemical Education*, 70(10), October, p861-862

8. Pelizzetti, E. Minero, C. Borgarello, E. Tinucci, L. Serpone, N. 1993. Photocatalytic Activity and Selectivity of Titania Colloids and Particles Prepared by the Sol-Gel Technique. *Langmuir*. 9, 2995-3001.

9. Parfitt, G.D. 1980. The role of the Surface in the Behaviour of Titanium Dioxide Pigments. *Croatica Chemica Acta*. 53(2), 333-339.

10. Rechmann, H. 1969. *Farbe und Lack*. 75, p51.

11. Shchekochikhin, Y.M., Tilimonov, V.M., Keier, N.P and Teremin, A.N. 1964. *Kinetika i Kataliz*. 5, 113.

12. Conley, R.F. 1974. Design, Functionality, and Efficiency of Pigment Dispersants in Water-Base Systems. *Journal of Paint Technology*. 46(594), 51-64.

13. Diebold, M.P. 1995. The Causes and Prevention of Titanium Dioxide Photodegradation of Paints. Part 2. *Surface Coatings International*. 7, 294-299.

14. Anderson, C. Bard, A.J. 1995. An Improved Photocatalyst of TiO_2/SiO_2 Prepared by Sol-Gel Synthesis. *Journal of Physical Chemistry*. 99, 9882-9885.

CHAPTER 5

Zeta Potential of TiO_2 Powders

CHAPTER 5

ZETA POTENTIAL OF TiO_2 POWDERS

5.1. INTRODUCTION

5.1.1. Origin and classification of electrokinetic effects

When two phases are placed in contact with one another,generally speaking, a difference in potential develops between them. If one of the phases is a polar liquid, like water, its molecules will tend to be oriented in a particular direction at the interface and this will generate a potential difference. If there are ions in one or both phases there will be a tendency for the electric charges to distribute themselves in a non-uniform way at the interface. An imaginary surface, the surface of shear, is considered to lie close to the solid surface and within which the fluid is stationary. A potential difference can also be created when charged colloidal particles eg. TiO_2 , are allowed to settle through a fluid under gravity or in a centrifugal field and this is known as the sedimentation potential.

Many important properties of colloidal systems are determined directly or indirectly by the electrical charge on the particles. According to Hunter [1] the potential distribution itself determines the interaction energy between the particles, and this is in many cases responsible for the stability of particles towards coagulation and for many aspects of the flow behaviour of the colloidal suspension.

Hunter [1] suggested that the four most important mechanisms which give rise to the spontaneous separation of charge between two phases in contact are:

(1) differences in the affinity of the two phases for electrons,
(2) differences in the affinity of the two phases for ions of one charge or the other,
(3) ionization of surface groups and
(4) physical entrapment of non-mobile charge in one phase.

Mechanism (3) is commonly observed with oxide surfaces where the degree of charge development depends on the pH of the solution and the behaviour is very much like mechanism (2) with H^+ and OH^- behaving as potential-determining ions. TiO_2 surfaces possess a large number of amphoteric hydroxyl groups which can undergo reaction with either H^+ or OH^- depending on the pH:

$$-O\text{-}MOH_2^+ \overset{H^+}{\longleftrightarrow} O\text{-}M\text{-}OH \overset{OH^-}{\longleftrightarrow} -O\text{-}M(OH)^-_2 \quad (1)$$

This equation is widely accepted as the charging mechanism of oxide surfaces [2,3]. The point where these two equations are in equilibrium represent the iso-electric point. However Morrison [4] gave a different mechanism:

$$-O\text{-}M\text{-}OH + OH^- \overset{K_1}{\longleftrightarrow} -O\text{-}M\text{-}O^- + H_2O \quad (2)$$

$$-O\text{-}M\text{-}OH + H^+ \overset{K_2}{\longleftrightarrow} -O\text{-}MOH_2^+ \quad (3)$$

According to Morrison the adsorption of univalent simple ions, except protons, can only decrease stabilization and the nett effect will be to reduce the charge. . The following equations illustrate the surface chemistry involved:

$$M\text{-}O^- + C^+ \longleftrightarrow MOC \quad (4)$$

$$MOH_2^+ + A^- \longleftrightarrow MOH_2A \quad (5)$$

Multivalent ions (e.g. phosphate) can cause charge reversal because they carry multiple charge:

$$MOH_2^+ + A^{n-} \longleftrightarrow MOH_2A^{(n-1)-} \quad (6)$$

Morrison also stated that if the metal atom has a high positive charge density , the surface hydroxyls will be acidic and vice versa. Silica which is a plus four cation and has a small ionic radius is very acidic while alumina contains a plus three cation and a large ionic radius and is therefore basic.

The point of zero charge (p.z.c.) is the average of the two pK's for equation (2) and (3) $pzc = (pK_1 + pK_2)/2$ and represent the average acid/base character of the surface.

5.1.2. Zeta potential and its applications

The potential yielded by any of the electrokinetic effects is referred to as the zeta potential and will be expected to be the potential at the surface of shear between the phases in relative motion. For all oxides there exist a particular bulk concentration of potential-determing ions for which the surface charge is zero and this condition is termed the point of zero charge (p.z.c.). There is another point which may or may not be coincident with the p.z.c. and this is the point at which the potential-determing ion concentration has been adjusted to make the zeta potential zero; this is called the isoelectric point (i.e.p). For all practical reasons the p.c.z. and the i.e.p. will be considered as the same point in this study.

Huter [1] showed that potential-determing ions can be regarded as specifically adsorbed and do not affect the p.z.c. but can reverse the sign of the zeta potential. A chemisorbed ion, on the other hand, shifts the p.z.c. and can remain adsorbed even when the underlying surface has the same sign as itself.

Zeta potential has long been recognized as a very good index of the magnitude of the repulsive interaction between colloidal particles and measurements of zeta potential are commonly used to assess the stability of a colloidal sol [5]. If stability is caused by the particle charge, the repulsion force depends on the degree of double layer overlap. The behaviour of marginally stable sols has been studied by Wiese and Healy [6]. They found that rapid coagulation occurs in all cases (including TiO_2) at an absolute value of 14 ± 4 mV for the zeta potential.

Pigments with good dispersion and dispersion stability are preferred in industry due to high optical performance, durability and long storage stability. The dispersion stability of the treated TiO_2 was tested in the previous report by a sedimentation technique. The surface charge of the pigments offers a widely acceptable explanation for the stabilities of slurries in waterbase systems. The surface chemistry of the pigments determine the value and sign of the charge.

5.2. EXPERIMENTAL

Treated samples as discussed in chapter 2 were used for measurements. The Zeta potential measurements were done on a Zetasizer 4 instrument. Samples were dispersed in 0.005M $NaClO_4$ solutions using a ultrasonic bath. pH adjustments were done with 6M HCl and NaOH solutions.

5.3. RESULTS AND DISCUSSION

5.3.1. ZETA POTENTIAL MEASUREMENTS AT pH 7.

Zeta potential values of treated TiO_2 pigments at pH 7 are reported in table 5.1. As a reference the coating materials were precipitated in the absence of TiO_2, in the same way as the surface treatments, as silica and alumina using the indicated starting material. From these samples it can be seen that the zeta potential of all alumina samples gave positive values indicating an i.e.p. higher than pH 7 while silica and titania samples gave negative values indicating an i.e.p lower than pH 7. The sign of the zeta potential for these oxides can be explained by the model suggested by Morrison [4] as discussed in section 5.1.1. Silica and titania are both plus four cations with relative small ionic radiuses and therefore the surface hydroxyls are acidic. This suggests that hydrogen will move into solution from the surface when the oxide is dispersed in a aqueous solution leaving behind a negatively charged surface. The opposite accounts for alumina.

Treatment of TiO_2 with SiO_2 resulted in more negative zeta potential values than untreated rutile and treatment with Al_2O_3 gave more positive values. These results agree with those reported by Mäkinen [7]. A relation between the zeta potential and the percentage of coating on the surface seems to exist only at low percentages. This is shown in figure 5.1 where the zeta potential of samples S1-S6 and A1-A4 are plotted against the percentage of silica or alumina precipitated on the surface. The zeta potential at zero percentage precipitated is that of rutile. Treatment of TiO_2 with increasing percentages of alumina resulted in a steady increase in zeta potential up to 1.5% coating from where the zeta potential stabilised. Silica treatment resulted in more negative zeta potential values. Samples S5 and S6 gave less

negative values than the trend predicted from the previous samples.

The trend observed here for both silica and alumina is due to incomplete coverage on the surface. At low concentrations the surface is not completely covered by the coating and the charge is mainly determined by the TiO_2 surface. But when the percentage of coating increases, a larger part of the surface is covered and the influence of the coating on the charge increases until the surface is completely covered.

TABLE 5.1 : Zeta potential measurements of treated TiO_2 at a pH of 7

Sample	SiO_2%	Al_2O_3%	Zeta Potential	Sample	SiO_2%	Al_2O_3%	Zeta Potential
Na_2SiO_3			-38.7	AS1	0.37	1.31	-28.22
$NaAlO_2$			+40.6	AS2	0.39	2.37	- 1.06
$Al_2(SO_4)_3$			+20.4	AS3	1.17	2.90	-27.55
$AlCl_3$			+30.8	AS4	0.77	0.74	-51.44
				AS5	0.52	0.79	-33.44
Rutile	<0.2	<0.2	-50.94	AS6	0.80	0.58	-62.17
				AS7	0.36	0.58	-38.06
S1	0.10	<0.2	-52.58	AS8	1.49	1.11	-62.65
S2	0.14	<0.2	-55.63	AS9	1.14	1.18	-53.23
S3	0.28	<0.2	-64.52	AS10	<0.2	0.67	-39.25
S4	0.33	<0.2	-66.62	AS11	0.29	0.65	-34.35
S5	0.69	<0.2	-59.47	AS12	0.75	0.73	-45.54
S6	1.51	<0.2	-61.69	AS13	0.71	0.58	-53.49
				AS14	0.35	0.29	-52.14
A1	<0.1	0.73	-37.59	AS15	0.29	0.83	+ 0.77
A2	<0.1	1.25	- 3.06	AS16	0.44	0.82	-29.41
A3	<0.1	2.39	+10.95				
A4	<0.2	3.25	+ 7.34				
A5	<0.1	0.37	-29.79				
A6	<0.1	0.33	-28.12				
A7	<0.2	0.48	-29.51				
A8	<0.1	0.29	-36.31				
A9	<0.1	0.30	-31.96				
A10	<0.1	0.31	-29.87				

The interesting relationship between the silica/alumina ratio and the zeta potential can be observed in figure 5.2. A linear relationship clearly exist between the silica/alumina ratio and zeta potential of the samples treated with both this surface agents. Higher silica percentages resulted in more negative zeta potential values, indicating a silica-like surface, while excess alumina on the surface did not result in a fully alumina-like surface. This result agrees with those of Parfitt and Ramsbotham [8] who explained this observation by the adsorption of stearic acid (co-ordinate bonding to Lewis sites) and stearylamine (ionic adsorption on hydrated Brönsted sites). The occurrence of Brönsted acidity for high alumina surfaces indicated a mixed oxide surface with aluminium associated with silicon atoms rather than a pure alumina-like surface, which would only exhibit Lewis acidity. This explanation also correlates with the conclusion made in chapter 2 that coating of TiO_2 with alumina and silica simultaneously resulted in an alumino-silica intermolecular mixture.

Figure 5.1: Relation between % surface agent and zeta potential

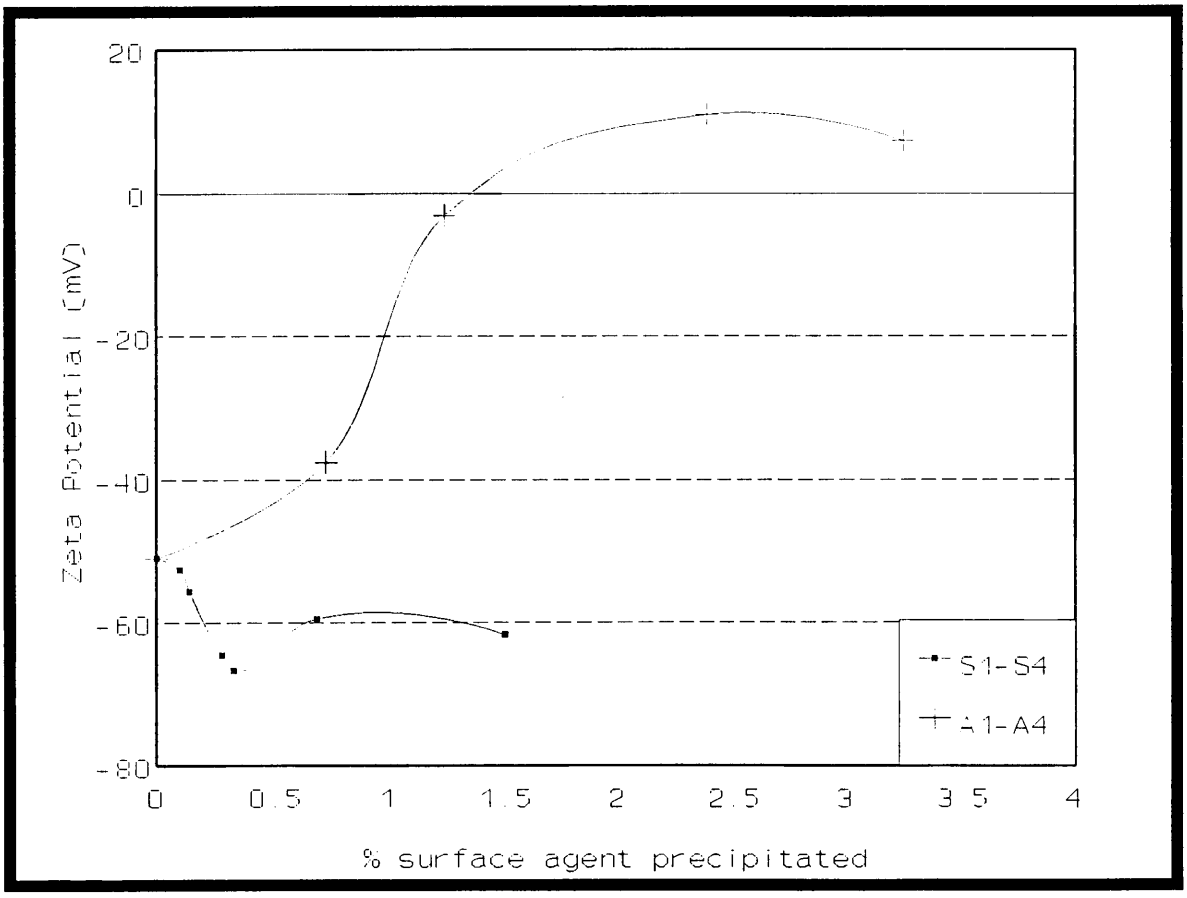

Figure 5.2: Si/Al Ratio versus zeta potential

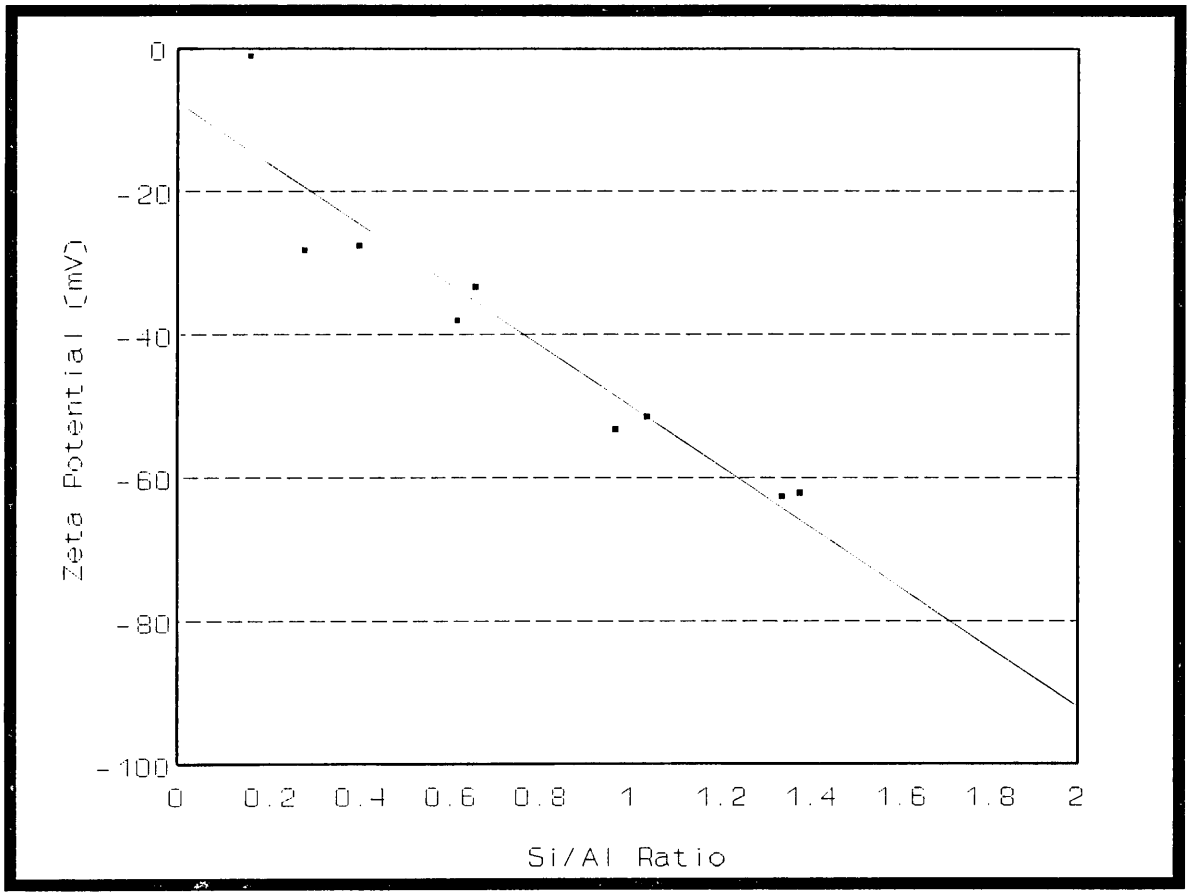

Because the zeta potential for silica is constant at pH 7, it is expected that the linear relation will hold up to a certain percentage from where it will stay constant.

Further proof for the mixed oxide coating can also be found in the fact that alumina only treated samples (A1-A10) resulted in alumina-like surfaces for high alumina percentages. The influence of silica on the zeta potential in a silica-alumina coating can be seen in figure 5.3. Only for a very low silica content in the coating, the zeta potential becomes positive, indicating a true alumina surface. Higher silica percentages in the coating result in a silica-like surfaces which is also proof of silica-alumina intermolecular mixture on the surface.

Figure 5.3: The influence of silica on the zeta potential in a mixed coating

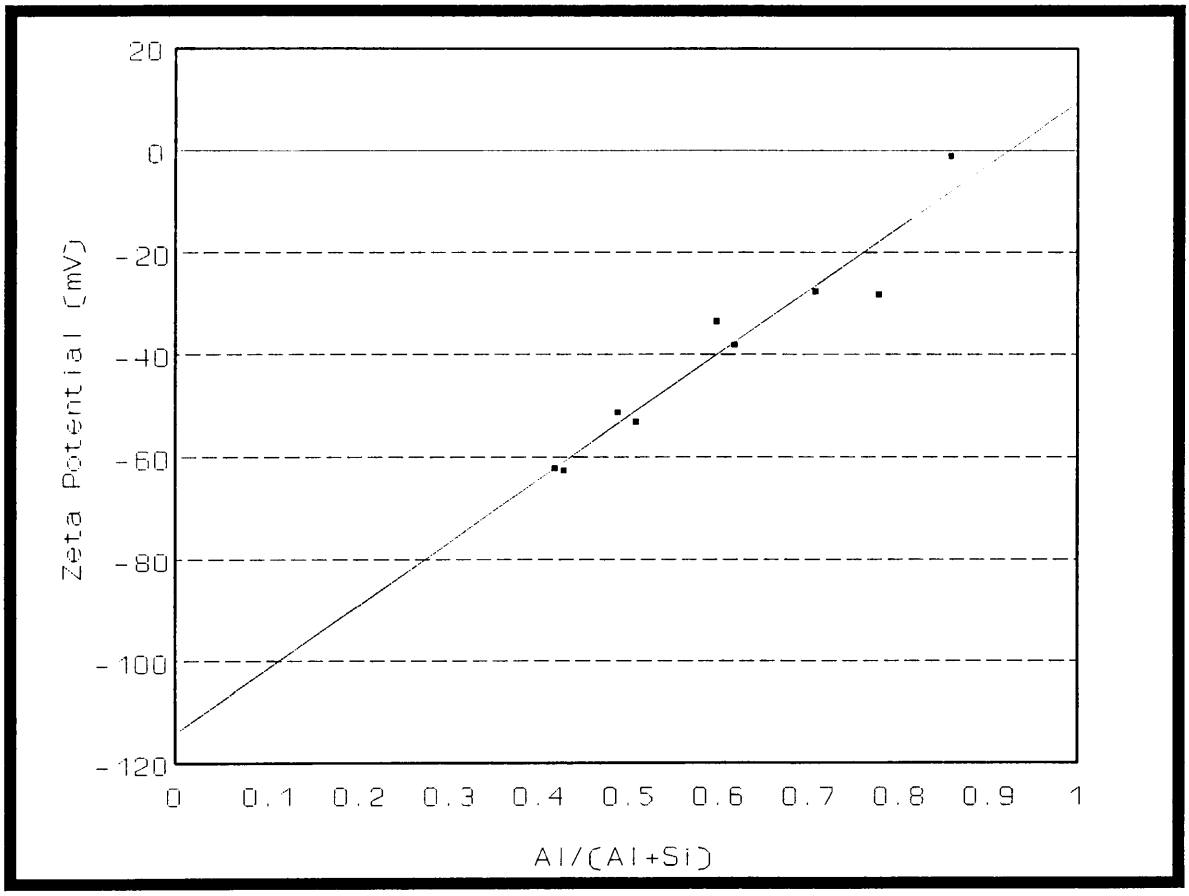

5.3.2. ISO-ELECTRIC POINT OF SAMPLES.

The dramatic effect that pH exerts on the zeta potential indicates that H^+ and OH^- are potential-determining ions in this system. In figure 5.4 the influence of the coating on the zeta potential of TiO_2 is clearly visible at different pH values. Silica treatment shifts the i.e.p. to lower values and an alumina coating resulted in a higher i.e.p. According Huter [1] this is an indication that the coatings are chemically adsorbed on the surface. The i.e.p. of the rutile sample is approximately at pH 2.6 which is lower than the pH 4.5-6.0 reported by Parks [2] and this might be due to different manufacturing processes. The lower i.e.p.

also gives an indication that the surface might be contaminated with different ions. The same author also reported the i.e.p. of alumina to be at pH 8.5-9.5 and the i.e.p. of silica between pH 1-2.

Surface treatment with alumina moved the i.e.p. 3.1 pH units up to pH 5.7, indicating an alumina-like surface, while treatment with silica moved the i.e.p. downwards to pH 2.3.

Figure 5.4: The iso-electric point of treated TiO_2

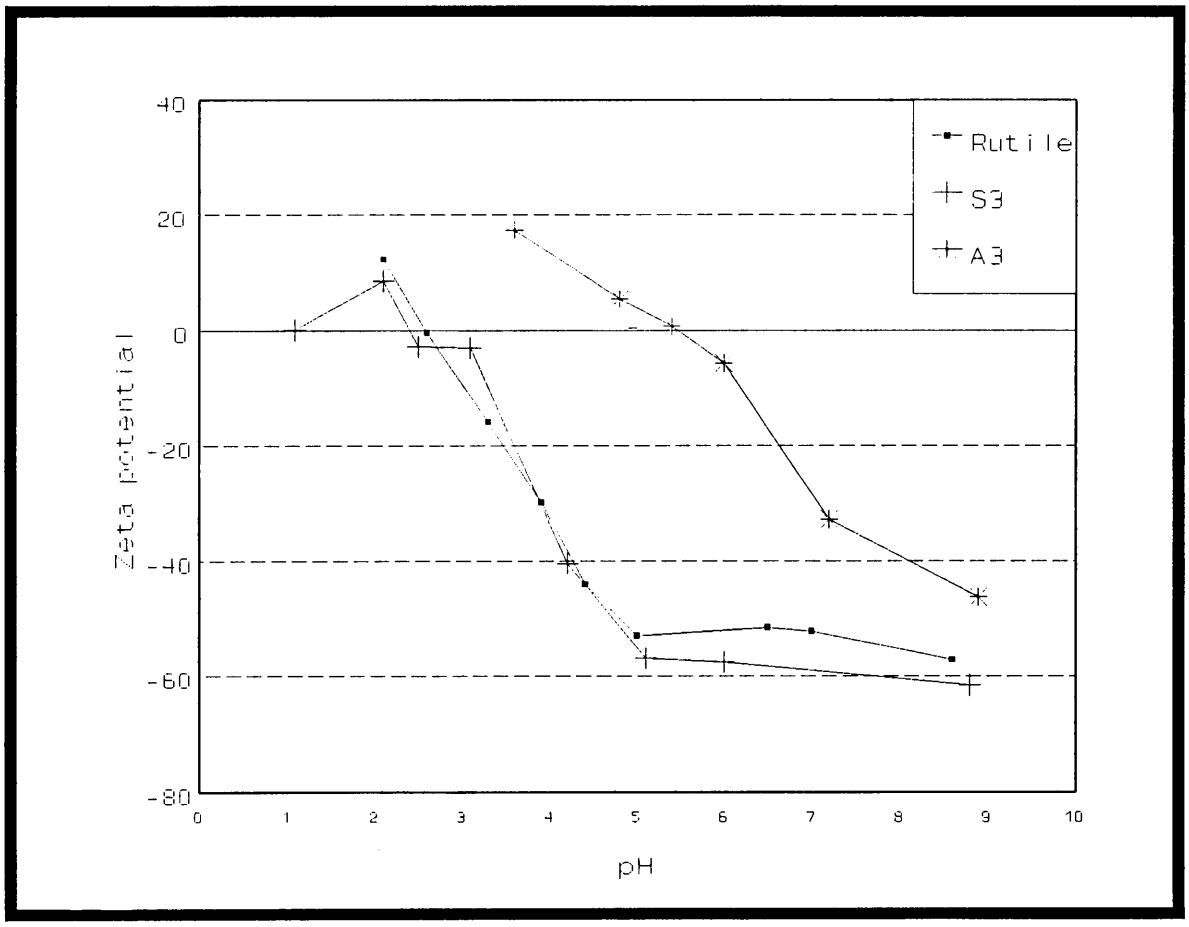

From these results it can be concluded that silica surfaces is more acidic than those of TiO_2 and alumina surfaces is more basic because the i.e.p. of silica surfaces were more negative than those of alumina and titania.

5.3.2. THE INFLUENCE OF ZETA POTENTIAL ON SURFACE TREATMENT

In chapter 2 the statement was made that the zeta potential plays an important role in the precipitation of oxides on TiO_2.

The i.e.p. of TiO_2 used in these experiments is at pH 2.6 and therefore the zeta potential is negative over a large pH range. The i.e.p. reported by Parks [2] is between pH 1 and 2 for silica and between pH 8.5 and 9.5 for alumina. This means that the zeta potential for silica is like TiO_2 negative over a large pH range while the zeta potential for alumina is positive over a large pH range.

When sodium aluminate or sodium silicate is used as starting material and added to a TiO_2 dispersion the pH increases from 6.5 to 11. At this pH the zeta potential for silica, alumina and titania is negative and therefore the repulsion forces between the particles are high. When the pH drops the silica and alumina start to precipitate and because of electrostatic forces on the surface of TiO_2, the colloidal particles start to grow on the surface. This is why the yield of the alumina precipitation is the highest at a pH of 8. At this pH, which is close to the i.e.p. of alumina, the zeta potential on the alumina is positive and electric attraction occurs between the TiO_2 surface and the Al_2O_3 particles.

The precipitation of SiO_2 on the surface can be explained by the fact that the TiO_2 surface consists of both positively and negatively charged sites. The measured zeta potential gives the net charge, which allows some positive sites to exist above the i.e.p. and electrostatic interaction between these sites and the negative sites on SiO_2 causes silica to adsorb on the surface.

When both surface agents are added simultaneously the pH also increases to 11 creating a negative zeta potential. In chapter 2 it was shown that in sample A4 alumina immediately adsorbs on the surface and at a pH 10 more than one percent already precipitated on the surface. This small percentage precipitation is enough to create some positive sites on the surface which will enhance the precipitation of silica. This might be one of the reasons for the higher yield in the silica precipitation when both surface agents are added compared to silica only. Silica then precipitates completely to form a alumino-silica intermolecular mixture followed by additional alumina precipitation. The conclusion that the precipitation of silica

is complete before that of alumina correlates with the results obtained by Mäkinen [7] who proved that no difference exist in the i.e.p. of samples treated with silica and alumina simultaneously compared to samples where alumina is precipitated on a layer coating of silica.

5.3.3. ZETA POTENTIAL AND COLLOID STABILITY

TiO_2 pigments are widely used in various aqueous and non-aqueous applications, where their good dispersion and dispersion stability are appreciated due to high optical performances and long storage stability of finished products. These properties depend on the interaction of TiO_2 particles between each other and between the binders. The surface charge offers a widely accepted model for the forces between TiO_2 particles and hence for the stabilities of slurries in water-based systems [9].

The absorbance values determined in the previous chapter (indicating the dispersion stability) are plotted against the zeta potential in figure 5.5. The dispersion became less stable when the zeta potential came closer to zero. This result agrees with that of Wiese et al [6] who found that rapid coagulation occurs at an absolute value of 14 $\pm$ 4 mV as mentioned in section 5.1.2. When the zeta potential becomes zero, the electric repulsion between the particles decreases and this causes a decrease in dispersion stability.

The large negative values reported for silica treated samples are the reason for their good dispersion stability because particles are prohibited from coagulation due to electric repulsion. Alumina treated samples gave poor dispersibility because the alumina coating was responsible for the positive or less negative charge on the surface. The repulsive forces decreased as a result of this and particles coagulate.

The poor coverage of samples A5-A10 can also be seen in the zeta potential measurements. The negative charge at pH 7 is because only part of the particle is covered.

Figure 5.5: The influence of surface charge on dispersion stability

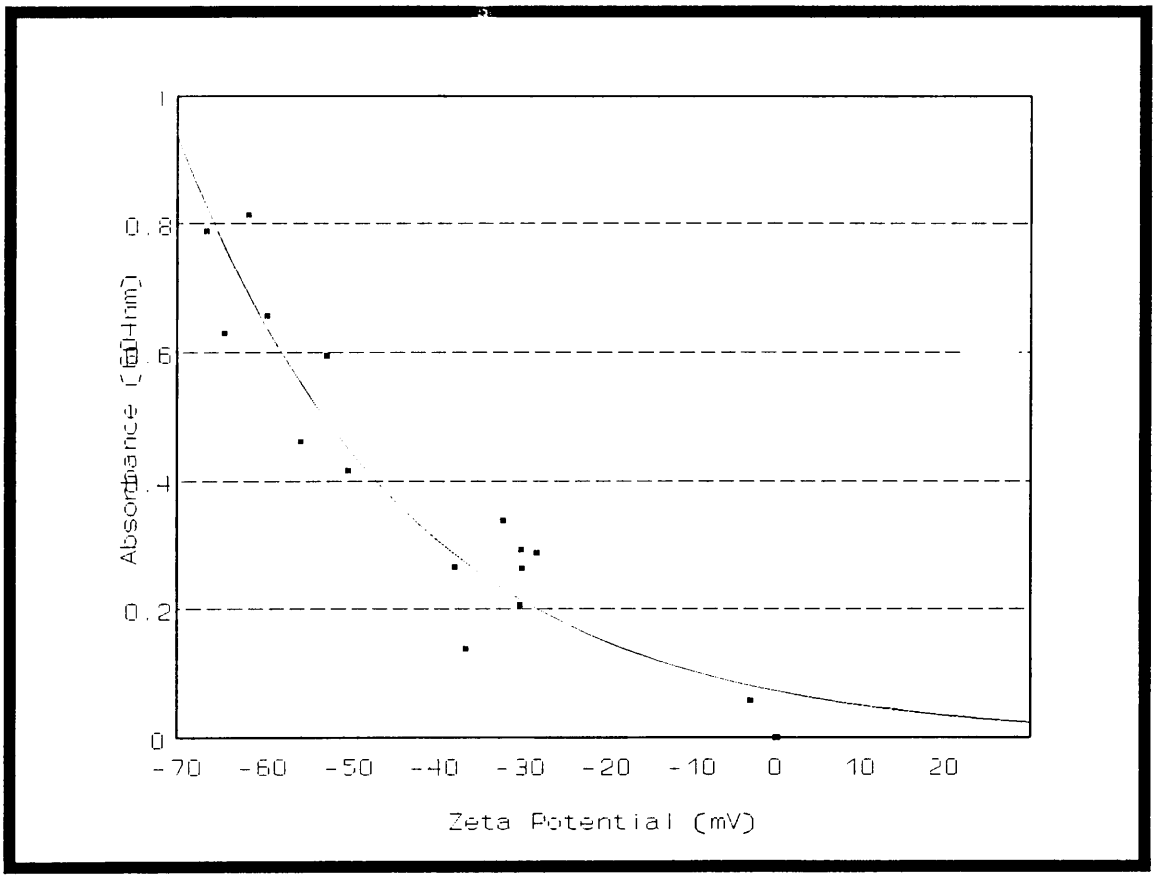

Figure 5.6 correlates the surface charge and dispersion stability for rutile at different pH values. The surface charge is minimal at low pH values because it is close to the i.e.p. Electric repulsion is low here and therefore dispersion stability is poor as indicated. The stability only increases when the zeta potential reaches values more negative than -20 mV at pH 3.5. At higher pH values the charge on the surface prevents the coagulation of particles and therefore the dispersion is more stable. At high pH values the NaOH ion concentration is so high that itself begins to contribute to the ionic strength, affecting the extension of the double layer and therefore stability decreases as observed.

Figure 5.6: The correlation between surface charge and stability at different pH values

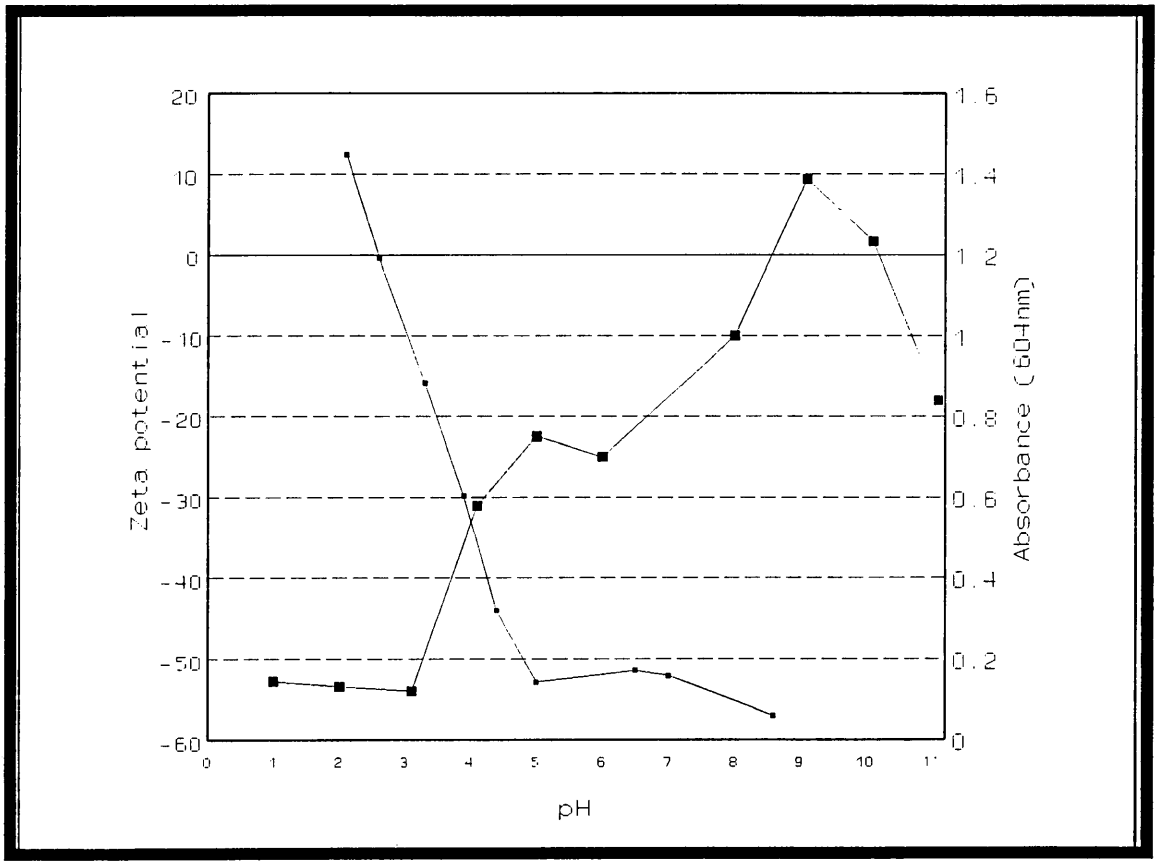

5.4. CONCLUSION

Many important properties of colloidal systems are determined directly or indirectly by the electrical charge on the particles. Zeta potential has long been recognized as a very good index of the magnitude of the repulsive interaction between colloidal particles and measurements of zeta potential are commonly used to assess the stability of a colloidal sol.

In this chapter zeta potential measurements were used to explain the results obtained for dispersion stability in the previous chapter. At pH 7 negative values were reported for silica and titania indicating iso electric points at lower pH values, while the zeta potential for alumina was positive at pH 7.

Treatment of TiO_2 with SiO_2 resulted in more negative zeta potential values than rutile and alumina treatment gave more positive values. Incomplete coverage of the coating resulted in a surface charge closer to that of TiO_2. TiO_2 treatment with a mixture of silica and alumina resulted in the formation of a alumino-silica intermolecular mixture with a silica like surface, even for low percentages. The large negative zeta potential values reported for samples with silica in the coating, are responsible for the good dispersion stability.

The iso electric point of untreated TiO_2 was reported to be at pH 2.6, while silica treatment moved the i.e.p. downwards to 2.3 and alumina treatment moved the i.e.p. upward to pH 5.7.

It can be concluded from these results that the precipitation of Al_2O_3 from sodium aluminate reach a maximum at pH 8 because this pH is close to the i.e.p. of alumina and therefore the particles are attracted to the negative TiO_2 surface. Silica adsorbs on positive sites on the surface and this causes the low precipitation yield reported. The yield is improved when the oxides are precipitated simultaneously because the alumina creates positive sites on which the silica can precipitate.

It was also proved that colloidal stability occurs if the surface charge is approximately 20 mV. Coagulation occurs at pH values lower than 4 because the surface charge becomes less than 20 mV and at pH values higher than 9 because the NaOH ion concentration is so high that itself begins to contribute to the ionic strength.

5.5. REFERENCES

1. Hunter, R.J. 1981. *Zeta Potential in Colloid Science.* Academic Press. London.

2. Parks, G,S. 1965. *Chemical Review.* 65,177.

3. Conley, R.F. 1974. Design , Functionality and Efficiency of Pigment Dispersants in Water-base systems. *J. Paint Tech.* 46: 51-64.

4. Morrison, H.H. 1985. Stabilization of Aqueous Oxide Pigment Dispersions. *Journal of Coatings Technology.* 57(721): p 55

5. Tuorilla, P. 1928. *Kolloid-Beih.* 27, 44.

6. Wiese, G.R. Healy, T.W. 1975. *Journal of Colloid Interface Science.* 52, 222.

7. Mäkinen, P.O. Losoi, T. Kohonen, A. 1988. Stability of aqueous dispersions of titanium dioxide. *12 th Concress of the Federation of Scandinvian Paint and Varnish Technologist Congress Book.* May 9-11. p 8.1-8.18.

8. Parfitt, G.D. Ramsbotham, J. 1971. *Journal of Oil and Colour Chemical Association.* 71,356.

9. Parfitt, G.D. 1972. *Dispersion of Powders in Liquids, 2nd Edition.* Applied Science Publishers. Chapter 3.

CHAPTER 6

Infrared Spectroscopy of TiO_2 Powders

CHAPTER 6

INFRARED SPECTROSCOPY OF TiO_2 POWDERS

6.1. INTRODUCTION

The use of infrared spectroscopy for the study of surfaces is comprehensively discussed by Little [1] and also Hair [2]. Since 1967 Parfitt and Rochester [3] discussed the use of infrared spectroscopy as a chemical method for the characterization of powder surfaces. Infrared spectroscopy proved to be the most useful technique for the characterization of functional groups, especially OH-groups, on the surface of TiO_2. The half width and position of the band is an indication of the type of hydroxyl group and the extent to which it is involved in hydrogen bonding interaction. According to Pimentel en McClellan [4] the involvement of hydroxyl groups in hydrogen bonding interaction causes the broadening and moving of the infrared band to a lower wavelength.

Parfitt [5] identified two different OH-groups on the TiO_2 surface which gave separate peaks on the IR-spectra at 3700 and 3670 cm^{-1}. The former is shown to have the greater thermal stability. Terminal groups are sufficiently close together to enable them to hydrogen bond and subsequently condense on heating to leave an oxygen bridge. There is a similar distance between the bridged OH groups but their surface attachment is very limiting with regard to mutual condensation. Therefore the bridged OH groups should have the greater thermal stability and Parfitt assigned the 3700 cm^{-1} band to them, and the 3670 cm^{-1} band to the terminal OH group.

These results differ from those reported later by Solomon and Hawthorne [6] who identified eight distinct OH adsorption bands and assigned the 3700 cm^{-1} band to terminal TiO-H on sites at lattice steps, edges, or apices. The 3680 cm^{-1} band was assigned to terminal TiO-H on (100) or (101) planes while bands at 3610, 3520 and 3410 cm^{-1} were assigned to bridged TiO-H groups. On the basis of chemical and structural considerations and theoretical

calculations, Solomon et al. [6] believed that the dissociative adsorption process involve the following sequence of events:

(i) An initial adsorption of water molecule at a five-coordinate surface Ti^{+4} site, preferably located on the (110) plane of rutile or the (100) plane of anatase.

(ii) Ionization of the water in the strong crystal surface field to give the Ti-OH species described as a terminal hydroxyl group (1); this dissociation is more extensive on rutile surfaces than on anatase.

(iii) Migration of the liberated proton to a neighbouring Ti-O-Ti site with formation of a bridged-hydroxylic species (2) from the lattice O^{2-} anion.

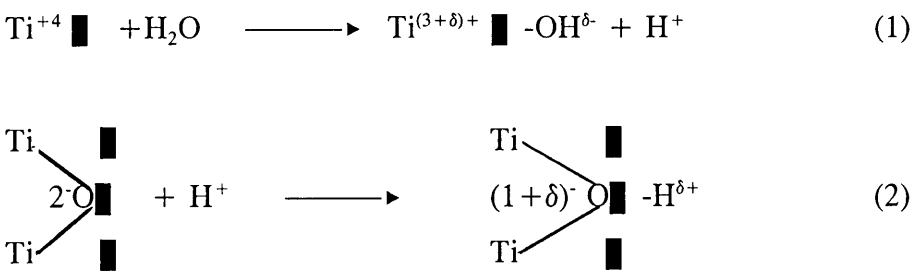

Weakly bound water may be adsorbed by hydrogen bond formation with terminal hydroxyl's, by non- or weakly dissociative adsorption on the surface cations contained in other crystal planes and by condensation in micropores.

These results also correlate with work done by Boehm [7] who suggested that the bridged groups are strongly polarized by the cations and therefore are acidic in character, while the terminal OH groups are basic and exchangeable with other anions.

Adsorption of ammonia can also be used in the characterization of the TiO_2 surface. Pichat en Mathieu [8] discovered that ammonia-molecules involved in H-bonding give Lewis acid-

base en Bronsted acid-base interactions with different characteristic bands.

Morterra [9] investigated dehydration, rehydration of TiO_2 surfaces with infrared spectroscopy and also studied the adsorption of CO at ambient temperatures. He proved that the OH stretching region of TiO_2 is characterized by a presence of strongly hydrogen-bonded species. After short evacuation at ambient temperature very little remained at 3300cm^{-1} of the ill-defined band leaving two well defined bands: the surface hydroxyl groups at 3600-3800cm^{-1} and un-dissociated water in the 3350-3500cm^{-1} range. Morterra assigned the broad band to physically adsorbed water showing the difference between physical adsorbed water and un-dissociated water coordinated to the surface. Morphological changes were assumed to be responsible for a complex change in the overall intensity in the 3600-3800cm^{-1} range but the dissociation of water molecules into OH groups was also a possible factor which was confirmed by rehydration. Morterra investigated the adsorption of CO on the surface and found that the CO adsorbed on Lewis-acidic sites and he believed that the sites were produced by the dehydration of undissociated water rather than OH groups.

Infra-red studies of the adsorption of ammonia may also be used as a diagnostic test for the Lewis acidity of surfaces instead of pyridine, which isused by the most authors. Infra-red spectra of ammonia adsorbed on the rutile surface showed a number of easily distinguishable adsorption bands which may be assigned to ammonia molecules involved in an electron donor interaction with two different types of Lewis sites [10]. The two types of Lewis acid sites are created by the removal of the isolated OH groups and by the removal of molecular water and the former is the strongest site.

Zettlemoyer et al. [11] proved that complete removal of the water monolayer took place after outgassing at 423K and at temperatures higher than 773K the surface is completely dehydroxylated. Morimoto et al. [12] showed that complete rehydroxylation occurs on exposure to water vapour after outgassing rutile at 523K but at higher temperatures the effect is only partial, suggesting the dehydroxylated oxide surface has become partially stabilized. These results were supported by previous work done by Ganichenko et al [13].

Tanaka & White [14] studied the adsorption of water, pyridine, carbon dioxide and carbon monoxide by infrared absorption spectroscopy on reduced and oxidized anatase. Two kinds of chemisorbed H_2O and two kinds of OH were found on anatase and four-coordinate Ti^{+4} ions at the surface of the anatase were proposed as the sites for adsorption of both OH and H_2O while five-coordinate ions are suggested as sites for OH adsorption only. Water was held more strongly on oxidized surfaces compared to reduced surfaces, which suggests that water adsorption is enhanced by the presence of four-coordinate Ti^{+4} ions and surface oxygen ions.

Most of the experiments mentioned above were done under evacuation, including the thermal treatment and the infra-red measurements. Because of instrumental restrictions measurements under thermal heating will not be investigated in this study, however enough information can be gathered to prove the importance of hydrogen bonding in dispersion stability and the important role of the OH groups in this bonding and in photo-activity.

6.2. EXPERIMENTAL

Mid-infrared spectra of all samples were taken at room temperature on a Bruker IFS 113 V spectrophotometer with a resolution of 4 cm^{-1}. Samples were prepared by mixing 0.03g of the sample with 0.3g KBr and measurements were done by placing the sample on a reflection cell. All the measurements were done under a vacuum of 10 KPa.

To determine the influence of pH and temperature on the surface of TiO_2, the rutile powder was dispersed in water as discussed in chapter 2. No surface treatment was done but the pH of the dispersion was changed with HCL or NaOH to pH values of 1, 4 and 11 after which the powder was filtered and dried for 3 hours at 383K. A dispersion of TiO_2 in distilled water at a pH value of 7 was used as a reference.

The influence of different temperatures on the spectra of TiO_2 was determined by respectively heating the rutile sample to 373K,473K, 673K, 873K and 1073K for one hour and then cooled to room temperature before the IR-spectra was measured.

Gas adsorption was done by heating TiO_2 (5g) at different temperatures for one hour and then the samples were exposed to water and different amine gases in a desiccator for one hour. The gas was generated by boiling the appropriate liquid in a flask with a outlet in the desiccator. Ethylene diamine (EDA),Dimethyl amine (DMA), ammonia (AM) and water (H) were used. Ethylene diamine with a purity of 99% was used, while ammonia and dimethyl amine gases were generated by boiling 25% solutions in a flat bottom flask with a outlet in the desiccator. To determine whether the water in the solution has an influence on the spectra, another experiment was done using ammonia gas(NH_3) with a purity of 99%. The samples were exposed as indicated by the following: gas:temperature(K)

EDA373, EDA473, EDA673, EDA873, EDA1073
DMA373, DMA473, DMA673, DMA873, DMA1073
AM373, AM473, AM673, AM873, AM1073
NH373, NH473, NH673, NH873, NH1073
H373, H473, H673, H873, H1073

The samples were heated with a Nabertherm programmable oven in stainless steel crucibles. After one hour exposure to the gas the samples were stabilized in air and IR spectra were measured in evacuation at room temperature.

Rehydroxylation is done by heating the EDA473R sample for one hour at 373K, 423K,473K and 573K respectively.

6.3. RESULTS AND DISCUSSION

6.3.1. INFRARED SPECTROSCOPY OF UNTREATED TiO_2 POWDERS

Infrared transmittance spectra of the rutile and anatase structure of TiO_2 can be seen in figure 6.1 and 6.2. Two different OH groups on the surface of anatase can be clearly seen in figure 6.2 at respectively 3694 cm^{-1} and 3670 cm^{-1}. Only one sharp band at 3703 cm^{-1} is visible in the IR spectra of rutile. This is because the 3703 cm^{-1} band is so broad and intense that it obscures the 3670 cm^{-1} band and consequently this band can not be seen clearly. The broad

bands at 3370 cm^{-1} and 1620 cm^{-1} in both spectra are probably due to adsorbed and undissociated water. These bands are always visible in the spectra of TiO_2 unless the spectra are measured under vacuum at high temperatures.

The influence of pH on the infrared spectra of rutile can be seen in figure 6.3 - 6.6. At a pH of 1 the band at 3670 cm^{-1} becomes more visible for the first time in rutile, while the 3700 cm^{-1} band had nearly disappeared. At a pH of 4 both bands have the same intensities and at a pH of 7 the original spectra with a slightly increase in intensities appeared. At a pH of 11 the intensity of the band at 3700 cm^{-1} increased significantly. It is also noticeable that at a higher pH the water bands are more intense than at a lower pH.

Considering the mechanism of the adsorption by Solomon, et al.[6] as discussed in the introduction the two different OH bands can be assigned to terminal and bridged OH groups on the surface of TiO_2. The hydrogen bond in the second reaction is weaker than the same bond in the first reaction in section 6.1, because the oxygen is strongly covalent bonded to two Ti atoms and less electrons are available for bonding. A weaker bond will cause the IR band to move to a lower wavelength and therefore the band at 3700 cm^{-1} is assigned to the terminal OH groups and the band at 3670 cm^{-1} to bridged OH groups.

This statement is supported by the IR spectra at different pH values. According to the second reaction in section 6.1 the H^+-ions are responsible for the formation of bridged OH groups. A logical acceptance can be made that an increase in H^+-ions will promote the formation of bridged OH groups. This can be seen in figure 6.3 where the 3670 cm^{-1} band (bridged OH) is clearly visible. An increase in OH^--ions will result in an increase in terminal OH groups as seen in figure 6.4 to 6.6 at the 3700 cm^{-1} band.

These results are also in accordance with suggestions by Boehm [7] that the bridged groups are acidic- and the terminal groups basic in character. At a lower pH the terminal groups will therefore disappear as seen in figure 6.3.

Figure 6.1: Infrared spectrum of TiO_2 (Rutile)

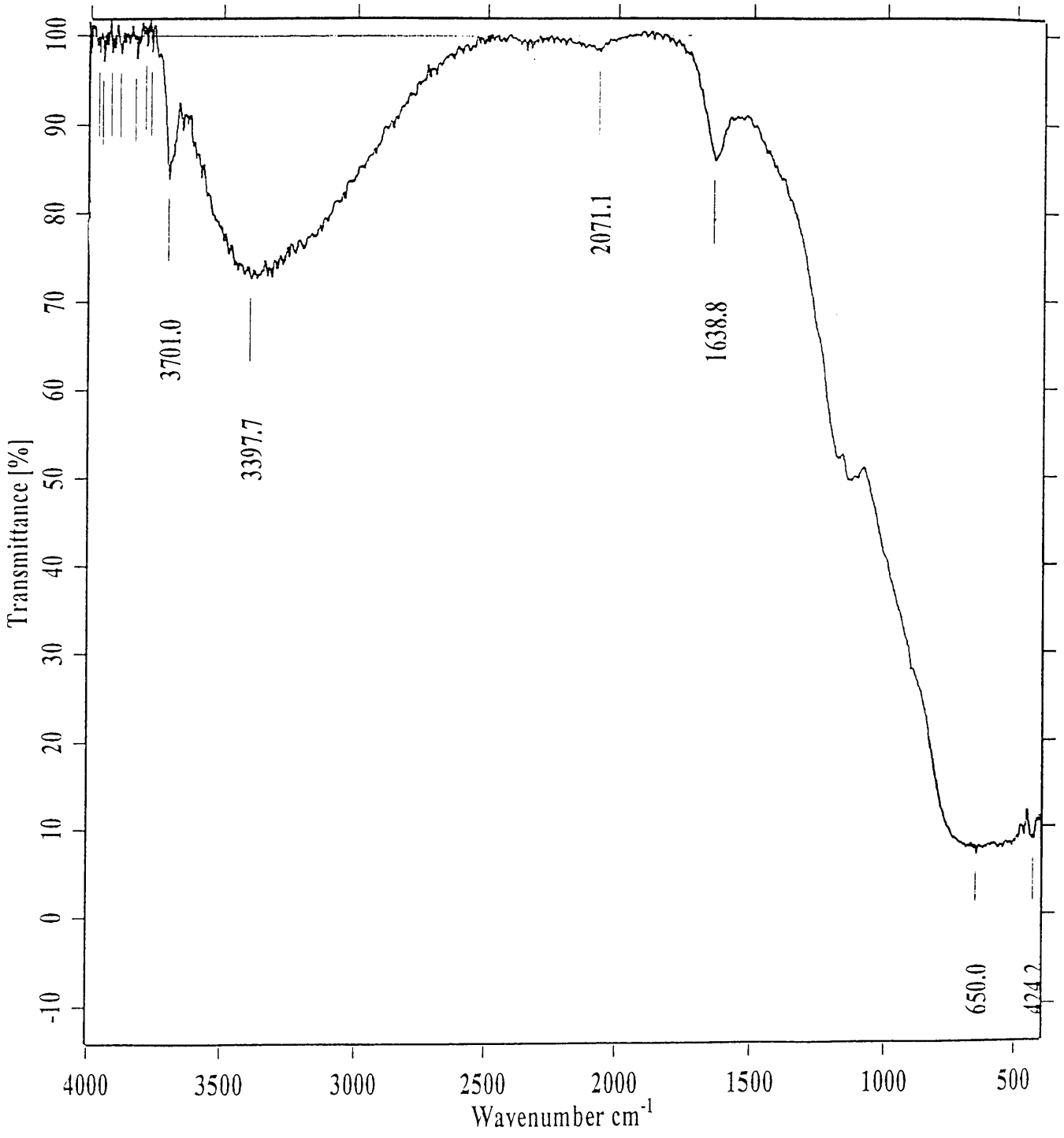

Figure 6.2: Infrared spectrum of TiO_2 (Anatase)

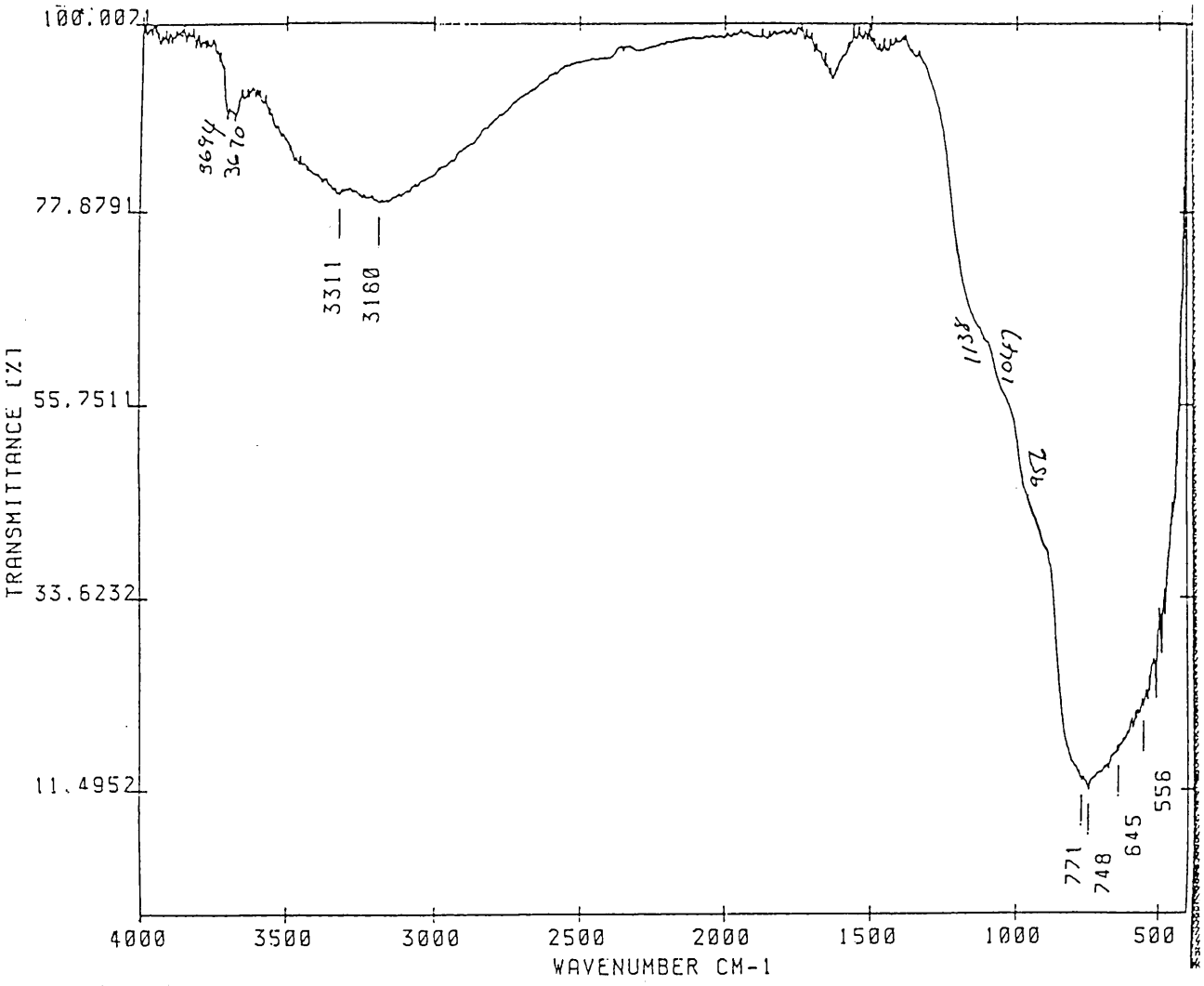

Figure 6.3: Infrared spectrum of TiO_2 at pH 1.

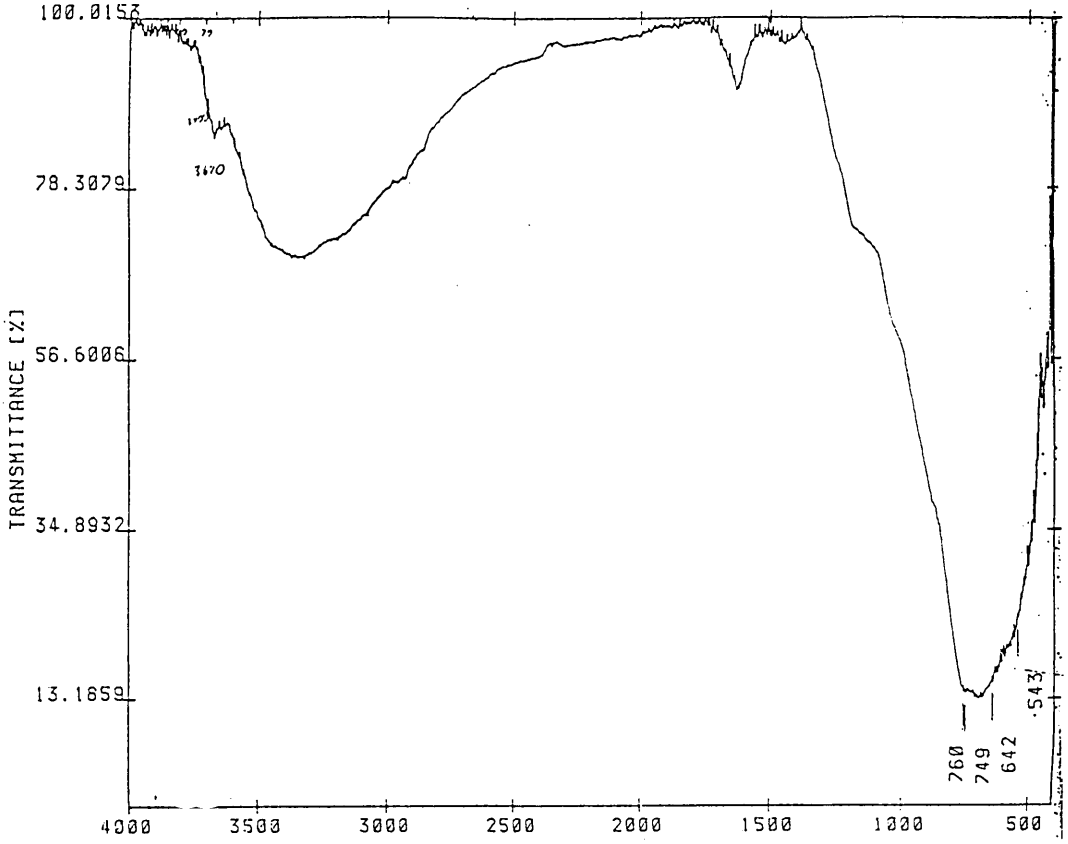

Figure 6.4: Infrared spectrum of TiO_2 at pH 4.

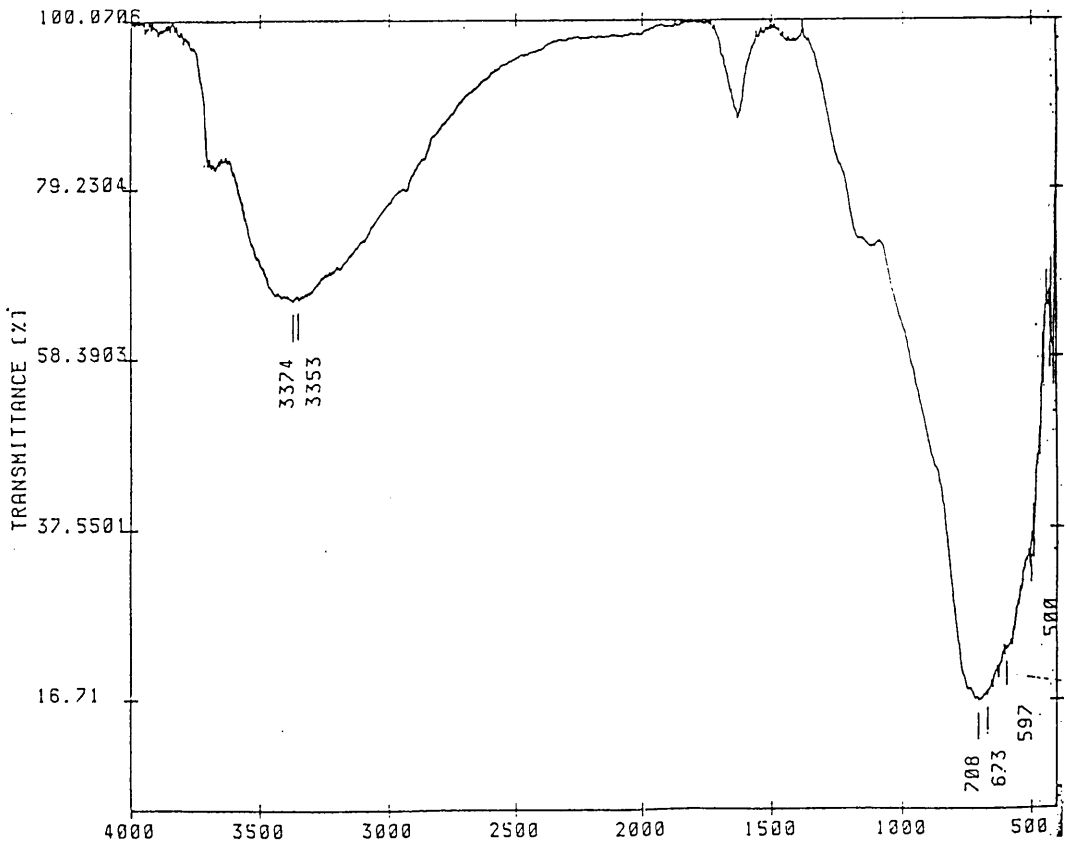

Figure 6.5: Infrared spectrum of TiO_2 at pH 7.

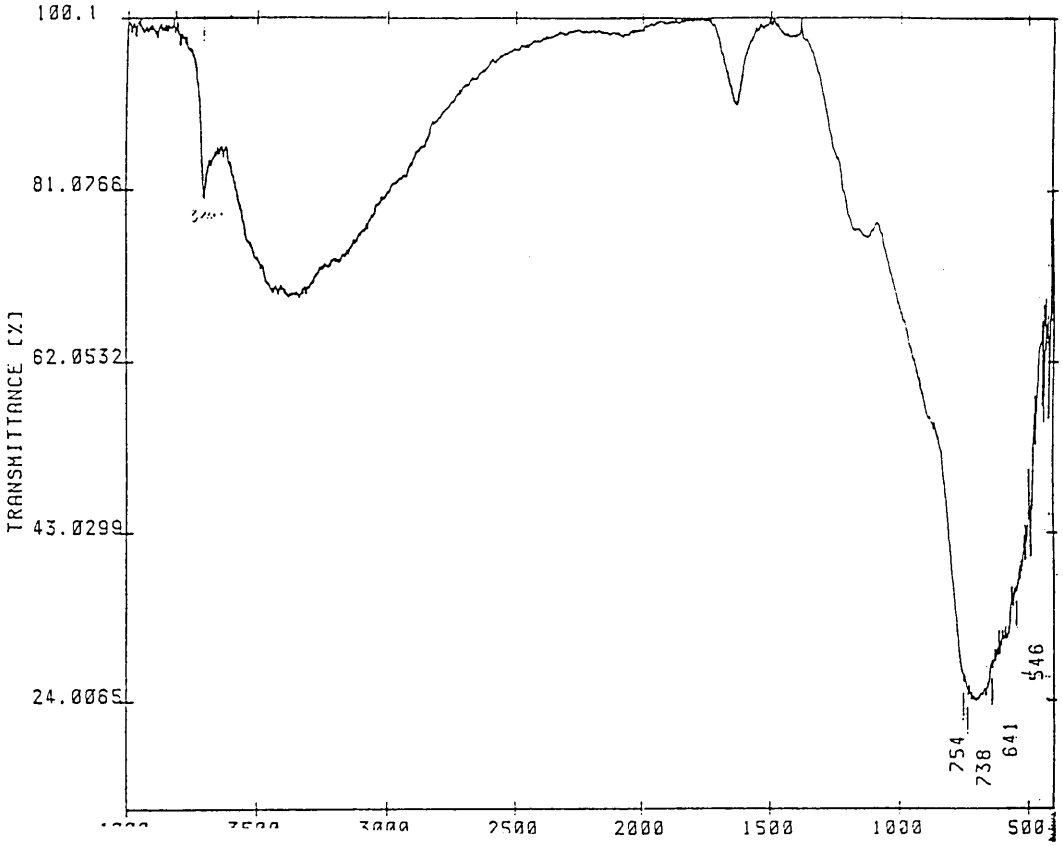

Figure 6.6: Infrared spectrum of TiO_2 at pH 11.

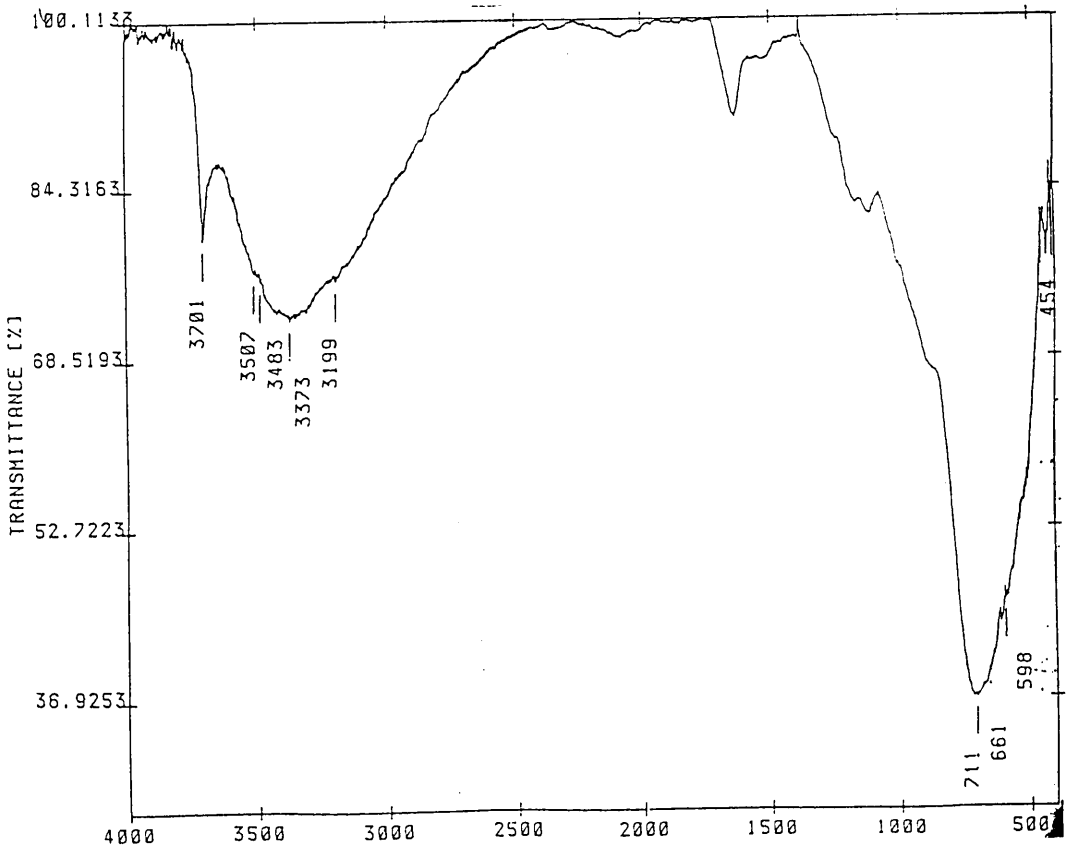

The zeta potential of TiO_2 was positive at low pH values and negative at higher pH values as discussed in chapter 5. According equation 4 in section 5.1 the positive zeta potential is created by the following reaction:

$$OM\text{-}OH + H^+ \dashrightarrow OM\text{-}OH_2^+$$

The infrared band of the terminal OH group ($3700nm^{-1}$) decreased at low pH values. It can therefore be assumed that the terminal OH groups allocate the positive charge on the surface and this is responsible for the instability in water. Because the terminal OH groups accepted a proton, they can be classified as basic.

Higher pH values simulate the formation of terminal OH groups as discussed previously. Although it is difficult to detect in the spectrum, it is expected that the bridge OH groups decreased at higher pH values, because of the following reaction:

$$M\text{-}OH + OH^- \dashrightarrow MO + H_2O$$

The bridge OH groups are therefore responsible for the negative zeta potential at higher pH values.

The increase in terminal OH groups at a higher pH is also responsible for the increase in photo-activity. More hydroxyls on the surface resulted in the formation of more hydroxyl radicals which increased the degradation of MB.

The influence of heat treatment on the rutile surface can be seen in figure 6.7. After heat treatment the samples were allowed to cool down in air. The terminal OH and undissociated water bands are clearly visible as discussed previously. The most significant change in the heated samples is the increase of the $3700cm^{-1}$ band which suggests an increase of terminal OH groups on the surface. A small increase in the bands at 3370 and 1620 cm^{-1} suggested that more water was absorbed on the surface.

The heat treatment provided sufficient energy to dissociate the water leaving terminal OH groups on the surface. The intensity of the OH groups increases with temperature up to 873K after which no changes were observed. There were no other significant changes in the spectra which suggested that the water on the surface returned to their normal concentration. The sites occupied by the additional OH groups could be created by the loss of undissociated water or the loss of surface oxygen as discussed by Tanaka et al [14].

These results can be explained by the mechanism of the adsorption by Solomon, et al.[6] as discussed in section 6.1. Other anions like sulphate or chloride process residues and also activated oxygen species can adsorb on the TiO_2 surface. With heat treatment these adsorbed species are driven off, leaving active Ti^{+4} sites behind. It is also possible that the energy at 1073K is enough to drive off same of the oxygen bonded to titanium on the surface also leaving active Ti^{+4} sites. When cooled down, water adsorbs on these active sites and form terminal OH groups on the surface according to the mechanism in section 6.1.

The spectra of the samples which have been exposed to water vapour, after heat treatment, can be seen in figure 6.8. The broad water band at 3400cm^{-1} becomes slightly bigger with increasing temperature as expected considering the fact that heat treatment provides more sites and the higher concentration of water vapour in the surroundings compared to air. It is expected that this change occurs because of physical adsorbed water rather than water coordinated to the surface, because this band increased significantly more in intensity compared to the previous spectrum. More visible is the change in intensity of the 3700cm^{-1} band in a similar way as the samples exposed to air. No difference is detectable when the intensity of this band is compared with the intensities of the samples exposed to air. Therefore it is believed that the additional OH groups originated from the dissociation of water on the surface and not from additional water adsorbed from the surroundings. Also significant is the increased intensity of the sample treated at 873K. No reason could be found for this deviation but it can be due to morphological changes at high temperatures.

Changes in surface area because of thermal treatment were too small to detect with the instrument available for BET measurements and therefore it can be safely said that the

influence of changes in surface area is minimal and have no significant influence on the spectra.

A conclusion which can be drawn from these results is that water, coordinated to the surface, starts to dissociate at 473K because it is believed that most physical adsorbed water is removed at this temperature. The dissociation is responsible for the increase in OH groups on the surface and reaches a maximum at 873K.

Figure 6.7: Infrared spectrum of TiO_2 after heat treatment

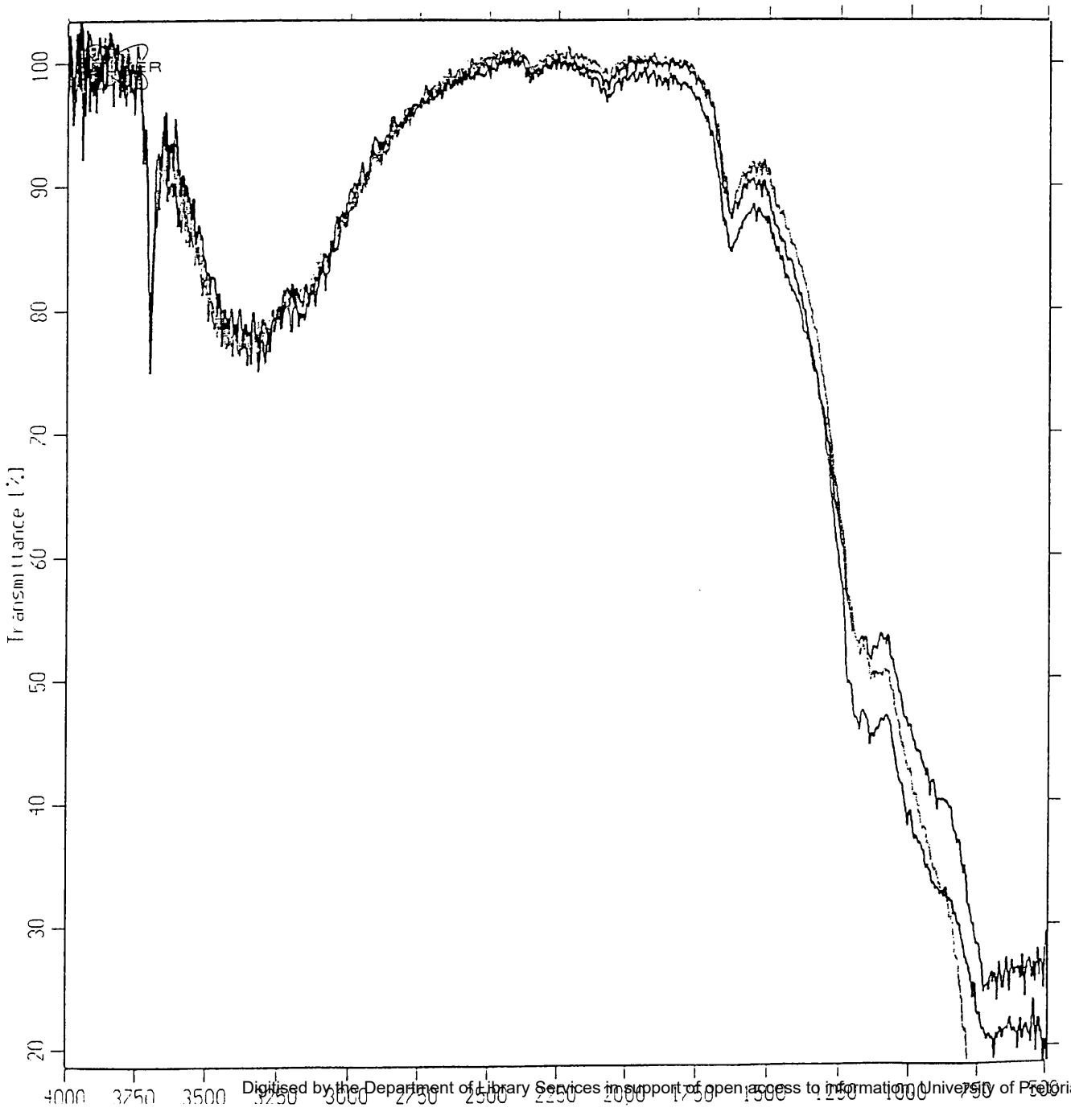

Figure 6.8: Infrared spectrum of TiO_2 exposed to water after heat treatment

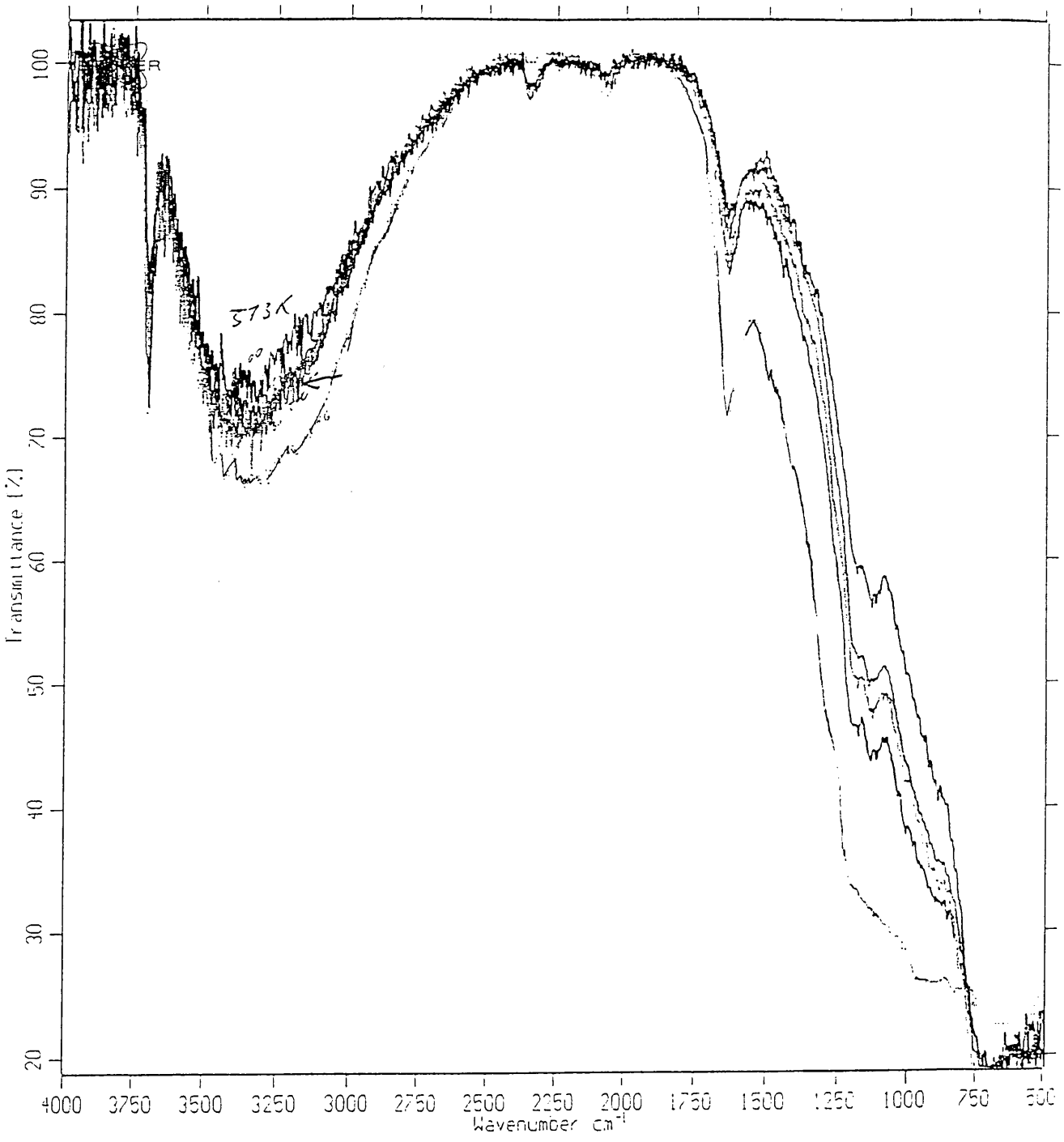

6.3.2 INFRARED SPECTROSCOPY OF INORGANIC TREATED TiO_2

6.3.2.1. SiO_2

The infrared spectra of the silica (S) treated samples can be seen in figure 6.9. The only difference from the rutile spectrum is a band at 3740cm^{-1} that becomes visible as the silica content increases. This band can be clearly seen in the spectrum of sample S5. This sharp band is typical of surface silanols (v SiO-H). The strong tail on the low-wavenumber side is due to H-bonded hydroxyls and the small amount of alumina present in the coating, as seen in the analytical results, is contributing to this band. The water band at 1638cm^{-1} moved slightly to a lower value, suggesting hydrogen bonding.

The finger print band for silica at 3740cm^{-1} can not be seen in the spectra of sample S1 because the percentage silica precipitated was too low as seen from the analytical results. In the spectra of samples S2 and S3 a clear shoulder is visible to the left of the OH-band on the rutile surface. Again this results correlate with the analytical results because the yield is still very low and therefore the TiO_2 surface is not completely covered by the silica.

According to Morterra et al [15] the asymmetric stretching modes of the Si-O-Si network give a complex adsorption at 1350-900cm^{-1}. No conclusions can be made from this band in the recorded spectra because only a broad band is observed although the intensity of the shoulder at 1200cm^{-1} is stronger for sample S5.

There seems to be a relation between the surface area and the intensity of the 3450cm^{-1} band and this seems logic because in a higher surface area more water and bounded hydroxyls are able to adsorb.

The silanol group on the silica coated TiO_2 is very acidic as discussed previously in section 5.1.2. The acidity of this OH group results in the equilibrium shift to the right of the following equation:

$$OM\text{-}OH + OH^- \dashrightarrow OM\text{-}O^- + H_2O$$

This results in a more negative zeta potential over a larger pH range for silica treated samples as seen in chapter 5 and accordingly a more stabile dispersion. The negative charge on the surface does not only result in bigger repulsive forces between the TiO_2 particles, but also causes an increase in the hydrogen bonding between the water molecules in solution and the surface. The hydrogen bonding between the water adsorbed on the surface and the $OM\text{-}O^-$ group caused the band at $1638cm^{-1}$ to move to lower value.

In chapter 4 it was stated that a reason for the increased photo-activity of silica treated samples, might be due to increased adsorption on the silica surface. This is proofed in figure 6.10. The characteristic band of MB can be seen at $1605nm^{-1}$ for three samples S1,A1 and rutile. MB was added to these samples as discussed in chapter 4 but instead of putting the samples in the sun, they were centrifuged and dried. In figure 6.10 it can be seen that MB adsorbs more on the silica treated sample than the untreated and alumina treated sample. This bring the MB more in contact with the hydroxyls on the surface, which enhances the degradation.

Figure 6.9: Infrared spectrum of silica treated samples.

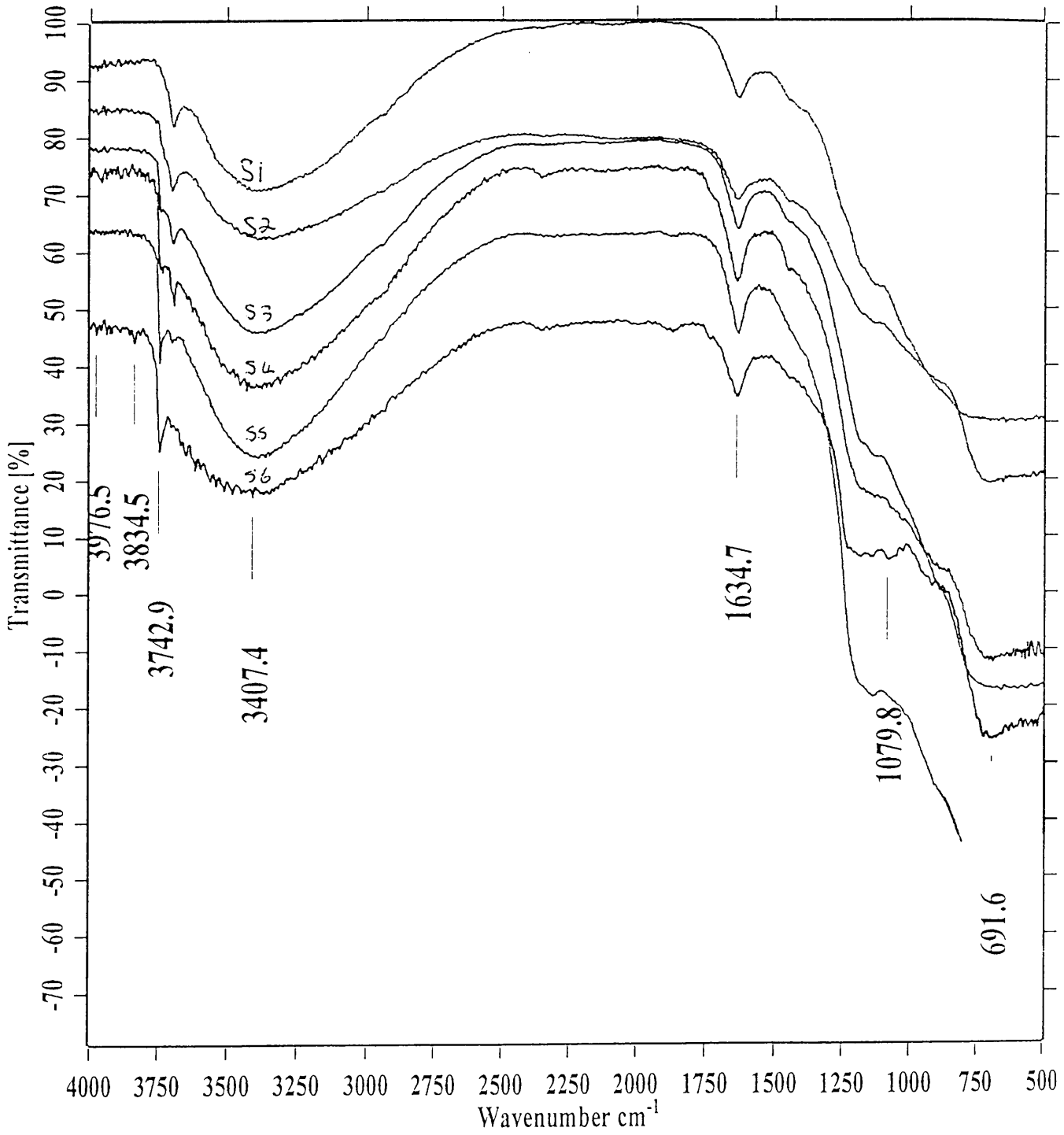

Figure 6.10: Infrared spectrum of MB adsorbed on TiO_2

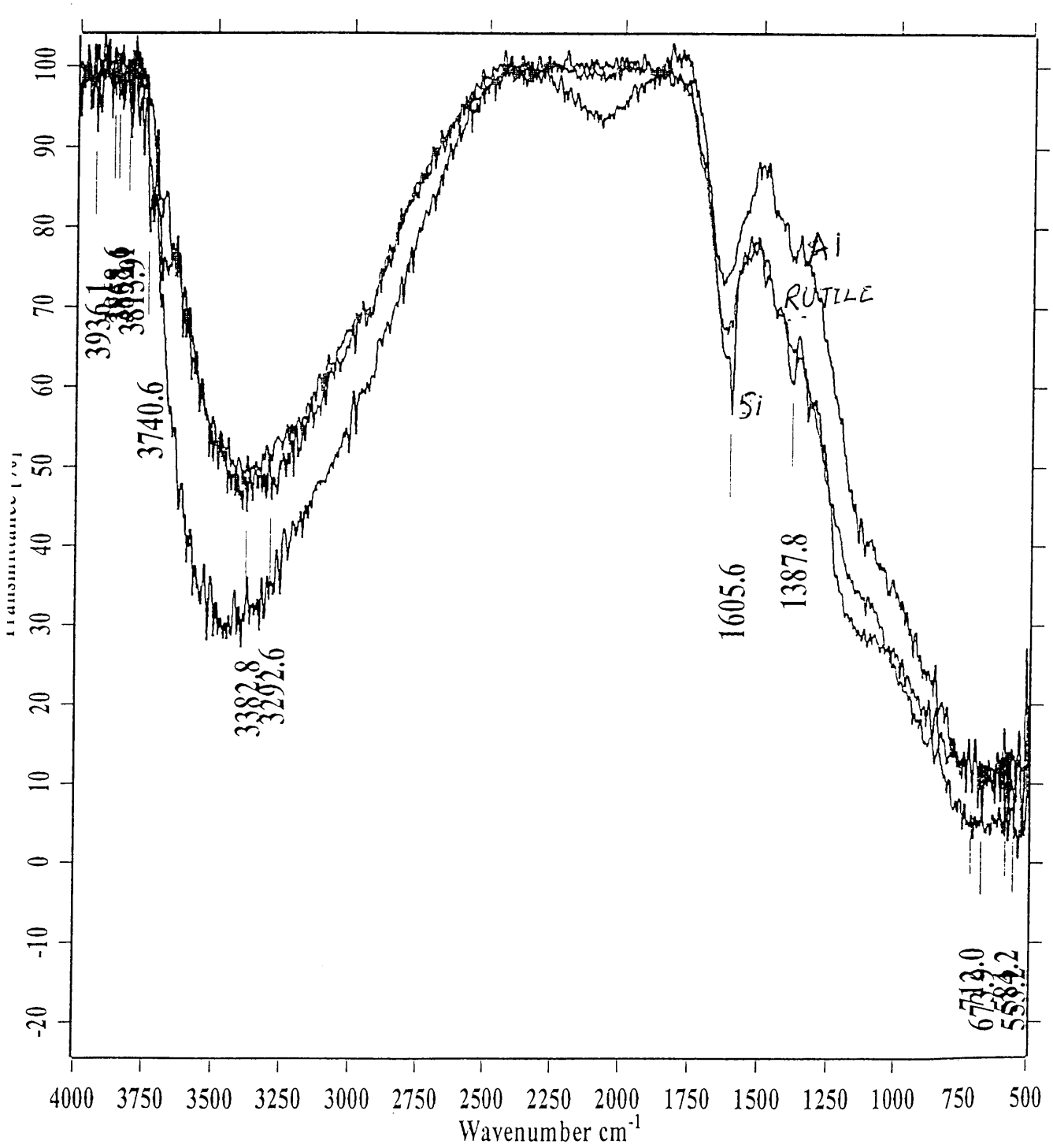

samples A1 and A2 also support t[illegible] in chapter 3 that these samples are covered by a dense coating. Although samples A2 is not completely covered the slow precipitation aloud a dense coating to be formed and therefore water band is smaller than samples A3 and A4.

The alumina acts as a physical barrier over the TiO_2 surface as stated in chapter 4. The OH band at 3700cm^{-1} in the infrared spectra of the alumina treated TiO_2 was completely covered and therefore the formation of hydroxyl radical were limited. Because of the energy difference between the valence band of the TiO_2 and Al_2O_3 the positive holes were prevented from moving to the surface.

Figure 6.11: Infrared spectrum of alumina treated samples

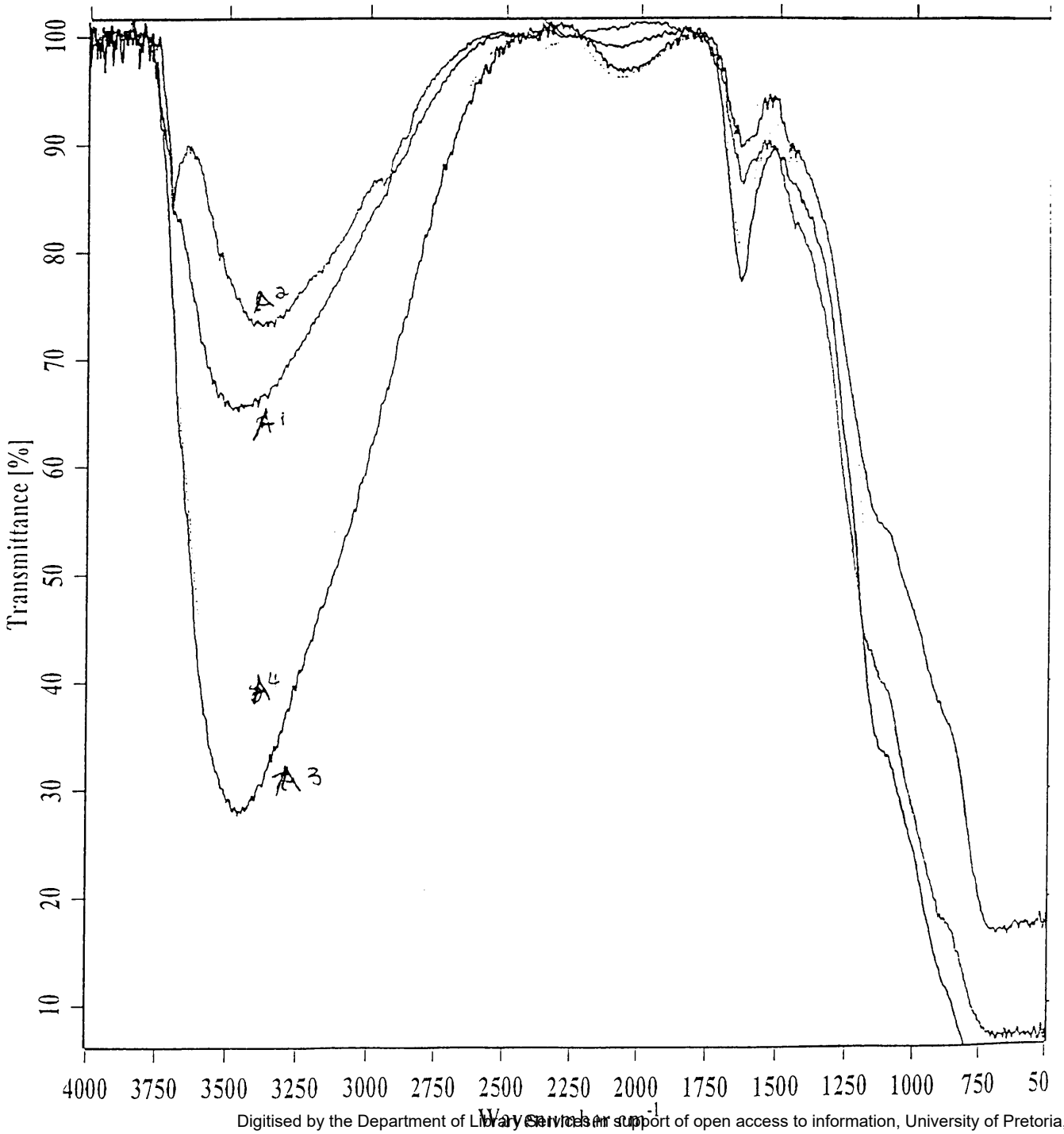

Figure 6.12: Infrared spectrum of alumina treated TiO_2 via $Al_2(SO_4)_3$

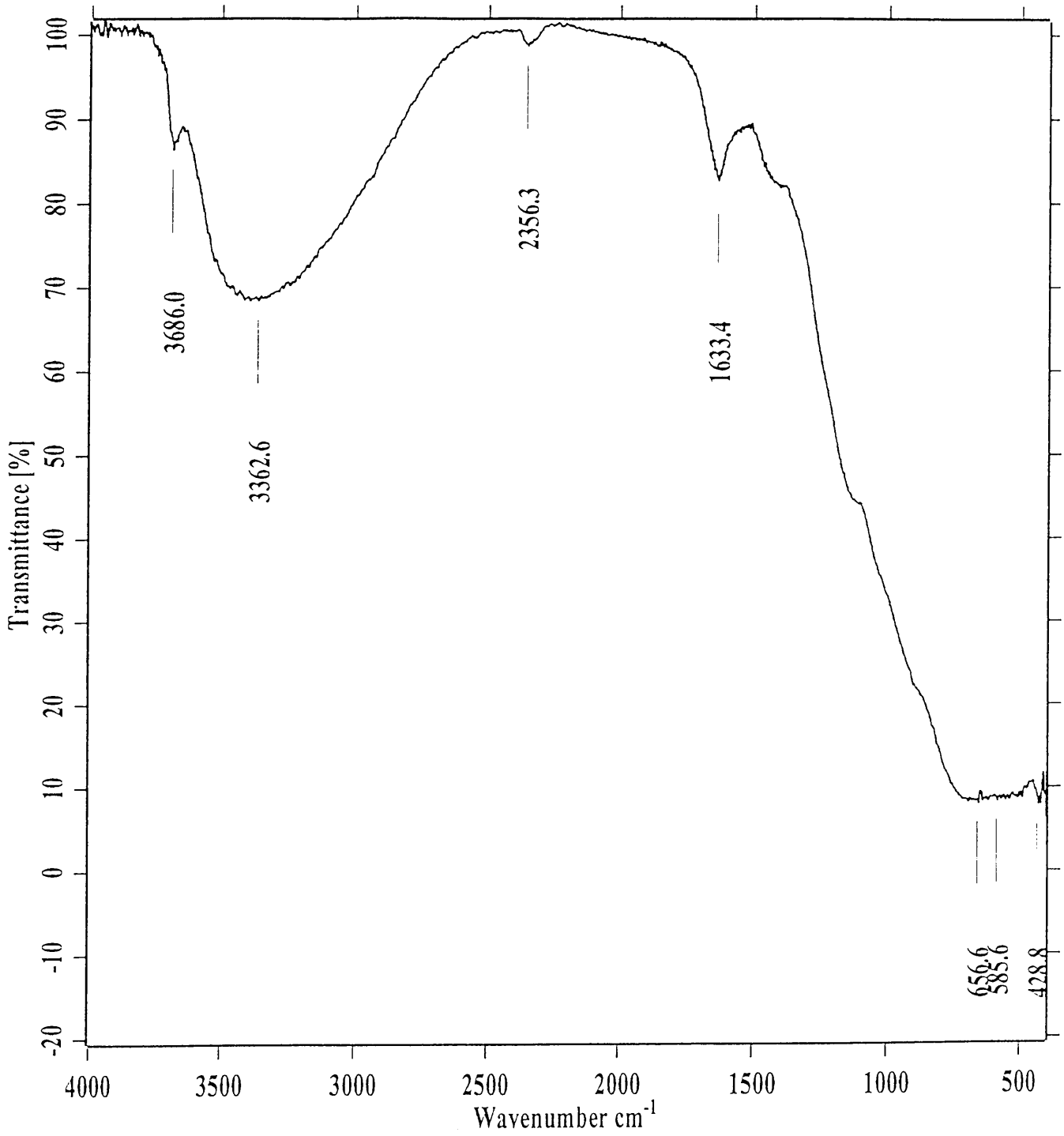

Figure 6.13: Infrared spectrum of alumina treated TiO_2 via $AlCl_3$

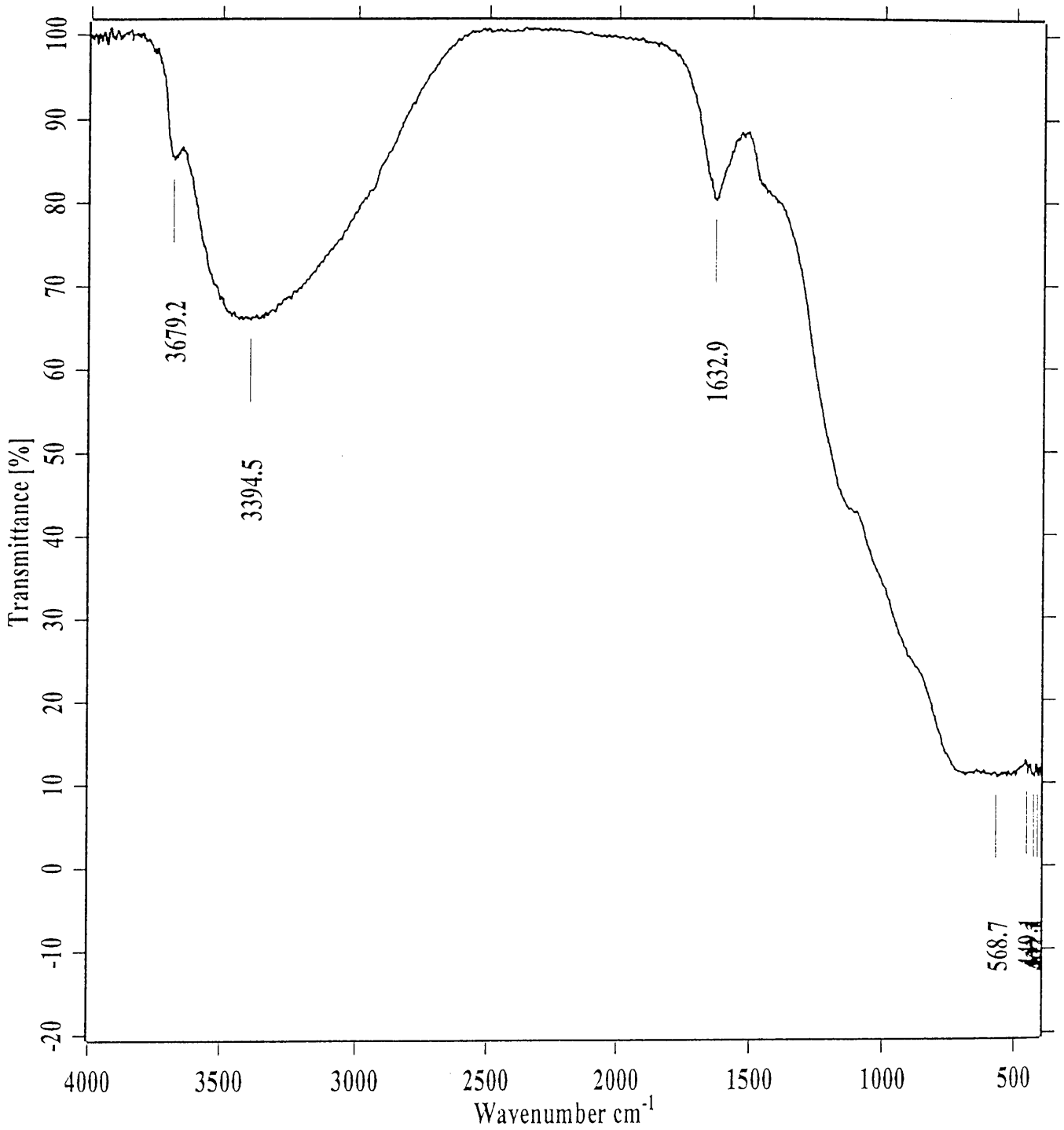

6.3.2.3. Mixed oxides

The infrared spectra of the TiO_2 samples treated with different ratios of Al_2O_3 and SiO_2 can be seen in figure 6.14 - 6.22. The spectra of sample AS1 is quite similar to that of sample A1 although the intensity is lower. The band for the surface hydroxyls on the TiO_2 surface appears only as a small shoulder at 3700cm^{-1} indicating good coverage from Al_2O_3. The fingerprint band for silica at 3740cm^{-1} can not be seen and this is due to the low silica yield.

The high alumina content of sample AS2 can also be seen in the infrared spectrum which is similar to that of sample A3 with a broad band at 3450cm^{-1} due to water captured in the alumina coating and hydrogen bonded hydroxyl groups. The silica band is again not visible due to a low yield.

In the spectra of sample AS4 and AS5 the fingerprint band for the silica coating can be clearly seen at 3723cm^{-1}. This is due to the higher silica content as seen from the analytical results. The alumina content is also lower and therefore the water band at 3450cm^{-1} is smaller than the previous samples. An interesting future from these spectra is that the characteristic band of silica moved to a lower band value. This might be due to hydrogen bonding with the high water contend on the alumina. The higher silica percentage in the coating of sample AS6 can also be detected at the silanol band in the infrared spectrum. The spectrum for sample AS 7 show both the silanol and hydroxyl groups on the TiO_2 surface. The large band at 3450cm^{-1} is characteristic of alumina in the coating. It must be mentioned that this sample gave good dispersion and low photo-activity and this also proof the importance of the hydroxyl groups in dispersion stability, while alumina is responsible for the low photo-activity.

The same trend can be seen in the samples with aluminium sulphate as reagent. In sample AS12 the influence of both the silica and alumina coatings can be seen. The silanol band is again moved to a lower wave number and this is evident for all the mixed coatings. In sample AS14 the OH band at 3700cm^{-1} is visible indicating that the surface is not completely covered.

The relationship between the 3450cm^{-1} band and the surface area can also be seen here except in sample AS1.

The OH band at 3700cm^{-1} is hardly visible in the infrared spectra of the TiO_2 treated with mixed oxides. This indicates a good coverage on the surface and this is the reason why the AS samples showed low photo-activity compared to rutile.

Figure 6.14: Infrared spectrum of sample AS1

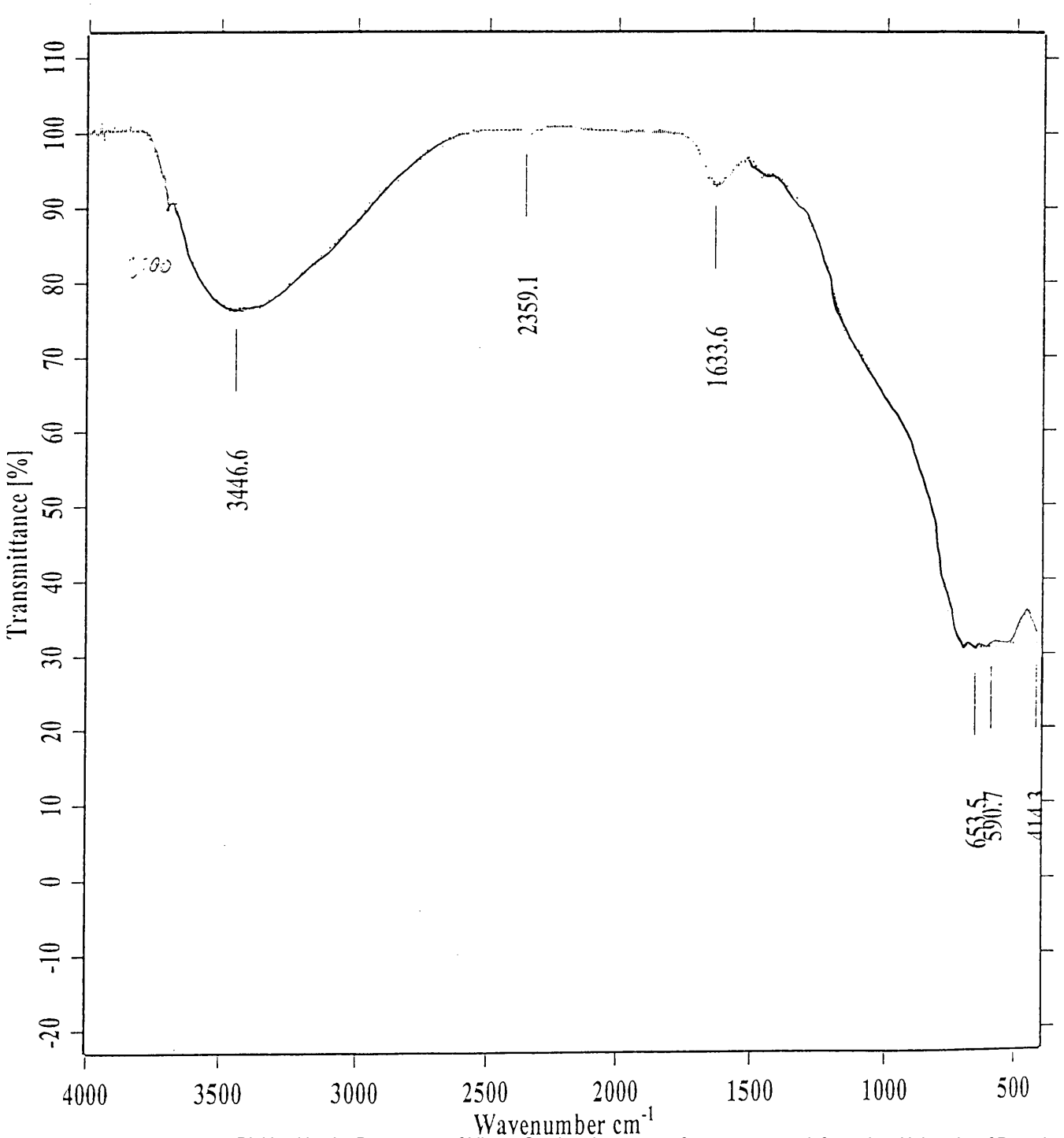

Figure 6.15: Infrared spectrum of sample AS2

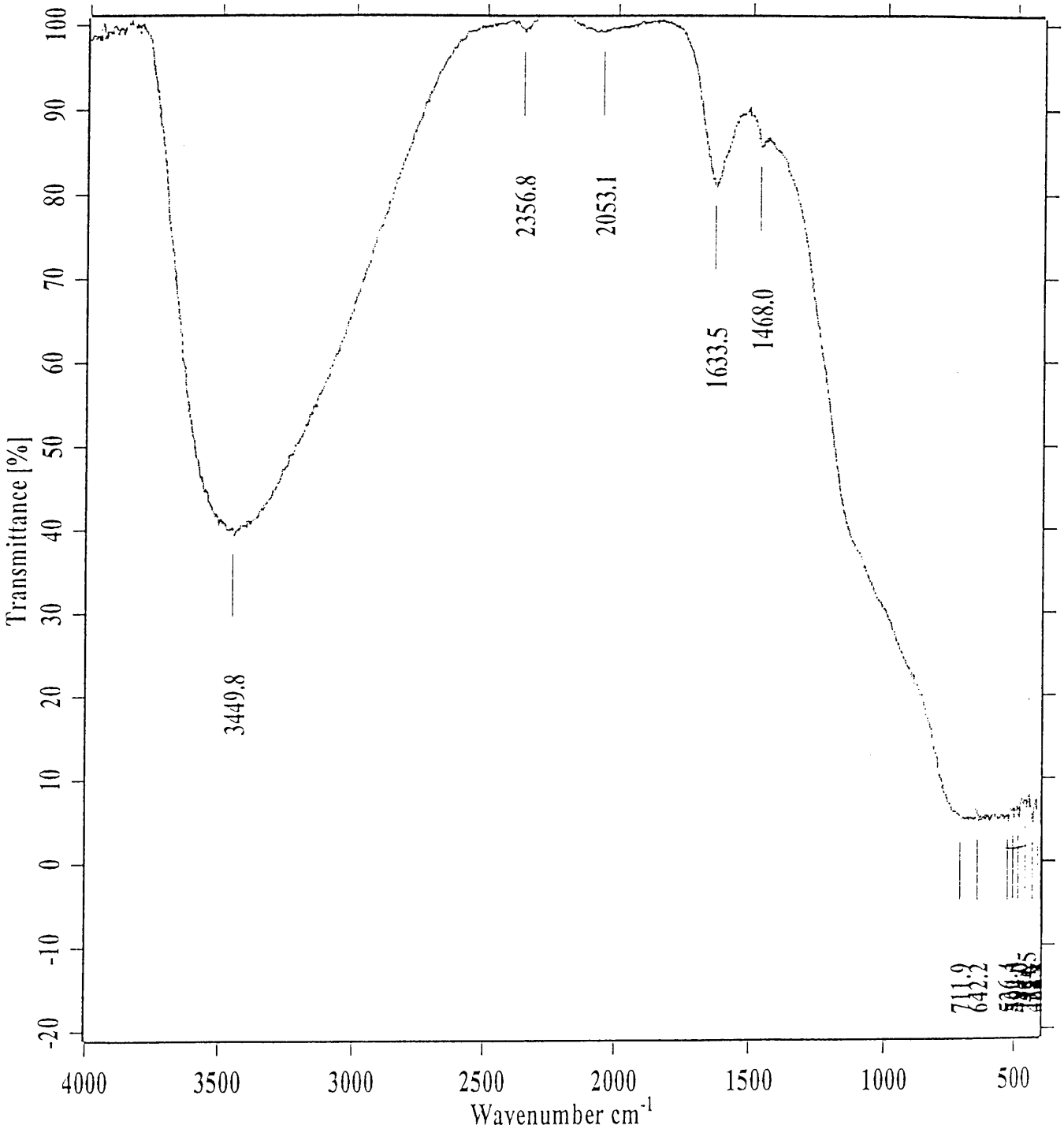

Figure 6.16: Infrared spectrum of sample AS3

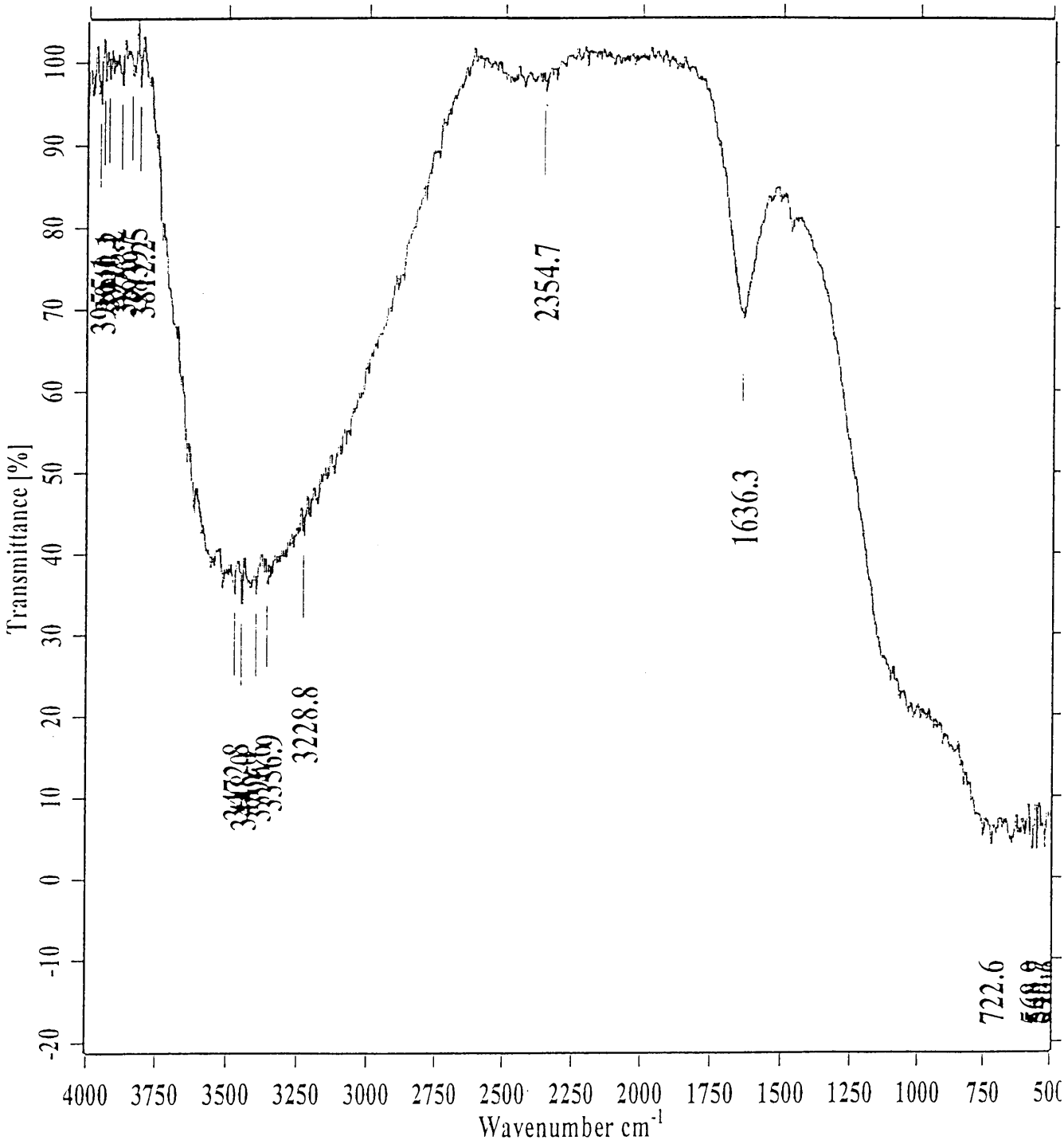

Figure 6.17: Infrared spectrum of sample AS4.

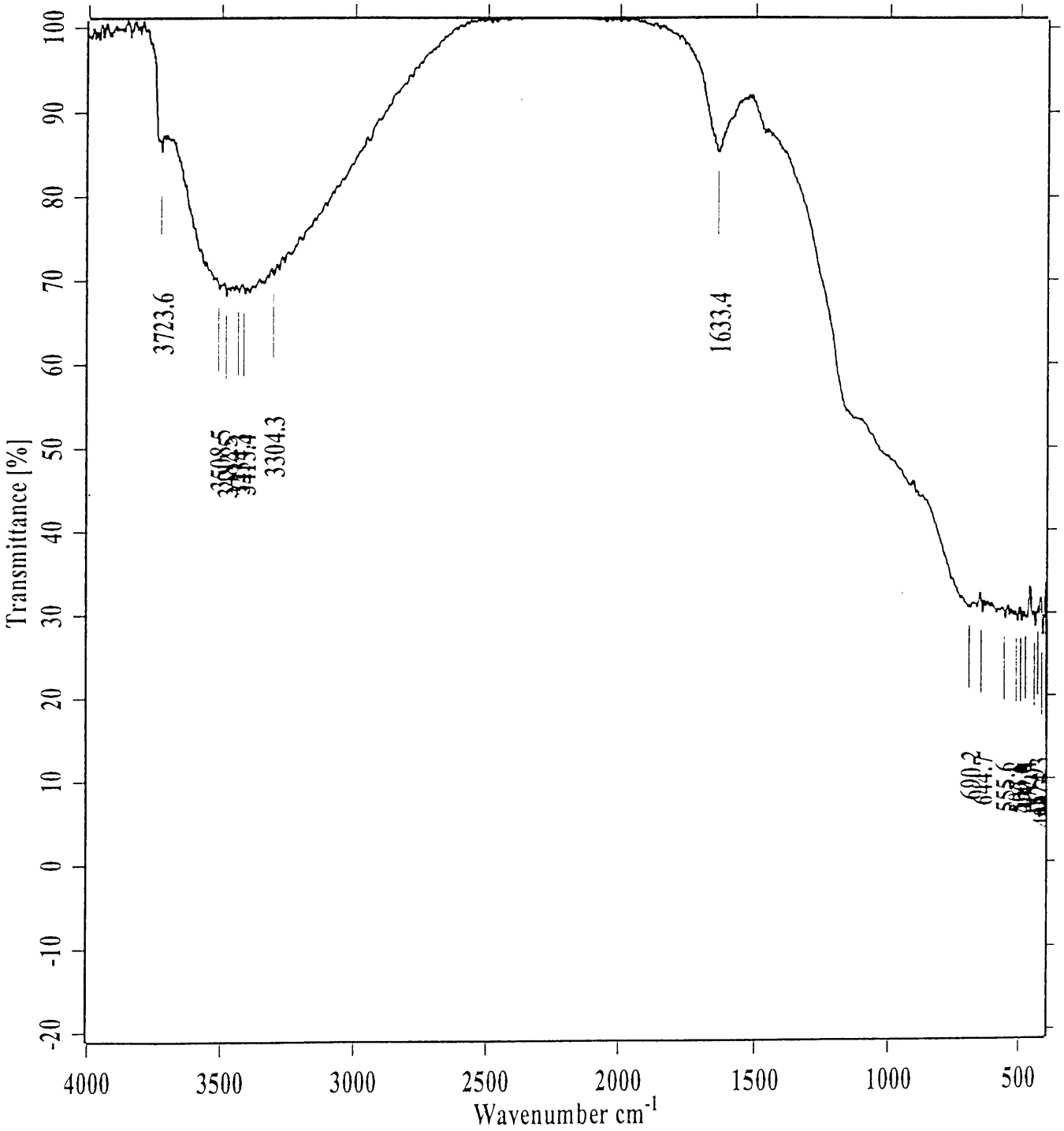

Figure 6.18: Infrared spectrum of sample AS5.

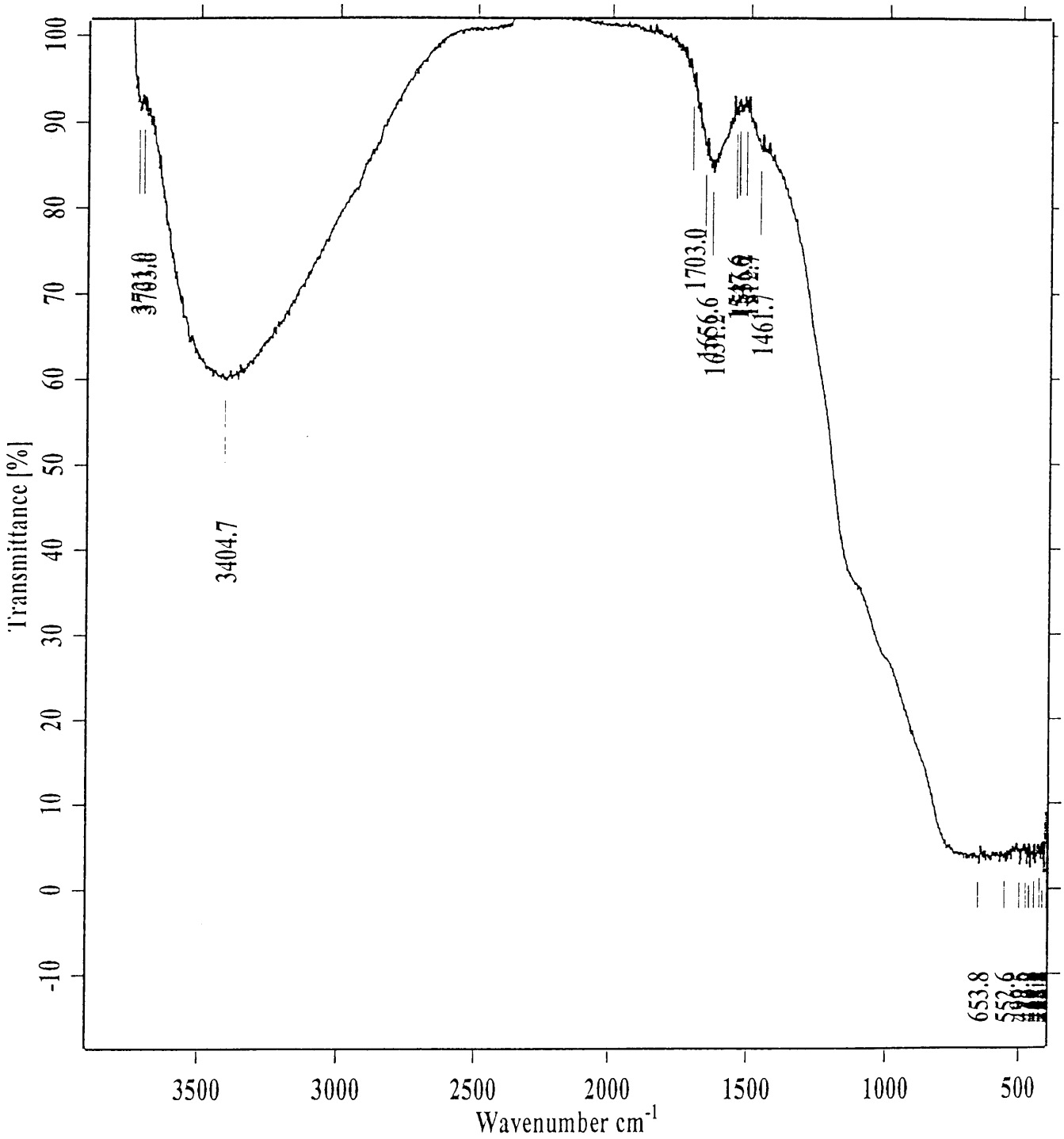

Figure 6.19: Infrared spectrum of sample AS6.

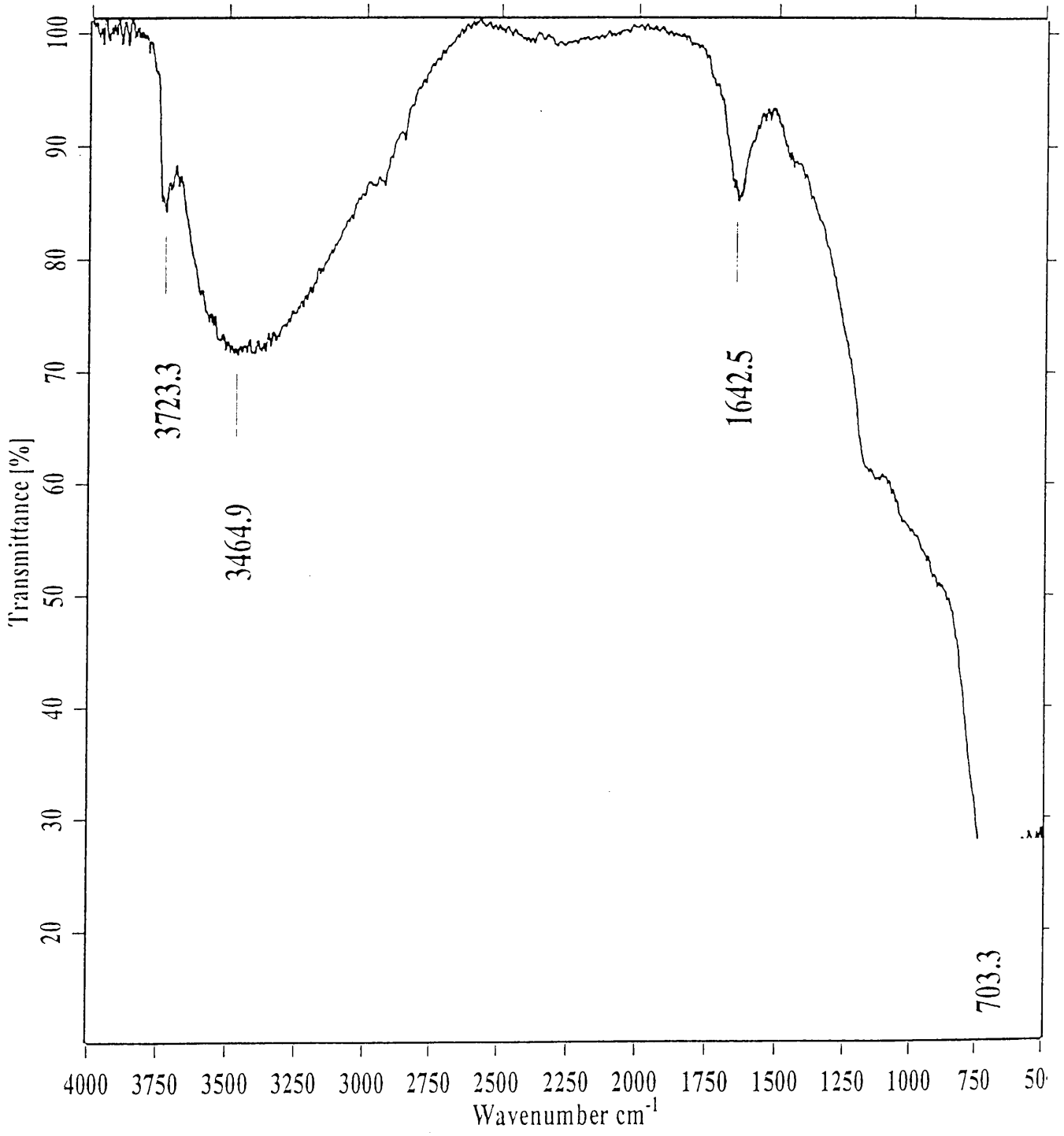

Figure 6.20: Infrared spectrum of sample AS7.

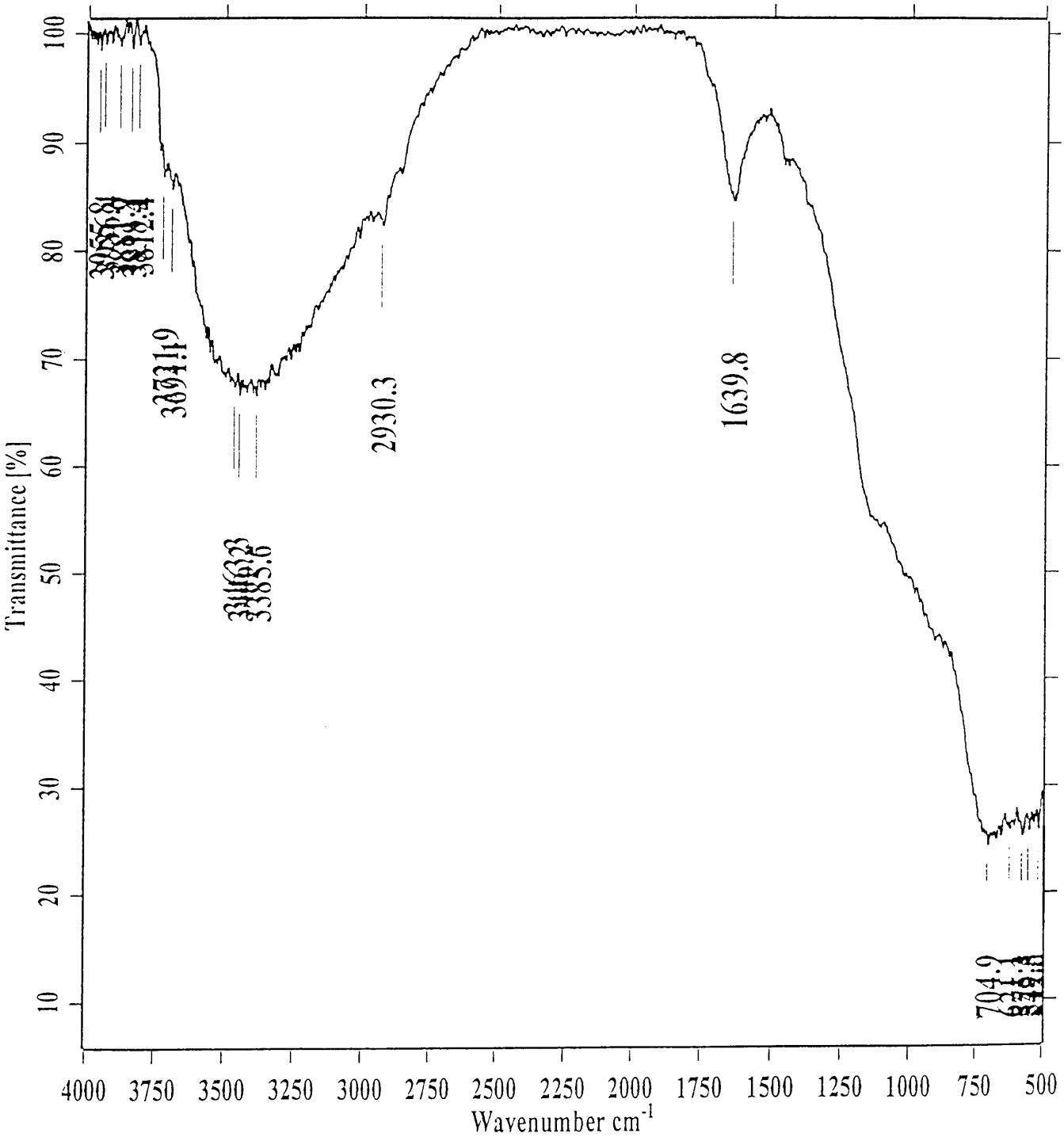

Figure 6.21: Infrared spectrum of sample AS12.

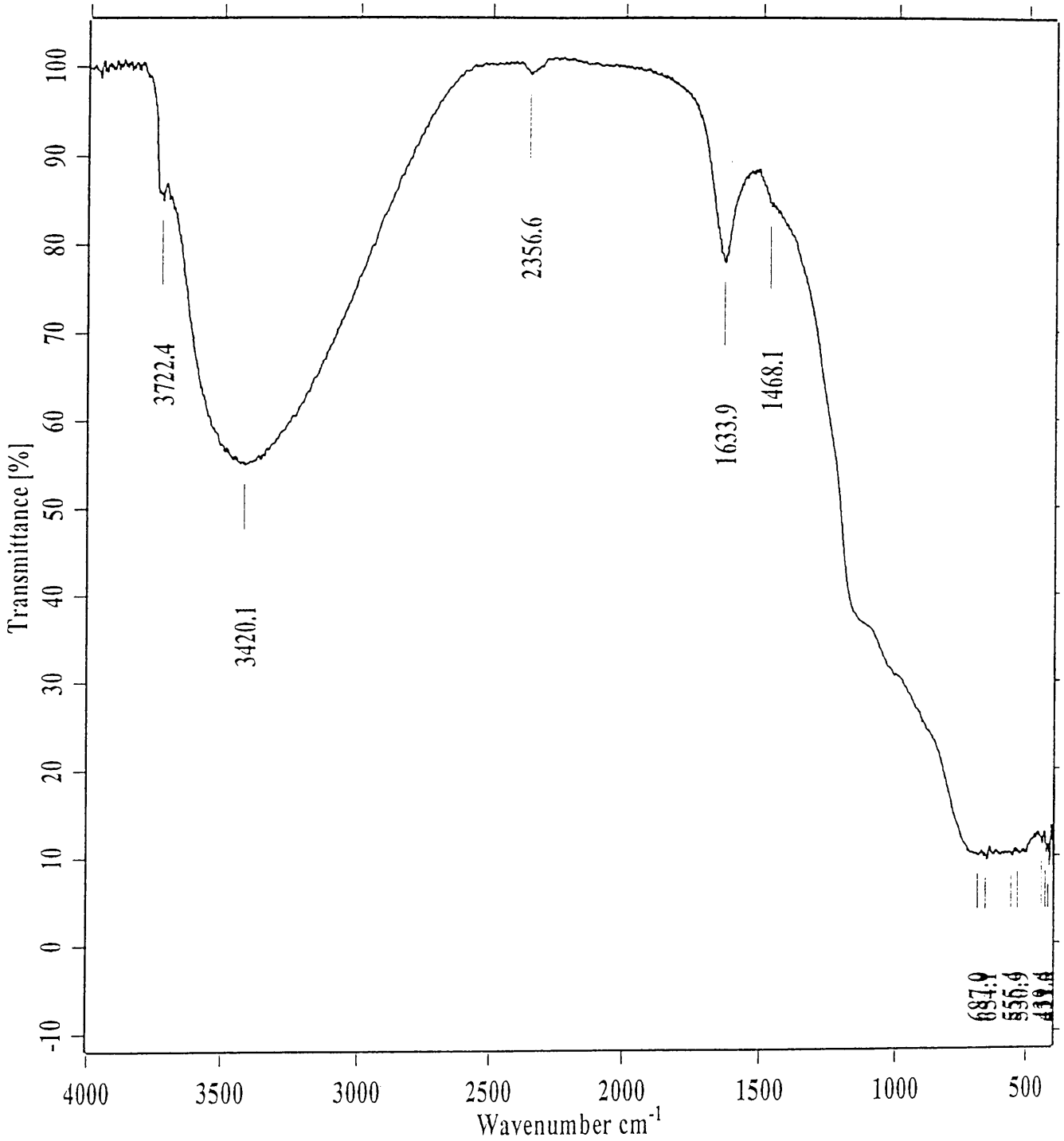

Figure 6.22: Infrared spectrum of sample AS14.

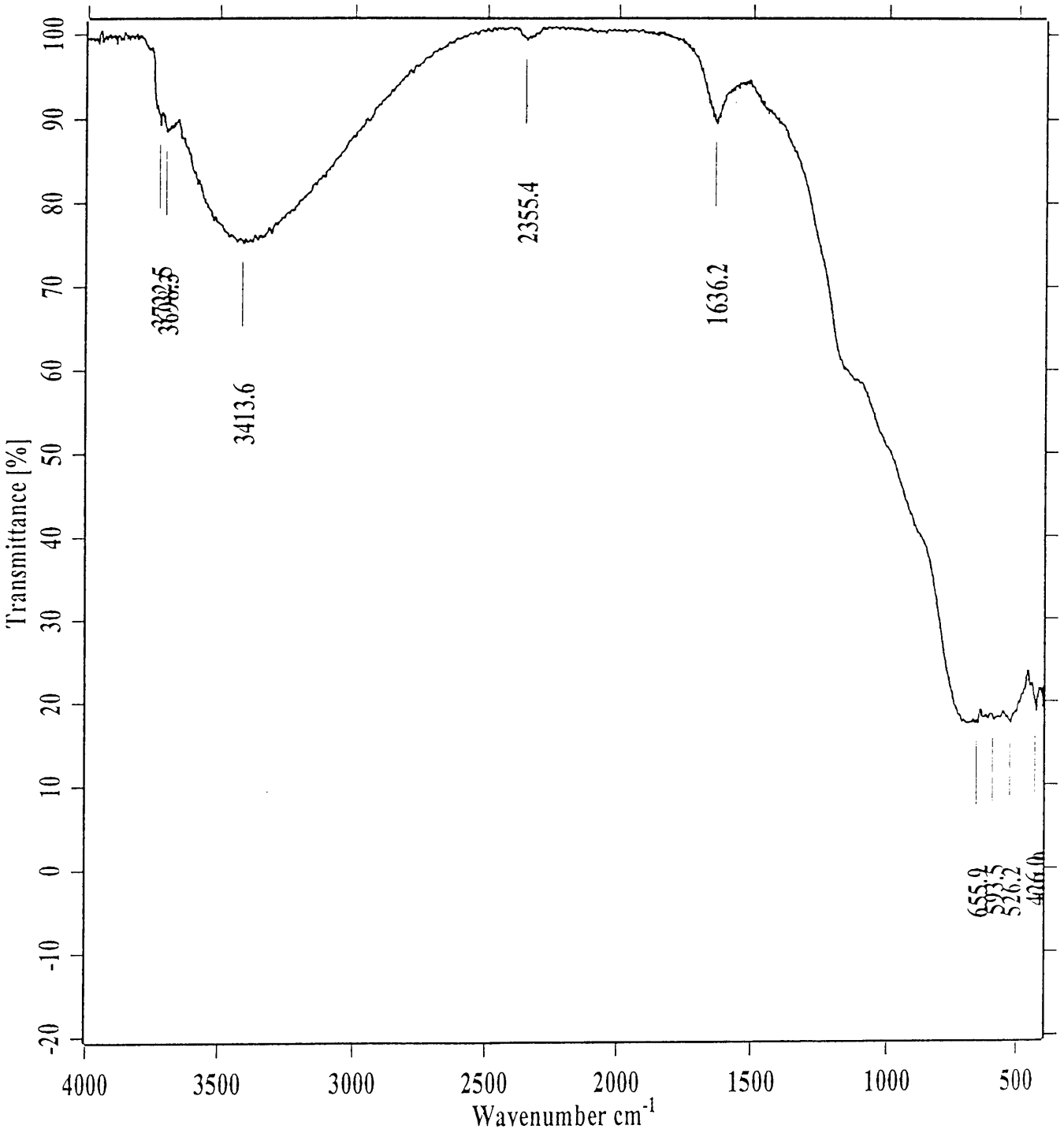

6.3.3. INFRARED SPECTROSCOPY OF ORGANIC TREATED TiO_2

The following spectra show the influence of dimethyl amine (figure 6.23), ammonia (figure 6.24) and ethylene diamine (figure 6.25) vapour on the surface of the TiO_2. The same trend is visible in all the vapours namely a decrease in the bands between 4000cm^{-1} and 2500cm^{-1} with an increase in temperature which is different from that of water. The most obvious difference in these spectra is that the samples treated with vapours generated from 25% solution, still show the broad water band at 3400cm^{-1} similar to the water treated samples while the spectra of the samples treated with ethylene diamine are completely different. A possible reason for this behaviour can possibly be found in the fact that both ammonia(bp 240K) and dimethyl amine(bp 279.8K) are more volatile than ethylene diamine(bp 390K). This means that ammonia and dimethyl amine adsorb on the surface as shown by previous authors [16] but evaporated under evacuation at room temperature. This can also be proved by the presence of an N-H band in the dimethyl amine spectrum while no band is observed for the samples treated with ammonia.

No significant difference is visible between the samples treated with ammonia gas and the samples treated with gas generated from the 25% ammonia solution. As in the case with the water treated samples the 873K sample deviates from the sequence.

In the spectra of the samples treated with ethylene diamine the N-H stretching vibrational bands are clearly visible at 3306cm^{-1} and the deformation bands at 1587cm^{-1}. The C-H stretch vibration of the ethylene is responsible for the band at 2950cm^{-1} with deformation bands at 1483cm^{-1}. More significant is the disappearance of the 3700cm^{-1} band suggesting a lower concentration of terminal hydroxyl groups.

Considering the fact that less oxygen is available for the samples exposed to amines compared to the samples exposed to air and water vapour, these results correlate with the work done by Tanaka et al. [14] proving that reduced samples showed less ability to retain water than oxidized samples. Tanaka suggested that reduction leads to lower coordination through the loss of surface oxygen ions and simultaneously the formation of Ti^{+3} sites which

are active for the dissociation of water.

Looking at the trend in the spectra for the samples treated with amines it is suggested that oxygen ions are driven off the surface by terminal treatment and the simultaneous formation of Ti^{+3} ion sites and this effect is more visible at higher temperatures. This is responsible for the decrease in the intensity of the water band at 3400cm^{-1} with increasing temperature. In both the ethylene diamine and dimethyl amine samples, the intensity of the N-H and C-H vibration bands also decrease with an increase in temperature. It is therefore suggested that the amines form hydrogen bonds with the water on the surface as a method of coupling. Therefore less amines adsorb on the surface when less water is available. Another proof for this statement is the broad band observed in the ethylene diamine spectrum which is an indication of hydrogen bonding.

There is also a difference in the intensities of the OH band at 3700cm^{-1}. The samples treated with dimethyl amine seems to have less hydroxyl groups bounded on the surface and in this spectrum the N-H stretch vibration from the amine is also visible at 2967cm^{-1}. In the ethylene diamine samples no hydroxyl band is visible at 3700cm^{-1}. This is a indication that the hydrogen bonding also take place between the amine and the hydroxyl groups on the surface because, even at low temperatures, no hydroxyl groups can be detected. These results correlate with work done by Primet, Pichat and Mathieu [10] on rutile surfaces using ammonia.

Figure 6.23: Infrared spectrum of DMA samples.

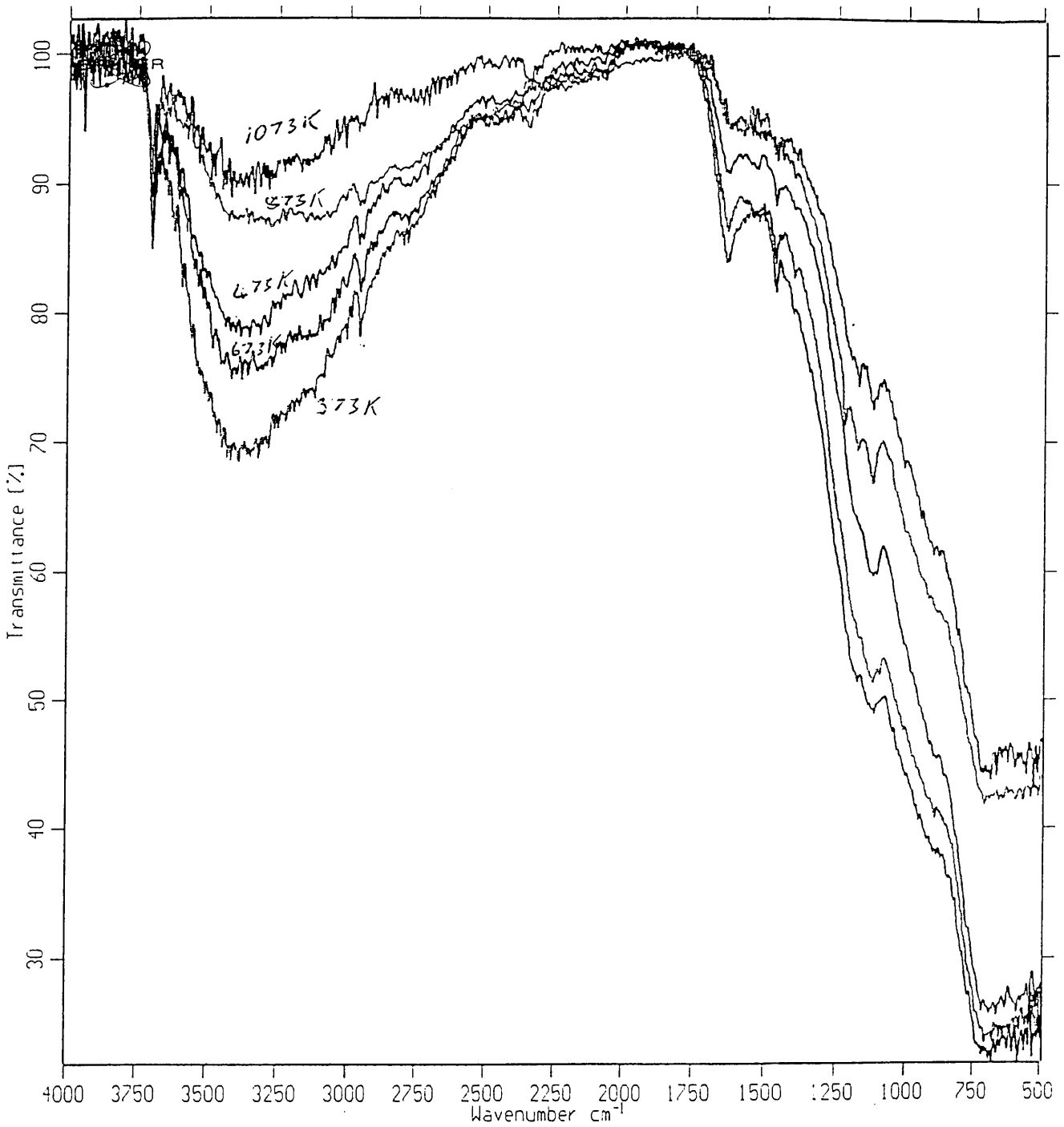

Figure 6.24: Infrared spectrum of AM samples.

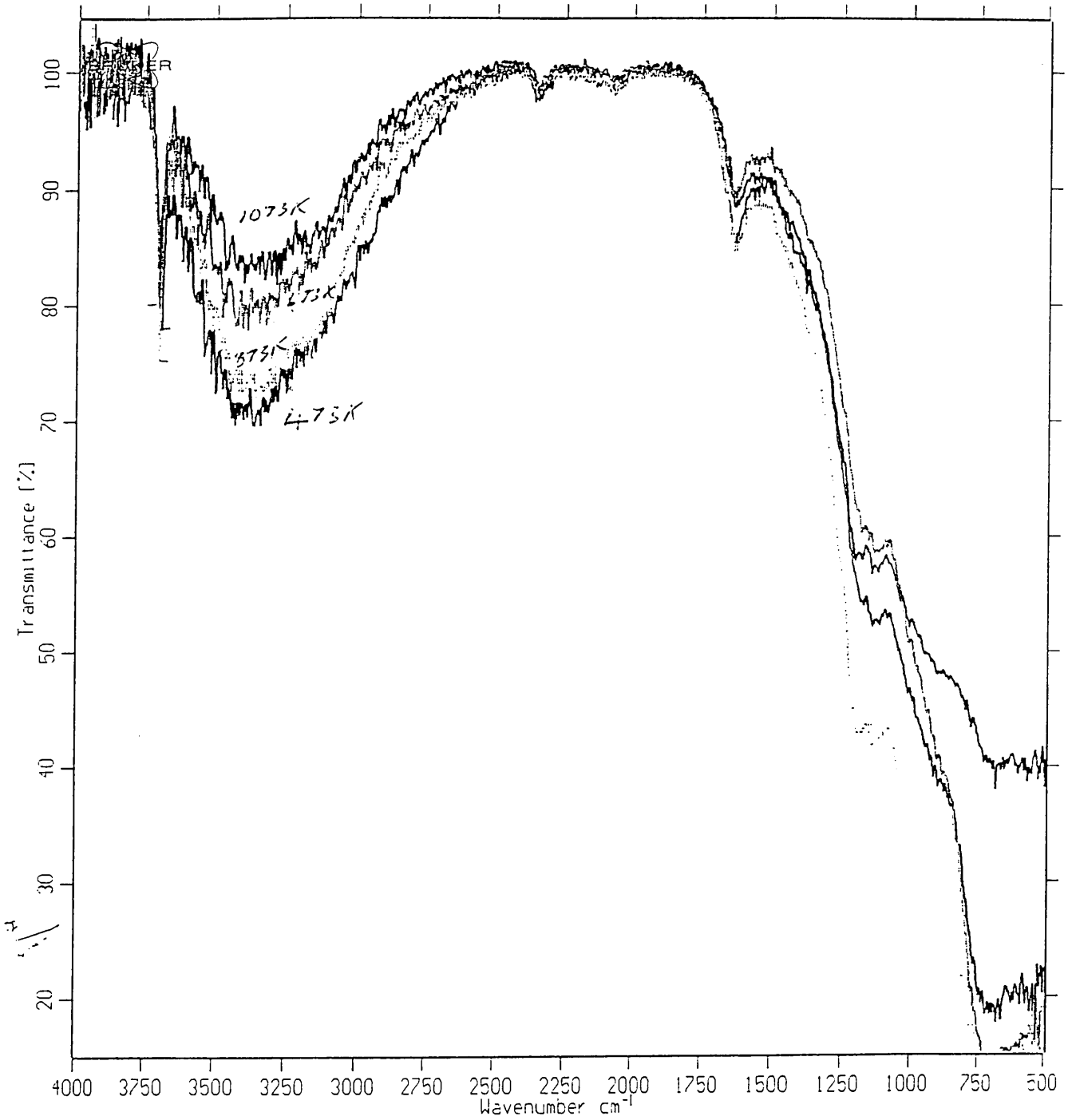

Figure 6.25: Infrared spectrum of EDA samples.

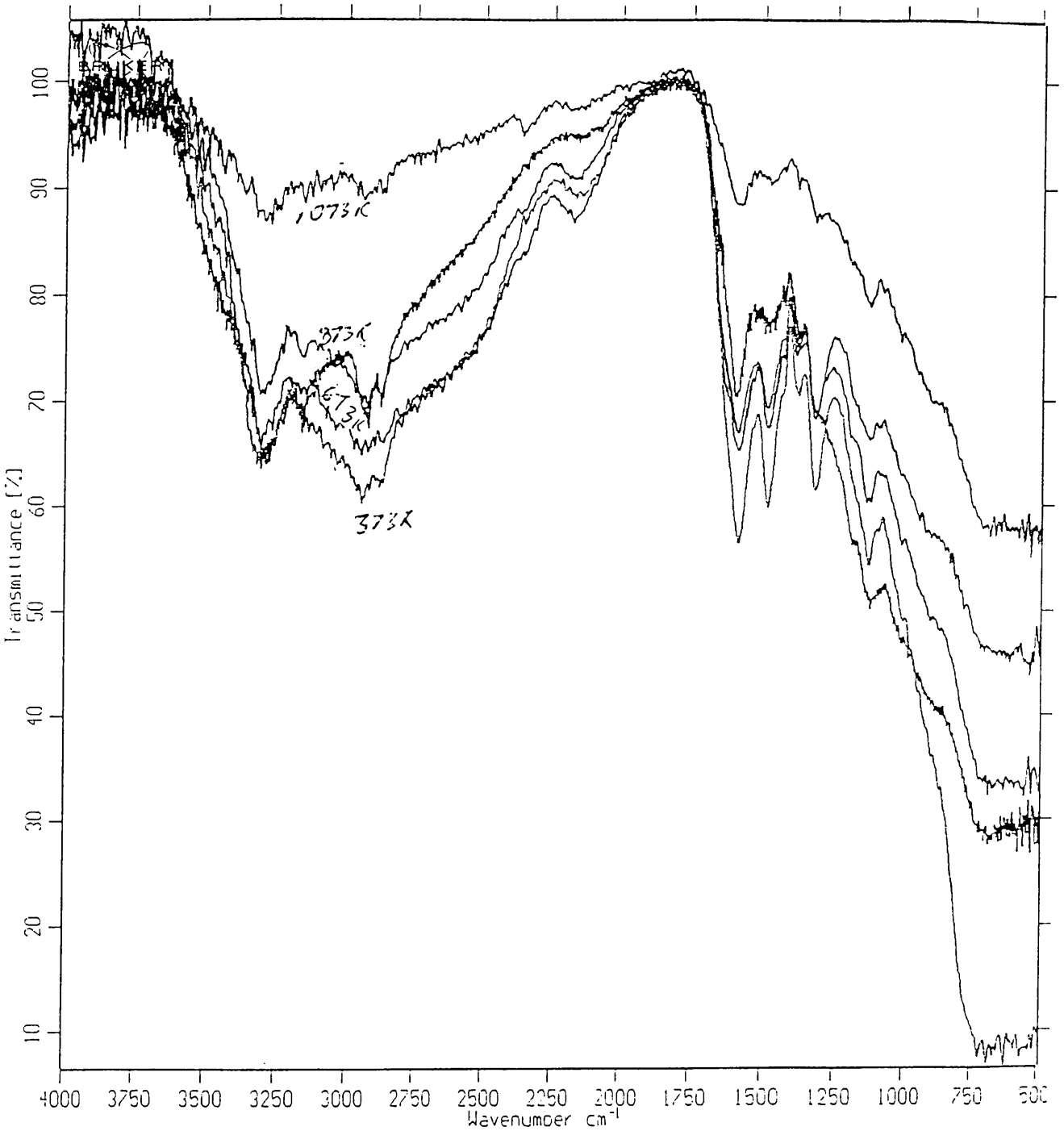

Evidence for hydrogen bonding can also be found by comparing the following spectrum for ethylene diamine from the literature [17] with the samples treated with ethylene diamine.

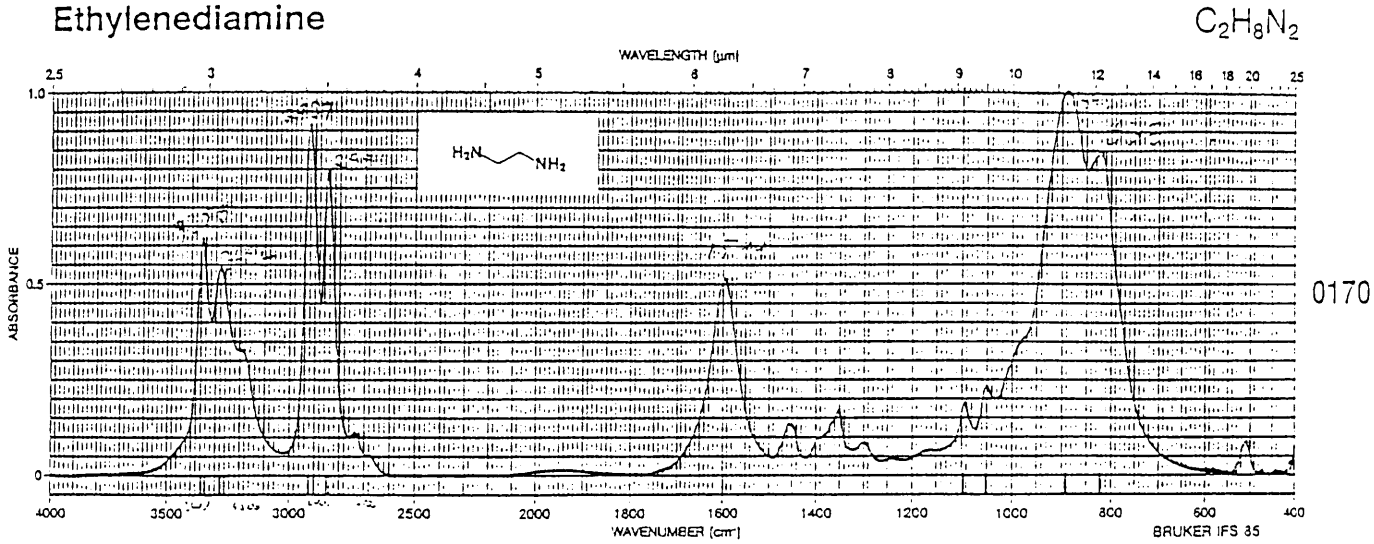

In the spectrum the two N-H stretch vibration bands are visible at 3358cm^{-1} and 3284cm^{-1} with a deformation band at 1599cm^{-1}. In the samples treated with ethylene diamine a significant shift to a lower wave number is observed for this band which is an indication of hydrogen bonding. When less water is available on the surface (higher temperatures) the N-H stretch band move to a higher wave number, closer to the original band.

The rehydroxylation of EDA473 sample can be seen in figure 6.26. In the original sample no OH band is visible at 3700cm^{-1} in the spectrum but rehydroxylation starts at 373K and increase until the original TiO_2 spectrum is visible at 573K. This is again an indication of hydrogen bonding between the amine and the hydroxyl groups on the surface because there is a relation between the intensities of the hydroxyl band and the amine bands. Because the N-H stretch vibration overlap with the broad O-H stretch vibration of water, it is very

difficult to quantify the intensities of the amine above 473K. This is also what happened with the samples treated with ammonia and dimethyl amine.

The good dispersion stability of amine treated TiO_2 showed in chapter 4 is because of hydrogen bonds formed between the adsorbed amines and the water causing structural viscosity. This shows the importance of hydrogen bonding in surface chemistry.

Figure 6.26: Infrared spectrum of the EDA473 sample indicating rehydroxylation.

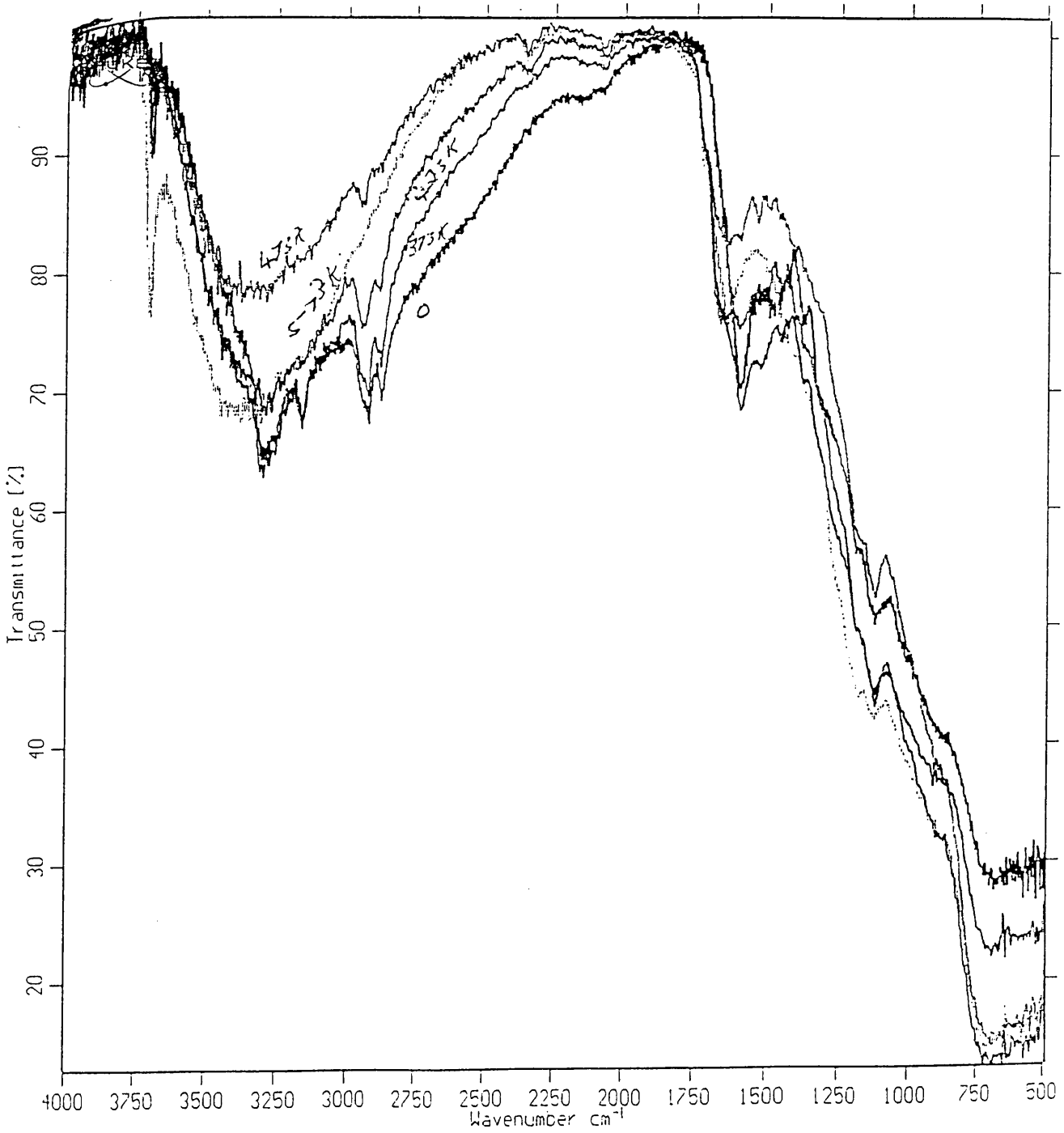

6.4. CONCLUSION

Infrared spectroscopy proved to be a useful technique for the characterization of functional groups on the TiO_2 surface. Different qualities of the treated TiO_2 were measured in the previous chapter. The purpose of this chapter was to explain some of these qualities.

Infrared transmittance spectra of rutile and anatase have been measured. Two sharp bands (3670 and 3700 cm^{-1}) in the OH-band region have been identified with the 3700cm^{-1} band very prominent at rutile surfaces. All the TiO_2 spectra showed a broad band at 3400cm^{-1} which is assigned to the ν_{OH} stretch band of water and the $\delta_{H\text{-}O\text{-}H}$ band was seen at 1636cm^{-1}.

The pH had a big influence on especially the 3700cm^{-1} band. At a lower pH the 3670 cm^{-1} band was more visible and at a higher pH the 3700 cm^{-1} band was more prominent.

The band at 3700 cm^{-1} was assigned to terminal hydroxyl groups and the band at 3670 cm^{-1} to bridged hydroxyl groups by considering the mechanism of adsorption discussed by Solomon, et al. [6] and this is supported by the results obtained from different pH values.

All the IR bands increase in intensities with temperature. This is because more Ti^{+4} sites were formed on the surface resulting from the loss of adsorbed species. The temperature supplied enough energy to dissociate adsorbed water on the surface, increasing the formation of terminal hydroxyl groups. Heat treatment provided sufficient energy to reduce the TiO_2 surface through the loss of surface oxygen ions, which lead to lower coordination and simultaneously the formation of Ti^{+3} sites. These sites are active in the dissociation of water coordinated on the surface resulting in the formation of hydroxyl groups. If the samples are exposed to water vapour after heat treatment there is an increase in physically adsorbed water.

6.5. REFERENCE

1. Little, L.H. 1966. *Infrared Spectra of Adsorbed Species*. London en New York: Academic Press.

2. Hair, M.L. 1967. *Infrared Spectroscopy in Surface Chemistry*. New York: Marcel Dekker.

3. Parfitt, G.D. Rochester, C.H. 1976. Surface Characterization: Chemical. In Parfitt, G.D. & Sing, K.S. *Characterization of Powder Surfaces*. London en New York: Academic Press.

4. Pimentel, G.C. McClellan, A.L. 1960. The Hydrogen Bond. In Parfitt, G.D. & Sing, K.S. *Characterization of Powder Surfaces.* London en New York: Academic Press.

5. Parfitt, G.D. 1976. The Surface of TiO_2. In *Progress in Surface and membrane Science.* **11**, 181-219.

6. Solomon, D.H. Hawthorne, D.G. 1983. *Chemistry of Pigments and Fillers.* New York en Brisbane: John Wiley & Sons.

7. Boehm, H.P. 1971. In *Progress in Surface and membrane Science.* **11**, 190.

8. Pichat, P. Mathieu, M.V. 1969. J. Chim. Phys. 66, 854. In Parfitt, G.D. & Sing, K.S. *Characterization of Powder Surfaces.* London en New York: Academic Press.

9. Morterra, C. 1988. An Infrared Spectroscopic Study of Anatase Properties. *J. Chem. Soc., Faraday Trans. 1.* 84(5), 1617-1673.

10. Primet, M. Pichat, P. Mathieu, M.V. 1971. Infrared study of the Surface of Titanium Dioxides. *The Journal of Physical Chemistry*. 75(9):1971.

11. Zettlemoyer et al .1966. In Parfitt, G.D. Cadenhead. Danielli. 1976. *Progress in surface and membrane science.* 11:186.

12. Morimoto et al . 1969. In Parfitt, G.D. Cadenhead. Danielli. 1976. *Progress in surface and membrane science.* 11:188

13. Ganichenko et al. 1961. In Parfitt, G.D. Cadenhead. Danielli. 1976. *Progress in surface and membrane science.* 11:188

14. Tanaka, K. White, J.M. 1982. Characterization of Species Adsorbed on Oxidized and Reduced Anatase. *The Journal of Physical Chemistry*. 86(24):4708.

15. Morterra, C. Cerrato, G. Visca, M. Lenti, D.M. 1991. IR Surface Characterization of Some TiO_2-Based Pigments. *Chem. Mater.* 3, 132-142.

16. Pichat,P. Mathieu, M.V. Imelek,B.(1969). In Parfitt, G.P. Sing K.S.W. 1976. *Characterization of Powder Surfaces*. Academic Press: London. 65.

17. Merck. 1988. *Merck FT-IR Atlas*. VCH Publishers:Weinheim, Germany. 57.

CHAPTER 7

Conclusion

CHAPTER 7

CONCLUSION

The economic importance of TiO_2 was discussed in chapter one. Considering the fact that South Africa has the largest economic reserves of ilmenite, it is not surprising that a lot of research is currently done on this mineral either on the mining and production side. In this industry huge amount of capital and technology is involved in surface treatment and therefore it is important to have a basic knowledge of the chemistry involved on the TiO_2 surface.

TiO_2 was treated with inorganic and organic surface agents under different conditions and the aim was to improve the qualities of the pigment. It was proved that the precipitation behaviour of silica and alumina is strongly dependant upon the experimental conditions. Silica precipitated with a poor yield, but this was improved by increasing the neutralization time. Sodium aluminate gave a good yield in the precipitation of Al_2O_3 on the surface and is less dependant on the rate of precipitation.

From these results it was concluded that the coating of TiO_2 with alumina and silica is a complex co-precipitation process where the silica is believed to precipitate first, followed by the formation of an alumino-silica intermolecular mixture.

Surface area measurements indicated a sharp increase for alumina treated samples and this increase was more prominent when silica was also present in the coating. An increase of 2.293 m^2/g was observed for each Al_2O_3 % coated on the surface. This increase was assigned to interstitial material not bounded to the surface and a porous alumina layer. The surface area of treated TiO_2 powders showed that the alumina-bearing chemical and the precipitation procedure have a tremendous effect on the morphology of the coating and therefore also on the qualities of the final pigment.

Good dispersion and durability are two important qualities in the TiO_2 pigment industry and

these qualities can be controlled by coating the pigment with organic and inorganic materials. It is a difficult matter to quantify the effectiveness of the coating, but in this study the surface treatment of TiO_2 was evaluated by using sedimentation and the degradation of methylene blue.

Silica treated samples gave a good dispersion stability and a high photo-activity, while alumina treated samples on the other hand gave poor stability and low photo-activity especially at coating percentages higher than one. The reason for the low photo-activity is because alumina act as a strong electron acceptor on the surface and prevent the formation of hydroxyl radicals. Silica increased the photo-activity because methylene blue adsorbs more on silica treated samples and this brings the MB molecules in closer contact with the hydroxyl radicals.

TiO_2 treated with mixtures of silica and alumina showed improved qualities. Good dispersion stability was observed with a Si/Al ratio higher than 0.6 but at this ratio the molecular mass of alumina had an effect on the stability.

For optimum durability and dispersion stability it is therefore suggested that TiO_2 is treated with a mixture of silica and alumina and preferably with a Si/Al ratio between 0.7 and 1. These results proved the importance of surface treatment in pigment manufacturing.

In this study zeta potential measurements were used to explain the dispersion stability of the treated TiO_2. Treatment of TiO_2 with SiO_2 resulted in more negative zeta potential values than rutile and alumina treatment gave more positive values. Incomplete coverage of the coating resulted in a surface charge closer to that of TiO_2. TiO_2 treatment with a mixture of silica and alumina resulted in the formation of a alumino-silica intermolecular mixture with a silica like surface, even for low percentages. The large negative zeta potential values reported for samples with silica in the coating, are responsible for the good dispersion stability.

The amphoteric dissociation of hydroxyl groups on the TiO_2 particle plays an important roll in the surface charge and therefore the precipitation of other particles on the surface. It was

concluded that the precipitation of Al_2O_3 from sodium aluminate reached a maximum at pH 8 because this pH is close to the i.e.p. of alumina and therefore the particles are attracted to the negative TiO_2 surface. Silica adsorbs on positive sites on the surface and this causes the low precipitation yield reported. The yield is improved when the oxides are precipitated simultaneously because the alumina creates positive sites on which the silica can precipitate. It was also proved that colloidal stability occurs if the surface charge is approximately -20 mV and this is why coagulation occurred at pH values lower than 4.

Infrared spectroscopy proved to be a useful technique for the characterization of functional groups on the TiO_2 surface. Two sharp bands (3670 and 3700 cm^{-1}) in the OH-band region have been identified and all the TiO_2 spectra showed a broad band at 3400cm^{-1} which is assigned to the ν_{OH} stretch band of water and the $\delta_{H\text{-}O\text{-}H}$ band was seen at 1636cm^{-1}. The band at 3700 cm^{-1} was assigned to terminal hydroxyl groups and the band at 3670 cm^{-1} to bridged hydroxyl groups.

Heat treatment provided sufficient energy to reduce the TiO_2 surface through the loss of surface oxygen ions, which lead to lower coordination and simultaneously the formation of Ti^{+3} sites. These sites were active in the dissociation of water coordinated on the surface resulting in the formation of hydroxyl groups.

The finger print band for silica treated samples (v SiO-H) was observed at 3740cm^{-1}. The dispersion stability increased for silica treated samples because of the acidity of this hydroxyl groups. Silica treated samples were more photo-active because MB adsorbed to a greater extend on silica surfaces.

A large broad band between 4000cm^{-1} and 2500cm^{-1} was characteristic of alumina treated samples. This was due to water retained in the porous coating layer and correlated with surface area measurements.

Treatment with mixed oxides showed that a controlled coverage of surface hydroxyl groups can result in good stability and low photo-activity.

Amines adsorb on the surface of TiO_2 by forming hydrogen bonds with the water coordinated on the surface and also with hydroxyl groups on the surface. N-H stretch vibrations were observed at 3306cm^{-1} for ethylene diamine with a deformation band at 1587cm^{-1} and C-H stretch vibrations at 2950cm^{-1} with a deformation band at 1483cm^{-1}, but ammonia and dimethyl amine were too volatile to detect under vacuum at room temperature.

No hydroxyl groups were visible in the spectra of the samples exposed to ethylene diamine because of hydrogen bonding. The N-H vibration bands shifted to lower wave numbers and the hydroxyl band re-appeared when the amine was driven off the surface by heat treatment.

The importance of steric stabilization was proved by the good dispersion stability of the samples treated with an amine. This stability was due to hydrogen bonding between the surface of the TiO_2 and the amine as well as the water in the surroundings and therefore the hydrogen bonding created a structural viscosity.

These experiments gave a clear indication that hydrogen bonding is very important in the dispersion stability of TiO_2. Dispersion stability in inorganic treated samples are mainly created by surface charge, although hydrogen bonding also play an important role. The terminal hydroxyl groups on the surface are therefore mainly responsible for dispersion stability and also photo-activity. For optimum pigment qualities it is therefore important to control the terminal hydroxyl groups on the rutile surface.

APPENDIX I

Surface Area

APPENDIX 1

SURFACE AREA

One form of the well-known BET equation [1] that describes the adsorption of a gas upon a solid surface is:

$$(P/P_0)/V[1-(P/P_0)] = 1/(V_mC) + [(C-1)/(V_mC)]P/P_0 \qquad (1)$$

where V is the volume (at standard temperature and pressure, STP) of gas adsorbed at pressure P, P_0 the saturation pressure which is the vapor pressure of liguified gas at the adsorbing temperature, V_m the volume of gas (STP) required to form an adsorbed monomolecular layer, and C a constant, related to the energy of adsorption.

The surface area S of the sample giving the monolayer adsorbed gas volume V_m(STP) is then calculated from

$$S = V_mAN/M \qquad (2)$$

where A is Avogadro's number which expresses the number of gas molecules in a mole of gas at standard conditions, M the molar volume of the gas, and N the area of each adsorbed gas molecule.

The constant C of equation 1 is typically a relatively large number, i.e., $C >> 1$, from which equation 1 reduces very nearly to

$$(P/P_0)/V[1-(P/P_0)] = (1/V_m)[(1/C)+(P/P_0)] \qquad (3)$$

Now if $P/P_0 >> 1/C$, equation 3 can be further represented by

$$(P/P_0)/V[1-(P/P_0)] = (1/V_m)(P/P_0) \qquad (4)$$

which rearanges to

$$V_m = V[1-P/P_0] \quad (5)$$

Substituting equation 5 into 2 yields

$$S = VAN\,[1-P/P_0]/M \quad (6)$$

from which the sample surface area is readily determined once the volume V of gas adsorbed (or desorbed, which must be identical) is measured and appropriate values for the other terms are incorporated.

The surface area of granulated and powdered solids is measured with the Flowsorb 2300 by determining the quantity of a gas that adsorbs as a single layer of molecules, a so-called monomolecular layer, on a sample [2]. This adsorption is done at or near the boiling point of the adsorbed gas. Under specific conditions the area covered by each gas molecule is thus directly calculated from the number of adsorbed molecules, which is derived from the gas quantity at the prescribed conditions, and the area occupied by each.

For a nitrogen and helium mixture of 30 volume % nitrogen, conditions most favorable for the formation of a monolayer of adsorbed nitrogen are established at atmospheric pressure and the temperature of liquid nitrogen.

REFERENCES

1. Brunauer, S. Emmett, P.H. Teller, E. 1938. J. Am. Chem. Soc. 60, 309A.

2. Micromeritics. 1985. Instruction manual, Flowsorbs II 2300. 15 June, p 2-1.

APPENDIX II

Infrared Spectroscopy

APPENDIX II

INFRARED SPECTROSCOPY

2.1. INTRODUCTION

IR spectroscopy can be considered as the first and the most important of the modern spectroscopic techniques that has found general acceptance in surface studies of solids. The most common application of IR spectroscopy is to identify adsorbed species on surfaces and to study the way in which these species are chemisorbed on the surface of the catalyst. In addition, the technique is useful in identifying phases that are present in precursor stages of the adsorbed species on a surface. Sometimes the IR spectra of an adsorbed probe molecules such as CO and NO give valuable information on the adsorption sites that are present on the surface.

Vibrations in molecules or in solid lattices are excited by the absorption of photons (infrared spectroscopy), or by the scattering of photons (Raman spectroscopy), electrons (electron loss spectroscopy) or neutrons (inelastic neutron scattering). In case the vibration is excited by the interaction of the bond with a wave field, as with photons and electrons, the excitation is subject to strict selection rules. Collisions, on the other hand, excite all vibrational modes.

Infrared spectroscopy is the most common form of vibrational spectroscopy, and the radiation falls into three categories, as is indicated in table 2.1. In this study the mid-infrared region is of interest to us.

Table 2.1: Classification of infrared radiation

Region	Wavelength (μm)	Energy (meV)	Wavenumber (cm^{-1})	Detection of
Infrared	1000-1	1.2-1240	10-10000	
Far	1000-50	1.2-25	10-200	Lattice vibrations
Mid	50-2.5	25-496	200-4000	Molecular vibrations
Near	2.5-1	496-1240	4000-10000	Overtones

2.2. HISTORY

A few words about the history of infrared spectroscopy. The first report of the systematic use of infrared radiation is due to Coblentz in 1905 who investigated water in minerals [1]. Investigations of hydroxyl groups and adsorbed molecules on oxides were made by Terenin and coworkers in Russia in the forties, as described by Kiselev and Lygin [2]. This work was done in the near-infrared region, which offers the advantage that glass is transparent for the radiation in this region and the construction of cells is easy. Commercial infrared instruments become available in the mid 1940's. Until then, Raman spectroscopy dominated the study of vibrations of molecules.

2.3. THEORY OF MOLECULAR VIBRATIONS

Molecules possess discrete levels of rotational and vibrational energy. Transitions between vibrational levels occur by absorption of photons with frequencies v in the mid-infrared range (Table 2.1). The C-O stretch vibration, for example, is at 2143cm^{-1}. For small deviations of the constituent atoms from their equilibrium positions, the potential energy V(r) can be approximated by that of the harmonic oscillator:

$$V(r) = 1/2\ k(r-r_{eq})^2 \qquad (1)$$

in which

- V(r) is the interatomic potential
- r is the distance between the vibrating atoms
- r_{eq} is the equilibrium distance between the atoms
- k is the force constant of the vibrating bond.

The corresponding vibrational energy levels are equidistant (see Figure 2.1):

$$E_n = (n + 1/2)hv \qquad (2)$$

$$v = 1/(2\pi)\sqrt{(k/\mu)} \qquad (3)$$

$$1/\mu = 1/m_1 + 1/m_2 \text{ or } \mu = (m_1m_2)/(m_1 + m_2) \quad (4)$$

in which:

E_n	is the energy of the n-th vibrational level
n	is an integer
h	is Planck's constant
v	is the frequency of the vibration
k	is the force constant of the bond
μ	is the reduced mass
m_i	is the mass of the vibrating atoms.

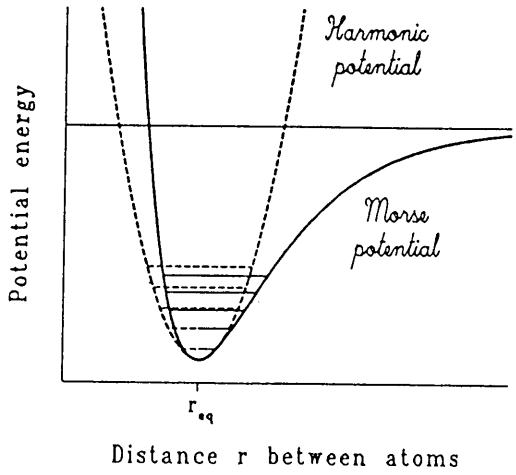

Figure .1: The harmonic potential and the Morse potential, together with vibrational energy levels. The harmonic potential is an acceptable approximation for molecular separations close to the equilibrium distance and vibrations up to the first excited level, but fails for higher excitations. The Morse potential is more realistic. Note that the separation between the vibrational levels decreases with increasing quantum number, implying, for example, that the second overtone occurs at a frequency slightly less than twice that of the fundamental vibration.

Thus, vibrational frequencies increase with increasing bond strength and with decreasing mass of the vibrating atoms. Allowed transitions in the harmonic approximation are those for which the vibrational quantum number changes by one unit. Overtones, i.e. absorption of light at a whole number times the fundamental frequency, would not be possible. A general

selection rule for the absorption of a photon is that the dipole moment of the molecule must change during the vibration. This distinguishes infrared from Raman spectroscopy where the selection rule requires that the molecular polarizability changes during the vibration.

The harmonic approximation is only valid for small deviations of the atoms from their equilibrium positions. The most obvious shortcoming of the harmonic potential is that the bond between two atoms cannot break. A physically more realistic potential is the Morse potential (Figure 2.1):

$$V(r) = D(1-e^{-a(r-req)})^2 - D \qquad (5)$$

in which

V(r) is interatomic potential

r is the distance between the vibrating atoms

r_{eq} is the equilibrium distance between the atoms

D is the dissociation energy of the vibrating bond

a is the parameter which controls the steepness of the potential well.

In this potential the energy levels are no longer equally spaced and overtones, i.e. vibrational transitions with $\blacktriangle n > 1$, become allowed. The overtone of gaseous CO at 4260 cm^{-1} (slightly less 2 x 2143 = 4286 cm^{-1}) is an example. For small deviations of r from equilibrium, however, the Morse potential is successfully approximated by a parabola and for the interpretation of IR spectra the harmonic oscillator description is usually sufficient.

The simple harmonic oscillator picture of a vibrating molecule has important implications. First, knowing the frequency, one can immediately calculate the force constant of the bond. Note that the latter corresponds to the curvature of the interatomic potential and not to its depth, the bond energy. However, as the depth and the curvature of a potential usually change hand in hand, it is often permissible to take the infrared frequency as an indicator for the strength of the bond. Second, isotopic substitution can be useful in the assignment of frequencies to bonds in absorbed species, because frequency shifts due to isotopic substitution (of for example D for H in absorbed ethylene, or OD for OH in methanol) can be predicted directly. See Table 2.2 for an example.

Table 2.2: C-O stretch frequency of different isotopic combinations

Molecule	V(CM^{-1})
$^{12}C^{16}O$	2143
$^{13}C^{16}O$	2096
$^{12}C^{18}O$	2091
$^{13}C^{18}O$	2042

The number of different vibrations that a molecule possesses, follows from the following considerations. A molecule consisting of N atoms has 3N degrees of freedom. Three of these are translational degrees of freedom of the molecule and three are rotations of the molecule along the three principle axes of inertia. Linear molecules have only two rotational degrees of freedom, as no energy change is involved in the rotation along the main axis. Thus, the number of fundamental vibrations is 3N-6 for a non-linear and 3N-5 for a linear molecule. In addition, there are overtones and combinations of fundamental vibrations. Fortunately, however, not all vibrations are visible.

There are four types of vibration, as illustrated by figure 2.2, each with a characteristic symbol:

- stretch vibrations (symbol v), changing the length of the bond,
- bending vibrations in one plane (symbol δ), changing bond angles but leaving bond lengths unaltered (in larger molecules further divided into rock, twist and wag vibrations),
- bending vibrations out of plane (symbol y), in which one atom oscillates through a plane defined by at least three neighbouring atoms,
- torsion vibrations (symbol τ) changing the angle between two planes through atoms.

Generally, the frequencies of these vibrations decrease in the order $v > \delta > y > \tau$. In addition, vibrations are divided into symmetric and asymmetric vibrations (v_s and v_{as}). For more details we refer to textbooks on infrared spectroscopy [3-6].

Not all vibrations can be observed: Absorption of an infrared photon occurs only if a dipole moment changes during the vibration. It is not necessary that the molecule possesses a permanent dipole, it is sufficient if a dipole moment changes during the vibration. The

intensity of the infrared band is proportional to the change in dipole moment. Although this statement is of little practical value, as the magnitude of dipole moments during the vibration are not known, it explains why species with polar bonds, such as CO, NO and OH, exhibit strong IR bands, whereas covalent bonds such as C-C or N=N absorb infrared light only weakly and molecules such as H_2, N_2 are not infrared active at all.

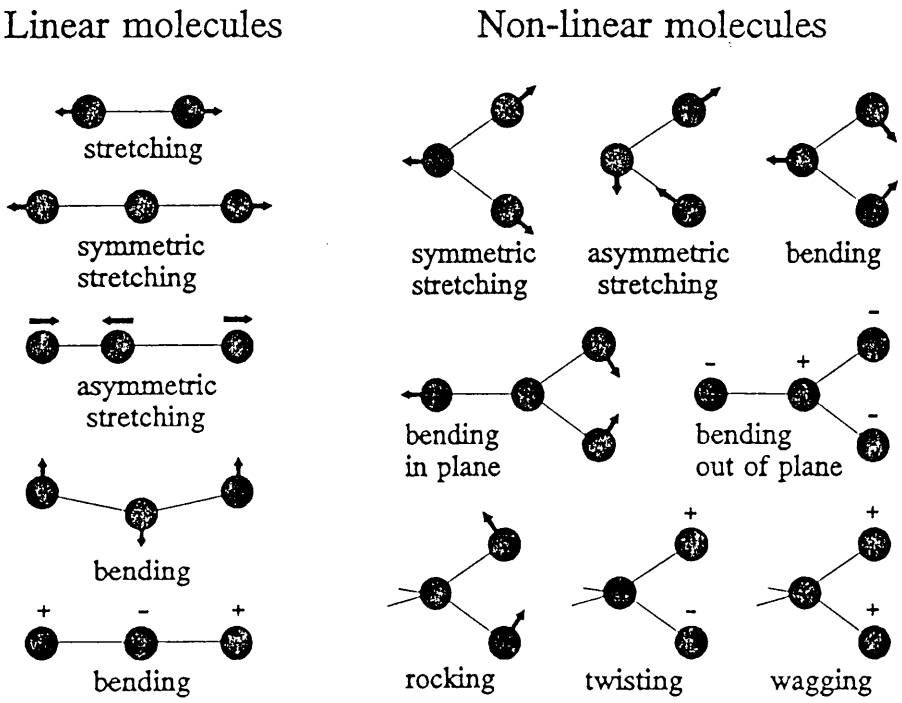

Figure 2: Fundamental vibrations of several molecules.

The group frequency concept states that functional groups in molecules may be treated as independent oscillators, irrespective of the larger structure to which they belong. For example, the C=C double bond of the -CH=CH_2 group varies no more than from 1651 cm^{-1} in propylene, where it is bound to a methyl group, to 1632 cm^{-1} when it is bound to the much heavier CH_2Br group in CH_2Br-CH=CH_2 [5]. As a consequence, infrared frequencies are characteristic for certain bonds in molecules and can also be used to identify species on

surfaces. The following classification of characteristic stretching frequencies is a good starting point for interpreting vibrational spectra.

The infra red region between 4000 and 200 cm^{-1} can roughly be divided into four regions:

- The X-H stretch region (4000 - 2500 cm^{-1}), where strong contributions from OH, NH, CH and SH stretch vibrations are observed,
- The triple bond region (2500 - 2000 cm^{-1}), where contributions from gas phase CO (2143 cm^{-1}) and linearly adsorbed CO (2000 - 2200 cm^{-1}) are seen,
- The double bond region (2000 - 1500 cm^{-1}), where in catalytic studies bridge bonded CO, as well as carbonyl groups in adsorbed molecules (around 1700 cm^{-1}) absorb,
- The fingerprint region (1500 - 500 cm^{-1}), where all single bonds between carbon and elements such as nitrogen, oxygen, sulphur and halogens absorb,
- The M-X or metal-adsorbate region (around 200 - 450 cm^{-1}), where the metal-carbon, metal - oxygen and metal - nitrogen stretch frequencies in the spectra of adsorbed species are observed.

Correlation charts should be consulted for more precise assignments [3-6]. Although we are mainly interested in adsorbed molecules, spectra often contain contributions from gas phase species and therefore some knowledge of gas phase spectra is essential. Molecules in the gas phase have rotational freedom, and as a consequence the vibrational transitions are accompanied by rotational transitions. For a rigid rotor which vibrates as an harmonic oscillator, the expression for the available energy levels is:

$$E_{n,j} = (n+½)hv + [h^2/(8\pi^2 I)]\, j(j+1); \qquad I = \mu r^2 \qquad (6)$$

where

$E_{n,j}$ is the energy of a level with quantum numbers n and j
n is the vibrational quantum number
j is the rotational quantum number
h is Planck's constant
v is the frequency
I is the moment of inertia

μ is the reduced mass

r is the distance between the vibrating atoms.

Here a third selection rule applies: For linear molecules, transitions corresponding to vibrations along the main axis are allowed if $\Delta j = \pm 1$. The $\Delta j = 0$ transition is only allowed for vibrations perpendicular to the main axis. Note that because of this selection rule the purely vibrational transition (called Q branch) appears in the gas phase spectrum of CO_2, but is absent in that of CO. In both cases, two branches of rotational side bands appear (called P and R branch), see figure 2.3 for gas phase CO.

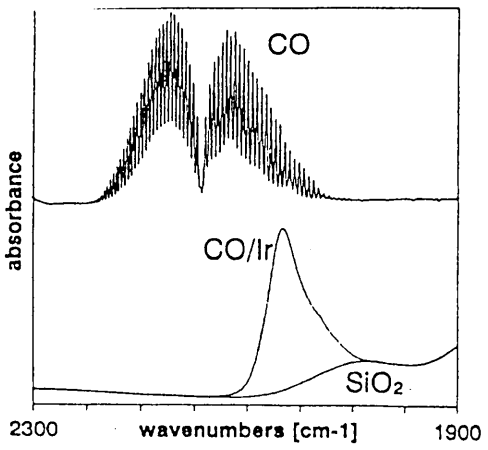

Figure 3: The infrared spectrum of gas phase CO shows rotational fine structure, which is absent in the spectrum of CO adsorbed on an Ir/SiO_2 catalyst (courtesy of L.M.P. van Gruijthuijsen, Eindhoven).

Upon adsorption, the molecule loses its rotational freedom and now only the vibrational transition is observed, however, at a different frequency, see figure 2.3.

In the case of CO, three factors contribute to this shift

a) mechanical coupling of the C-O molecules to the heavy substrate increases the C-O frequency, about 30 cm^{-1} for CO adsorbed on platinum [7],

b) the interaction between the C-O dipole and its image in the conducting, polarizable metal weakens the C-O frequency by 25 - 50 cm^{-1} [8],

c) the formation of a chemisorption bond between the C-O and the substrate alters the distribution of electrons over the molecular orbitals and weakens the C-O bond.

Thus, one must be careful to interpret the frequency difference between adsorbed and gas phase C-O in terms of chemisorption bond strength only.

2.4. INFRARED SPECTROSCOPY

Several forms of infrared spectroscopy are in use, as illustrated in figure 2.4. The most common form of the technique is transmission infrared spectroscopy. In this case the sample consists typically of 10-100mg of catalyst, pressed into a self supporting disk of approximately 1cm^2 and a few tenths of a millimetre thickness. Transmission IR can be applied if the bulk of the catalyst absorbs weakly. This is usually the case with typical oxide supports for wavenumbers above about 1000cm^{-1}, whereas carbon-supported catalysts cannot be measured in transmission mode. Another condition is that the support particles are smaller than the wavelength of the IR radiation, otherwise scattering losses become important.

A great advantage of infrared spectroscopy is that the technique can be used to study catalyst in situ. Several cells for in situ investigations have been described in the literature [3,4]. The critical point is the construction of infrared transparent windows that withstand high temperatures and pressures.

In the diffuse reflectance mode samples can be measured as loose powders, with the advantage that not only the tendinous preparation of wafers is unnecessary but also that diffusion limitations associated with tightly pressed samples are avoided. Diffuse reflectance is also the indicated technique for strongly scattering or absorbing particles. The often used acronyms DRIFT or DRIFTS stand for diffuse reflectance infrared Fourier transform spectroscopy. The diffusely scattered radiation is collected by an ellipsoidal mirror and focused on the detector. The infrared absorption spectrum is described the Kubelka-Munk function:

$$K/S = (1-R_\infty)^2/(2R_\infty) \qquad (7)$$

in which

K is the absorption coefficient, a function of the frequency v

S is the scattering coefficient

R_∞ is the reflectivity of a sample of infinite thickness, measured as a function of v.

If the scattering coefficient does not depend on the infrared frequency, the Kubelka-Munk function transforms the measured spectrum $R_\infty(v)$ into the absorption spectrum K(v). In situ cells for DRIFT studies of catalysts have been described [9] and are commercially available.

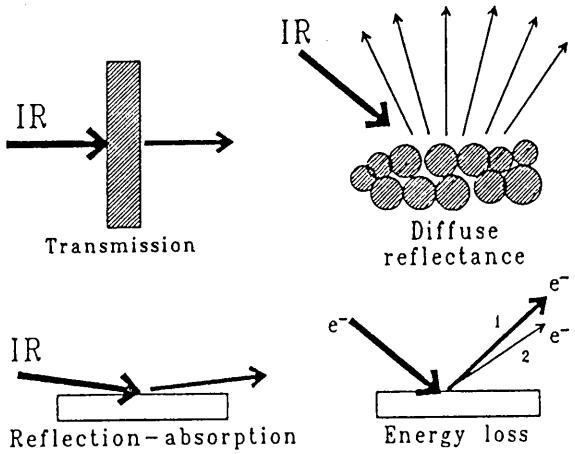

Figure .4: Five different forms of performing vibrational spectroscopy: a) transmission infrared and Raman spectroscopy on a wafer pressed from catalyst powder, b) diffuse reflectance infrared spectroscopy on catalyst powder, c) reflection-absorption infrared spectroscopy of adsorbates on a flat metal surface and d) electron energy loss spectroscopy, also on a flat surface, based on dipole scattering (1) or impact scattering (2).

For measuring infrared absorption spectra of gases adsorbed on the surfaces of metal single crystals or polycrystalline foils, one uses reflection absorption infrared spectroscopy (RAIRS), sometimes also referred to as infrared reflection absorption spectroscopy (IRAS). In RAIRS, the IR beam comes in at grazing angle, i.e. almost parallel to the surface, see Figure 2.4. During reflection the p-component of the IR light (the component perpendicular to the surface) excites those vibrations of the chemisorbed molecule for which the component of the dipole moment perpendicular to the surface changes. This rather strict 'metal surface selection rule' is typical for RAIRS. Although absorption bands in RAIRS have intensities

that are some two orders of magnitude weaker than in transmission studies on supported catalysts, RAIRS spectra can be measured accurately with standard spectrometers.

2.5. EQUIPMENT

The first generation of infrared spectrometers was of the energy dispersive type: A monochromator (initially a prism, after the mid 1960s a grating) selects the wavelength of interest from the continuum emitted by the infrared source, and the transmission corresponding to that particularly frequency by the sample can be measured. Nowadays energy-dispersive instruments have largely been abandoned in favour of Fourier-Transform Infrared (FTIR) spectrometers operating on the principle of the Michelson interferometer. These instruments have the great advantage that the entire spectrum is obtained for each scan the interferometer makes, with the result that the total collection time needed to measure a spectrum is much lower. The treatment of the Fourier transform technique is outside the scope of this book; the reader is referred to the literature [7,13].

Optical components can be made of NaCl (transparent from 650 - 4000 cm^{-1}), KBr, with a low energy cut-off of 400 cm^{-1} or CsI, with an even more favourable cut-off of 200 cm^{-1}. The source is usually a temperature-stabilized ceramic filament operating around 1500 K. The detector may be a slowly reacting thermocouple in energy dispersive instruments, but has to be a fast response device in FTIR. The standard for routine applications is the deuterium triglycine sulphate or DTGS detector, while the liquid nitrogen cooled mercury cadmium telluride or MCT detector is used for more demanding applications, as for example in RAIRS.

2.6. REFERENCES

1. Coblentz, W.W. 1911. *J. Franklin Inst.* 172, 309.

2. Kiselev, A.V. Lygin, V.I. 1966. In *Infrared Spectroscopy of Adsorbed Species.* L.H. Little (Ed), Academic Press. New York.

3. Hair, M.L. 1967. *Infrared Spectroscopy in Surface Chemistry.* Dekker. New York.

4. Little, L.H. 1966. *Infrared Spectroscopy of Adsorbed Species.* Academic Press. New York.

5. Fadini, A. Schnepel, F.M. 1989. *Vibrational Spectroscopy.* Ellis Harwood Ltd. Chichester.

6. George, W.O. McIntyne, P.S. 1987. *Infrared Spectroscopy.* Wiley. Chichester.

7. Lund, P.A. Tevault, D.E. Swardzewski, R.R. 1984. *J. Phys. Chem.* 88, 1731.

8. Heidberg, J. Weiss, H. 1987. In *Thin Metal Films and Gas Chemisorption.* Wissmann, P. (Ed). Elsevier. Amsterdam. 191.

APPENDIX III

Publications

APPENDIX III

PUBLICATIONS

The following research publications were submitted/published:

1. A.C. van Dyk and A.M. Heyns, Dispersion Stability and Photo-activity of TiO_2 powders, Journal of Colloid and Interface Science, submitted May 1997.

2. A.C. van Dyk and A.M. Heyns, Untreated and Treated TiO_2, An FT-IR DRIFT Study, Journal of Materials Science, submitted July 1997.

3. A.C. van Dyk and A.M. Heyns, The FT-IR spectra of TiO_2 surfaces treated with Dimethyl Amine, Ammonia and Ethylene Diamine, Journal of Applied Spectroscopy, to be submitted.

4. A.C. van Dyk, L.C. Prinsloo and A.M. Heyns, The use of Methylene Blue in Determining the Photo-activity of TiO_2 surfaces, Journal of Applied Spectroscopy, to be submitted.